

Retention of elements relevant for a high-level nuclear
waste disposal on Opalinus Clay as model for a host rock
and Ca-bentonite as potential buffer
and backfill material

Dissertation

zur Erlangung des Grades des Doktors der Naturwissenschaften
der Naturwissenschaftlich-Technischen Fakultät
der Universität des Saarlandes

von

Kristina Brix

Saarbrücken, 2019

Tag des Kolloquiums: 07.02.2020

Dekan: Prof. Dr. Guido Kickelbick

Berichterstatter: Priv. Doz. Dr. Ralf Kautenburger

Prof. Dr. Gregor Jung

Vorsitz: Prof. Dr. Marc Schneider

Akad. Mitarbeiter: Dr. Andreas Rammo

„Das ist in meinen Augen gerade der große moralische Wert der naturwissenschaftlichen Ausbildung, daß wir lernen müssen, Ehrfurcht vor der Wahrheit zu haben, gleichgültig, ob sie mit unseren Wünschen oder vorgefaßten Meinungen übereinstimmt oder nicht“

– Lise Meitner (1878 - 1968)

Danksagung

Mein besonderer Dank gilt zunächst Dr. PD Ralf Kautenburger für die freundliche Aufnahme in die WASTE-Arbeitsgruppe, was mir nicht nur die Möglichkeit zur Durchführung dieser Arbeit gab, sondern auch die Gelegenheit den Actinoidenverbund kennenzulernen und internationale Konferenzen zu besuchen. Ich möchte aber auch für die Unterstützung, die Ratschläge und die Herausforderungen danken.

Des Weiteren möchte ich mich bei Dr. Jonas Sander, Traudel Allgayer und insbesondere Dr. Christina Hein für ein jahrelanges angenehmes und konstruktives Arbeitsumfeld, Tipps und Hilfe, sowie ein immer offenes Ohr bedanken. Zusätzlich vielen Dank für das Korrekturlesen dieser Arbeit an Tina und Sandra Baur.

Den beiden Watergirls Geli Meyer und Lis Fünfroeken, sowie dem restlichen fluktuierenden, studentischen WASTE-Team, danke ich für die angenehme (Arbeits-)Atmosphäre, die produktiven Mittagessen, die Gespräche zwischendurch, sowie die unvergesslichen Ausflüge.

Mein Dank gilt ebenso Prof. Dr. Guido Kickelbick und den Mitgliedern des Arbeitskreises Nadja, Achim, Patrick, Bastian, Susanne Limbach, Dennis Becker, Nils, Max, Dennis Meier, Christel, Christina Odenwald, Mana, Sandra Schäfer, Jessica, Susanne Harling, Robert, Thomas, Matthias, Charlotte, Stefan und Sylvia für die Aufnahme in den Arbeitskreis und ein freundliches Arbeitsklima.

Prof. Dr. H. P. Beck möchte ich für seine Anregungen und Ratschläge danken, aber auch dafür, dass er mit seiner Vorlesung *Einführung in die Radiochemie* mein Interesse an diesem Thema geweckt hat.

Ebenso möchte ich Prof. Dr. Gregor Jung und seinem Arbeitskreis (insbesondere Dr. Christian Spies, Dr. Tobias Staut und Dr. Andreas Grüter) danken, die im Rahmen meiner Bachelor- und Masterarbeit mein Interesse am wissenschaftlichen Arbeiten stets gefördert haben.

Bei dem Projektträger PTKA-WTE und dem BMWi bedanke ich mich für die finanzielle Förderung des Projekts *Geochemische Radionuklidrückhaltung an Zementalterationsphasen* in dessen Rahmen diese Arbeit entstanden ist.

Ich danke auch meinen Eltern, Cornelia & Peter Schorr, sowie Axel Brix, für die jahrelange Unterstützung, insbesondere meiner Mutter für die Zeit während des Studiums.

Zuletzt möchte ich mich bei Julian bedanken: danke, dass du immer da bist.

Table of contents

Abbreviations and symbols	I
1. Abstract	1
2. General part.....	3
2.1 Introduction	3
2.2 Final disposal problem	5
2.2.1 Civilian use of nuclear power	5
2.2.2 Radioactive waste disposals in Germany	7
2.2.3 Radioactive waste disposals in other countries	9
2.2.4 Waste Cocktail elements	10
2.3 Concept for a high-level nuclear waste disposal in clay formations in northern Germany	14
2.3.1 Geology and hydrogeology	14
2.3.2 The multi-barrier system	16
2.3.3 Fundamentals of ion immobilisation on potential barriers of a disposal.....	18
2.3.4 Opalinus Clay as a model for the host rock.....	19
2.3.5 Bentonite as buffer and backfill material	21
2.4 Experimental methods and data analysis	23
2.4.1 Retention experiments	23
2.4.2 Elemental quantification via mass spectrometry with inductively coupled plasma..	24
2.5 Geochemical modelling.....	30
2.5.1 Theoretical background	30
2.5.2 Adsorption models for Eu^{3+} , UO_2^{2+} and Cs^+	33
3. Results and Discussion	34
3.1 Insights into the retention behaviour of europium(III) and uranium(VI) onto Opalinus Clay influenced by pore water composition, temperature, pH and organic compounds	34
3.2 Simultaneous quantification of iodine and high valent metals via ICP-MS under acidic conditions in complex matrices.....	53
3.3 Adsorption of caesium on raw Ca-bentonite in high saline solutions: Influence of concentration, mineral composition, other radionuclides and modelling	60
4. Summary and outlook	81
5. References.....	III

Abbreviations and symbols

ΔG	Gibbs energy
ΔH_0	standard enthalpy
ΔH_{ads}	adsorption enthalpy
ε	ion interaction parameter
γ	activity coefficient
A	Debye-Hückel parameter
a	activity
ACW	artificial cement pore water
B	$1.5 \sqrt{\frac{kg}{mol}}$, empirical constant
c	concentration
c_{ads}	amount of adsorbed substance
CEC	cationic exchange capacity
c_{eq}	concentration or partial pressure of the non-adsorbed amount of a substance
c_{im}	immobilised amount of a substance
D_e	diffusion coefficient
HLW	high-level nuclear waste
HPLC	high pressure liquid chromatography
I	ionic strength
IAP	ion activity product
ICP-MS	mass spectrometry with inductively coupled plasma
K	formation constant of separated ions from a solid
K_d	distribution coefficient
K_F	Freundlich coefficient
K_H	Henry coefficient
K_L	Langmuir coefficient
k	velocity constant
m_u	molality of the ion u
n	Freundlich exponent
OPA	Opalinus Clay
PW	Opalinus Clay reference pore water

R_d	retention coefficient
SI	saturation index
SIT	specific ion interaction theory
SP	sodium perchlorate
T	temperature
$t_{1/2}$	half-life
WC	waste cocktail
z	ion charge

1. Abstract

The safe storage of high-level nuclear waste in deep geological formations is nowadays a great task for humanity since the materials will be harmful for several hundreds of thousands of years. To ensure the safe storage, all relevant interactions between the radionuclides, the technical barriers, the construction material and the surrounding host rock have to be known. This work contributes to a long-term safety case for a potential repository in clay formations in northern Germany as a model region. The retention behaviour of Eu^{3+} and UO_2^{2+} on Opalinus Clay as reference host rock is investigated in 0.01 M NaOCl_4 and 0.4 M reference Opalinus Clay pore water. In this experiments, the pH value (2-12), the temperature (25 and 60 °C) and the content of organic matter are varied. Furthermore, the adsorption of Cs^+ on Calcigel as potential buffer and backfill material is determined in high saline solutions (0.1-5 M). This is also done in presence of other relevant elements (Eu^{3+} , UO_2^{2+} and I^-). For the latter, a new method to measure iodine under acidic conditions via mass spectrometry with inductively coupled plasma is developed. Therefore, iodide gets oxidised by NaOCl to iodate. Following this, it is possible to quantify the metals and iodide in one measurement. The adsorption of Cs^+ on Calcigel takes place under all investigated conditions but decreases with increasing ionic strength. The experiments can also be simulated very well via ion exchange modelling.

Heutzutage ist die sichere Lagerung von hochradioaktivem Abfall in tiefen geologischen Formationen eine der größten Herausforderungen für die Menschheit, da seine Radiotoxizität für mehrere hunderttausend Jahre bestehen bleibt. Um die sichere Lagerung zu gewährleisten müssen alle relevanten Wechselwirkungen zwischen den Radionukliden, den technischen Barrieren, dem Konstruktionsmaterial und dem Wirtsgestein bekannt sein. Diese Arbeit trägt zur Langzeitsicherheitsanalyse eines potentiellen Endlagers in Tongesteinsformationen in der Modellregion Norddeutschland bei. Der Rückhalt von Eu^{3+} und UO_2^{2+} an Opalinuston als Referenzwirtsgestein wird in 0,01 M NaOCl_4 und 0,4 M Referenzporenwasser untersucht. In diesen Experimenten wird der pH-Wert (2-12), die Temperatur (25 und 60 °C) und der Gehalt an Organik variiert. Des Weiteren wird die Adsorption von Cs^+ an Calcigel als potentielltem Buffer- und Verfüllmaterial in hochsalinen Lösungen (0,1-5 M) bestimmt. Dies wird auch in Anwesenheit anderer relevanter Elemente (Eu^{3+} , UO_2^{2+} und I^-) durchgeführt. Dafür wird eine Methode entwickelt, um Iod mittels Massenspektrometrie mit induktiv gekoppeltem Plasma im

sauren Milieu zu bestimmen. Diese Methode ermöglicht es, die Metalle und Iodid in einer Messung zu quantifizieren. Die Adsorption von Cs^+ an Calcigel findet unter allen untersuchten Bedingungen statt, sinkt jedoch mit zunehmender Ionenstärke. Die Experimente können zudem sehr gut mittels Ionenaustauschmodellierungen simuliert werden.

2. General part

2.1 Introduction

In 1934, Enrico Fermi irradiated uranium atoms with neutrons (Fermi et al., 1934). Around four years later, on 17th December 1938, Otto Hahn and Fritz Straßmann showed, that the result of Fermi's experiment were non-natural barium isotopes, amongst others (Hahn and Strassmann, 1939). When Lise Meitner and Otto Frisch described the process theoretically in 1939, this was the hour of birth for the use of nuclear power both in civil and military way (Flügge, 1939; Meitner and Frisch, 1939a, 1939b; Reed, 2014).

Since then, also a great task for humanity arose: the safe storage of nuclear waste, which radiates for many hundreds of thousands of years. The danger for humans and the environment comes not only from the radiotoxicity. Most of the substances are heavy metals and also chemotoxic (Duffield and Williams, 1986; Buchheim and Persson, 1992; Grivé et al., 2015). These toxic substances have to be stored in a place, where no interaction with the environment is possible and additionally safe from unauthorised access.

Today, it is international consensus to store the high-level nuclear waste (HLW), which emits > 99% of the radioactivity contained in the whole radioactive waste (Röhlig et al., 2012), in deep geological formations such as salt rock, clay formations or granite bedrock.

Owing to the very long half-lives ($t_{1/2}$) of some radionuclides, a long-term safety case for a HLW repository is absolutely necessary. For this purpose, a lot of laboratory experiments were and are done concerning the reversible and irreversible immobilisation of radionuclides or their homologues (Dickson and Glasser, 2000; Lee et al., 2006; Kautenburger and Beck, 2010; Hamed et al., 2019; Missana et al., 2019). For such experiments, which require the determination of many different elements at trace levels, mass spectrometry with inductively coupled plasma (ICP-MS) is a useful tool. Certainly, it is not feasible to anticipate every possible process or interaction concerning the HLW for the next million years. Therefore, the experiments were additionally simulated via computer programs to develop a model which enables a prognosis of the radionuclides' and barriers' behaviour under varying conditions (Seveque et al., 1992; Montes-H et al., 2005; Marty et al., 2010; Cao et al., 2019; Ma et al., 2019).

In the present work, adsorption experiments and their geochemical simulations are done as a contribution to the long-term safety case for a potential HLW disposal under conditions occurring in claystone in the model region northern Germany.

Raw Opalinus Clay (OPA) is studied as reference clay for a possible host rock. The retention behaviour of Eu^{3+} and UO_2^{2+} on OPA is described at room and elevated temperature T (60 °C), since HLW emits heat in the first hundreds of years. This is done in 0.01 NaClO_4 as inert reference background electrolyte and OPA pore water (0.4 M). The salinity of clay pore waters in northern Germany is expected to be high saline (up to 5 M NaCl with additional high valent cations) (Klinge et al., 2002). Adsorption experiments are done in a wide pH range (2-12) with respect to different dissolution and precipitation effects of the OPA minerals and are also simulated by ion exchange modelling. The influence of humic acid and lactate as natural occurring, potential complexing agents on the retention behaviour of the two metals is also described.

Calcigel, a raw Ca-bentonite, is investigated as potential buffer and backfill material in a HLW disposal. The adsorption of different Cs^+ concentrations, as very mobile cation, on Calcigel in very high saline (0.1-5 M), NaCl based solutions is analysed by batch experiments as well as theoretically via ion exchange modelling. Adsorption experiments on pure Na-montmorillonite in comparison to Calcigel are also done. Hereby, the influence of the inhomogeneity of non-threatened Calcigel is tested.

Furthermore, the development of new measurement applications is indispensable to investigate the phenomena concerning the long-time storage of HLW under realistic conditions. Here, a new method to quantify iodine via ICP-MS under acidic conditions is presented. It allows experiments with iodine or iodide in the presence of other, even high valent metal ions and a simultaneous quantification. This is highly time- and resource-saving compared to the alkaline iodine measurement techniques via ICP-MS known from the literature (Reid et al., 2008; Novo et al., 2019). High valent metals could precipitate under non-acidic conditions whereas iodine forms volatile compounds at $\text{pH} < 7$. So, every sample would have to be measured twice without the new method. Since the HLW will not be separated before the storage, the Cs^+ adsorption on Calcigel is also investigated in the presence of other HLW relevant elements (Eu^{3+} , UO_2^{2+} and I^-) by using this method. The results are published in peer-reviewed scientific journals.

2.2 Final disposal problem

2.2.1 Civilian use of nuclear power

Since 1954, nuclear fission is used in power plants to produce energy and the first reactor could supply 5 MW (Petros'yants, 1964; Sinev et al., 1964). Today, this technology is applied worldwide and altogether more than 450 nuclear reactors are operating in power plants, with each of them generating an average power of around 900 MW. The most common reactor type is the pressurized water reactor (65% in numbers, 70% in supplied energy) (International Atomic Energy Agency, 2019) which is constructed with three separated water circuits. The first provides the cooling of the reactor core and transfers the heat originating from the core's chain reaction to a steam generator, where water in the second circuit is evaporated and activates a turbine to generate power. The heat that cannot be used for power generation is carried off by the third circuit, the cooling water system (Lips, 2005).

The huge advantage of nuclear power plants is the potential to produce a lot of electricity, whereas no exhaust emissions are produced, such as CO₂. For many countries, the nuclear power is a high-performance source of energy in accordance with environmental protection. However, there are also two disadvantages. Therefore, some countries including Germany stop their generation of energy out of nuclear fission (Nohrstedt, 2008; Jahn and Korolczuk, 2012; Hayashi and Hughes, 2013).

The first and perhaps most urgent disadvantage are serious accidents, which could happen and happened before, due to human or technical failure with disastrous consequences for humanity and the environment. On 28th March in 1979, the core of a reactor in Three Mile Island (Harrisburg, USA) melted partially leading to the release of a small amount of radioactive material (mainly Xe-133 and Kr-85) (Collier and Davies, 1980; Rogovin and Frampton Jr., 1980; Bartlett et al., 1983; Marksberry et al., 2016). The worst accident in the context of nuclear energy so far happened on 26th April in 1984 in Chernobyl (Ukraine) where a reactor exploded. It released plenty of radioactive material in the earth atmosphere. A plume, loaded with radioactive isotopes, gathered over the complete northern hemisphere. As a consequence of this, the cancer rates increased significantly in some regions. A combination of human incompetence and a fatal construction failure of the reactor's control rods was the reason for this disastrous accident. It led to the dead of assumed 4,000 - 93,000 people (official number: 31, which died due to the blast or acute radiation exposure) and a 30-km exclusion zone around the reactor (~2,600 km²) for the next thousands of years (Joshi, 1987; Nichoisson and

Hedgecock, 1991; Kazakov et al., 1992; Reponen et al., 1993; Molero et al., 1999; Nuclear Energy Agency, 2002; Williams, 2002). The latest incident was in 2011. A submarine earthquake (magnitude 9.0) caused a blackout in the region of Fukushima Daiichi. Due to this, the power plant's reactors were shut down automatically and the emergency generators started to work. This ensured a permanent cooling of the reactor cores and the nuclear fuel in the spent fuel pit. Around one hour later, a tsunami hit the east coast of Japan, flooded the nuclear power plant and destroyed the emergency power supply. In the following, the cores of three reactors melted and several explosions and fires damaged the reactor buildings. These led to a release of radiant material into the atmosphere and (direct and indirect) into the sea (Nagatani et al., 2013; Wada et al., 2013; International Atomic Energy Agency, 2015; Kubo et al., 2018).

Beside this pervasive danger, there is another disadvantage of nuclear power plants and it is growing bigger, with every year the reactors are in operation: the radioactive waste. It originates not only from nuclear power plants, but also uranium mines, hospitals and some research institutions are generating radioactive waste. However, they produce it only in a small amount. Commonly, the waste is distinguished in three different types: low-, intermediate- and high-level nuclear waste (International Atomic Energy Agency, 1981, 1994; Baisden and Choppin, 2007). Low-level nuclear waste contains mainly contaminated materials such as shoe covers, clothing, syringes and other laboratory equipment which was in short contact with radiant material. Its activity is normally slightly higher than natural background activity and no heating is expected. Intermediate-level nuclear waste has a higher activity but still no generation of heat is expected. The most problematic waste are high-level radioactive materials such as non-spent fuel, fission products and radiated parts of reactor buildings. In Germany, these kinds of nuclear waste are nowadays also considered but they are classified in only two groups: negligible heat-generating waste and heat-generating waste. The first includes low- and intermediate-level nuclear waste whereas the second category describes HLW (Nuclear Energy Agency, 2005, 2016). Currently, the International Atomic Energy Agency proposes even six subclasses of nuclear waste, based on the half-life and activity content (International Atomic Energy Agency, 2009). In agreement with the economic efficiency, these kinds of waste have to be stored separately with regard to variable safety requirements.

Some research focuses on the transmutation of HLW. This means the separation and subsequently neutron irradiation of long-lived radionuclides. It is possible to shorten the necessary storage time of HLW around a hundred times with this procedure (Salvatores, 2005; Wallenius, 2019). Whether this procedure is feasible depends on the economic efficiency. A safe storage for the remaining several thousands of years is still needed.

The present work focuses on the long-term safety aspects of a HLW disposal in deep geological formations.

2.2.2 Radioactive waste disposals in Germany

Until 1996 when the United Nations ratified the London Protocol, it was almost common to dispose radioactive waste simply in a preferable easy way, by dumping it into the sea, in rivers or just burying it somewhere in the environment (Weißenburger, 1996; International Atomic Energy Agency, 1999; International Maritime Organization, 2006). Nowadays, it is international consensus to store at least the HLW in deep geological formations, to pretend humanity and the environment from the radioactive materials for the next hundreds of thousands of years.

In Germany, the history of nuclear waste disposal is controversial and full of challenges, because the acceptance of the general public in almost every decision concerning this topic is very low. In the 1960s, a former salt mine in Morsleben was determined for the storage of low- and intermediate-level nuclear waste in East Germany (HLW could be restored to the USSR). Even before the license was accorded and structural measures were operated, the deposition of waste from Dresden began due to lack of space in the intermediate store. A long-term proof of safety was never adduced. Meanwhile the mine is in danger of collapsing because of the excessive mining and has to get stabilised. The actual consensus is to close the repository, while the 37,000 m³ of radioactive waste remain there (Bundesamt für Strahlenschutz, 2017a; Bundesgesellschaft für Endlagerung, 2019).

Also in West Germany, the final repository should be in a salt stock. They are already stable since many million years and are able to creep and following this, to close small leakages. The former salt mine Asse was chosen as research mine to investigate technical aspects for a nuclear waste disposal in 1965. Six years later, this research mine was additionally used as repository for low- and intermediate-level waste, without completed long-term safety considerations. There are a lot of digging chambers very close to each other based on the extraordinary intensive lining in Asse. For this reason, the intermediate ceilings trend to break, leading to instability and water intrusions. Nowadays, Asse is going to be closed and the stored radioactive waste has to be removed and stored additionally in a HLW disposal, once it is constructed (Bundesamt für Strahlenschutz, 2017b). Simultaneously to the research in Asse, it was looked for a real

repository for every kind of nuclear waste. In 1979, Gorleben was chosen as experimental mine, although there were also other salt stocks supposed and almost no geoscientific investigations conducted. An interim storage was built but no nuclear waste was embedded in the deep salt stock. Today the interim storage Gorleben is still in operation, but the storage is interrupted, until a final decision for the safest place for a HLW disposal is made.

Before, almost every decision in relation to Morsleben, Asse and Gorleben was made without respect to the general public, which explains the negative atmosphere coming up when the government is talking about final disposals for nuclear waste. Besides this, the Konrad mine, which was also investigated in the 1970s, applies as repository for negligible heat generating nuclear waste. Since 2007, there is a valid license to build and operate the former iron mine as repository for 303,000 m³ low- and intermediate-level nuclear waste (Bundesamt für Strahlenschutz, 2017c). In the context that there was no comparative site selection and several delays during the construction (so far, it will last until 2027) and consequently much higher costs, there are still some protests against the Konrad mine.

Nevertheless, in 2013 the German government declared by law a restart concerning the search for a HLW disposal and additionally, they underlined that the waste must not be stored abroad (Standortauswahlgesetz, 2013). Until 2031, different geological formations (clay, salt rock and crystalline rock) in the whole country should be investigated as potential sites (Figure 1), without consideration of existing structures and former studies (“white map”). The complete process should be transparent and the concerns of the public should be listened. At the end of the process, the long-term safety of sites coming into question will have the first priority for the decision (Kommission Lagerung hoch radioaktiver Abfallstoffe, 2016).

Studies have shown that the fissured crystalline rock formations in Germany seem to have a too high permeability to be considered as a suitable host rock (Bundesgesellschaft für Geowissenschaften und Rohstoffe, 2007). So, most of the actual host rock research focuses on salt rock or clay formations. In the context of this work, clay is treated as possible host rock.

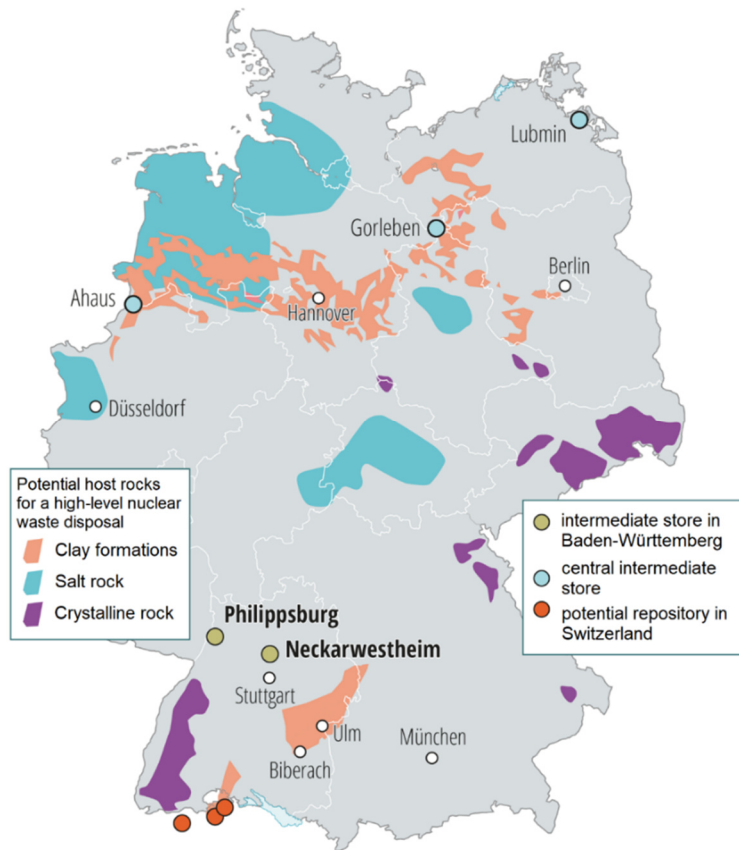


Figure 1. Geological formations of potential host rocks for a high-level nuclear waste disposal in Germany (Link, 2018).

2.2.3 Radioactive waste disposals in other countries

Since 37 countries all over the world operate nuclear power plants (International Atomic Energy Agency, 2019), the search for a final disposal is not only a German problem. Whereas several low- and intermediate-level nuclear waste disposals are under construction or even operating, no repository for HLW exists worldwide. The first HLW disposal, Olkiluoto, is under construction in granite bedrock in Eurajoki, Finland (Miller and Marcos, 2007; Aaltonen et al., 2016). The storage may begin in 2020.

The plans of France and Switzerland to build their HLW repositories near the border to Germany are causing worries to the German general public. France is considered a nuclear country where the advantage of low-emission electricity weights higher than the worries about perturbations or the final storage of the nuclear waste. The French government even asked for communes which volunteered for research laboratories in geological formations in their region. One of these 30 volunteered communes is Bure in the department Meuse (around 120 km distant

from the German border). In 2012, the French government declared the clay formation near Bure as future intermediate- and HLW disposal (Kommission Lagerung hoch radioaktiver Abfallstoffe, 2016). Also in Switzerland, clay formations are considered as favourite host rock and regions in different cantons were investigated, but until now, no final decision concerning the location is made.

Recently, the USA had to restart the research for a HLW disposal. In the 1980s, Yucca Mountain was chosen as appropriate storage location and every state, except Nevada where the formation is located, agreed. The geological formation in this area is volcanic tuff. In 2011 president Obama stopped the research and development in this region, mainly due to doubts on the suitability of this material as host rock. One of the requirements for the final location is now the agreement of the concerned state and commune (Kommission Lagerung hoch radioaktiver Abfallstoffe, 2016).

2.2.4 Waste Cocktail elements

In the context of a HLW disposal, europium(III), caesium(I), uranium(VI) and iodide are chosen as representatives in this work for the element cocktail in spent fuel which has to be stored. A calculated composition of spent fuel is shown in Table 1.

Table 1 Composition of spent nuclear fuel (Neles et al., 2008).

Radionuclides	Content [%]
uranium-235	0.8
uranium-236/237/238	91.8
plutonium	1.2
fission products and transuranic elements	6.2

There are over 200 possible fission products of U-235 such as Sr-90, Zr-93, I-131 or Cs-137. Transuranic elements such as plutonium and americium can also arise from neutron capture of U-238 (Figure 2). The four representatives were investigated separate and in composition as the so-called waste cocktail (WC).

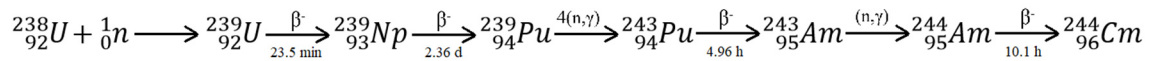


Figure 2. Genesis of americium and curium out of U-238.

As main component of spent fuel, uranium has to be considered in every wide-ranging research concerning the chemical safety aspects of a disposal for HLW. Beside its comparatively low radiotoxicity, the chemical toxicity of uranium has to be taken into account. It is harmful to plants, animals and microorganisms with different effects (Gao et al., 2019). In animals and humans, it mainly deposits in bones, liver and kidney and can cause renal failure beside other harms (Pavlakis et al., 1996).

In the present work, the initial uranium species is uranyl (UO_2^{2+}). Naturally, uranium occurs only in oxygenic minerals, for example, uranitite (UO_2), coffinite ($\text{U}[(\text{SiO}_4)(\text{OH})_4]$) or carnotite ($\text{KUO}_2\text{VO}_4 \cdot 1.5\text{H}_2\text{O}$), including three different natural isotopes: U-234 (0.005%), U-235 (0.72%) and U-238 (99.275%). Altogether, 26 isotopes of uranium are known (23 are fission products of transuranic elements). Most of them are α -emitters, this means they emit an ${}^4_2\text{He}$ -particle and energy, transmuting into a thorium atom. The half-lives range between a few microseconds and $> 10^9$ a. Four different oxidation states are known for uranium. Triple and fivefold charged uranium is not stable in aqueous solutions, whereas compounds with fourfold and sixfold charged uranium can exist in minerals and solutions (Holleman et al., 2007). Uranium chemistry is very complex, because there are a lot of known minerals containing uranium and in solution, it forms complexes with many other elements. In Figure 3, potential species of uranium in solution depending on pH value and background electrolyte are shown. Mainly, hydroxo and carbonate complexes are formed which can get neutralised by other ions in solution and also precipitate. In calcium containing solutions, the highly mobile, neutral complex $\text{Ca}_2\text{UO}_2(\text{CO}_3)_3$ is formed in the neutral pH range (Stewart et al., 2010). Especially, at pH 7.6 (shown in dashed lines in figure 3), the natural equilibrium pH value of Opalinus Clay pore water, $\text{Ca}_2\text{UO}_2(\text{CO}_3)_3$ is the dominant species in calcium containing electrolytes. This mobile complex plays a major role in safety considerations of HLW disposals because it is very hard to immobilise with methods based on retention via electrostatic interactions.

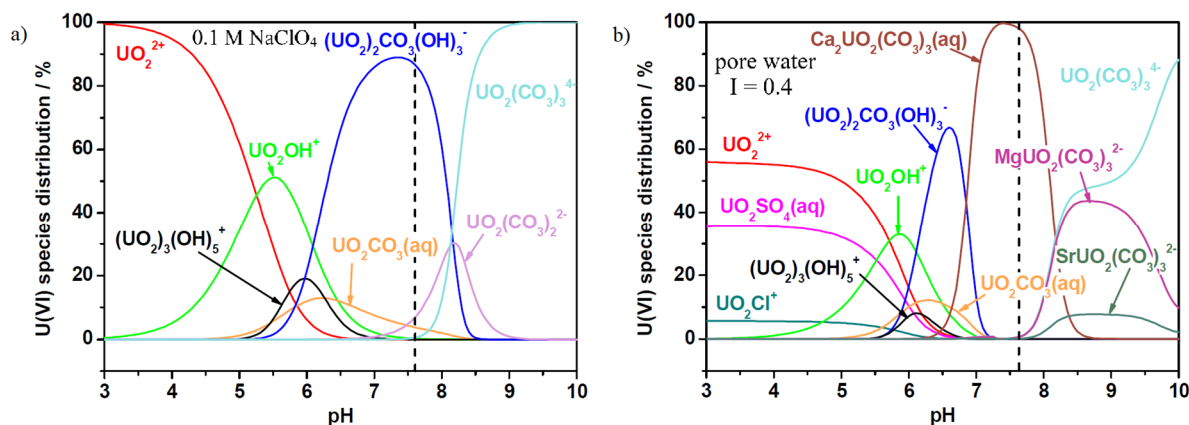


Figure 3. Calculated species distribution of uranyl in 0.1 M NaClO₄ (a) and 0.4 M Opalinus Clay pore water (b) with the equilibrium pH value 7.6 of Opalinus Clay pore water as dashed line (Joseph, 2013).

Europium(III) is another component of the WC investigated in the present work. It is not only a fission product contained in the HLW, but it can also be considered as homologue of the three valent actinides such as americium or curium (Eisenbud et al., 1984; Krauskopf, 1986). These transuranic elements are chemical and radio toxic (Breitenstein Jr. and Palmer, 1989). In animal studies they were found to deposit in liver and skeleton. Long-time effects were cancers of liver, lung and bone (Taylor, 1989). Consequently, a release to the environment has to be urgently prevented.

Due to their partial short half-life, transuranic elements are hard to study by themselves, especially with regard to the long-term behaviour. Since europium and americium are in the same column of the periodic system of elements, their electronic configuration and their chemical behaviour are very similar. As a consequence, the retention properties and reactivities of americium (and other actinides) can be estimated by studying europium. In solution, Eu(III) forms different species depended on the available anions. Under atmospheric conditions, Eu(III) mostly interacts with carbonate, which arises e.g. from atmospheric carbon dioxide or mineral dissolution (Figure 4a). In the absence of CO₂, europium hydroxo complexes are the dominant species (Figure 4b). Both, carbonate as well as hydroxo complexes have low solubility products in water and are precipitative in slightly basic solutions (Holleman et al., 2007).

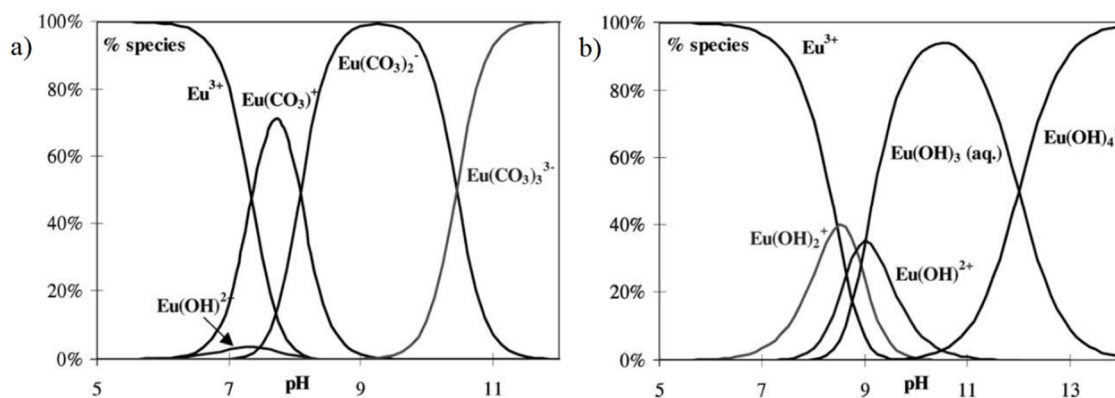


Figure 4. Speciation of Eu(III) in 0.1 M NaClO₄ in presence (a) and absence (b) of CO₂ (Plancque et al., 2003).

As monovalent cation, Cs⁺ is also considered in the WC. The caesium isotopes Cs-135 ($t_{1/2} = 2.3 \cdot 10^6$ a) and Cs-137 ($t_{1/2} = 30$ a) are two of the major fission products of U-235. Both are β^- -emitters which means they emit an electron and an antineutrino resulting in the element with one atomic number higher while the atomic mass remains constant. In the special case of Cs, the preferred decay product is a metastable Ba isotope which relaxes into stable barium under the release of γ -rays. Therefore, caesium is considered as main source of nuclear radiation in the first hundreds of years (Cherif et al., 2017). In solution, caesium is a monovalent, highly soluble cation, which does not precipitate under natural conditions. This implies a very high mobility of Cs⁺ in aqueous solutions. Consequently, in case of a release into the environment, radiant Cs can contaminate a wide area (Staunton and Roubaud, 1997; Poinssot et al., 1999; Bradbury and Baeyens, 2000; Dzene et al., 2015). Natural occurring Cs-133 acts similar to potassium in the human body, depositing in bones, muscles and soft tissue and is generally seen as non-toxic (Yamagata, 1962; Leggett et al., 2003). Only high amounts can cause confusion in the metabolism (because of the similarity to potassium) and provoke diseases such as cardiac arrest, arrhythmia or hypokalemia among others (Melnikov and Zanoni, 2010). The radioactive isotopes are mainly harmful due to their radioactivity and resulting radiation in living beings (Rasheed et al., 2019; Turner et al., 2019).

Iodine is one of the few fission products with anionic character and therefore chosen as representative in the investigated WC. Its preferred species in natural solutions are IO₃⁻, I⁻ or bound to organic molecules (Bruchertseifer et al., 2003) although iodine can be available in many different oxidation states (7, 5, 1, 0, -1). The isotopes occurring in HLW are I-129 ($t_{1/2} = 15.7 \cdot 10^6$ a) and I-131 ($t_{1/2} = 8$ d). Like the caesium isotopes, they are β^- -emitters. Based on its high volatility (as I₂ or HI) and high mobility (as iodide) in ground- or seawater, radioactive iodine is able to contaminate a large territory. In human body, iodine is metabolised

in the thyroid, where the chemical radiation can cause thyroid cancer (Drozdovitch et al., 2019; Kutsen et al., 2019). Therefore, many governments provide potassium iodide tablets in case of the release of radioactive material. This natural iodide saturates the thyroid for some days, so no new uptake is necessary for the metabolism and additional intake of perhaps radiant iodide isotopes can be segregated fast. Nevertheless, only people younger than 45 are recommended to use the tablets, because the risk of a permanent hyperthyroidism triggered by the iodide excess is much higher since then (Rønnov-Jessen and Kirkegaard, 1973; Nordyke et al., 1988).

2.3 Concept for a high-level nuclear waste disposal in clay formations in northern Germany

2.3.1 Geology and hydrogeology

Different studies were made to evaluate the suitability of potential host rocks in Germany such as granite, salt rock or clay formations (Bräuer et al., 1994; Kockel and Krull, 1995; Bundesgesellschaft für Geowissenschaften und Rohstoffe, 2007; Hoth et al., 2007). In the present work, clay is considered as host rock under conditions occurring especially in northern Germany. This disposal model is based on the ANSICHT project (Jobmann et al., 2017).

Abundant clay deposits from lower Cretaceous are located in the Lower Saxony Basin (Mutterlose and Bornemann, 2000). The maximum thickness is 1,300 m. Herefrom, the sections Hauterivian and Barremian in a depth of around 200 to 1,000 m are mostly suitable for a repository. Hauterivian is divided in two layers with different geological composition: the lower Hauterivian with mainly lime and marl lime benches alternating with pyrite and siderite containing illite or kaolinite claystone as well as the upper Hauterivian with pyritic and bituminous claystone. The sediment of Barremian can also be divided in an upper and lower Barremian. Both mainly consist of illite or kaolinite claystone with some enclaves of pyrite (Reinhold et al., 2013). Samples from different boreholes are available, but they are very different in their specific mineral composition. An exemplary overview of the borehole Konrad 101 is given in Table 2 with averaged mineral values from the different layers of the two lower Cretaceous sections of interest respectively (Jahn and Sönnke, 2013). Although the boreholes were in the same area, the range of fluctuation in the mineral composition is partly very large.

Table 2 Composition of the drilling core from Konrad 101 of the sections Barremian and Hauterivian in lower Cretaceous in the Lower Saxony Basin (average values are given and range per complete section in brackets) (Jahn and Sönnke, 2013).

Mineral	Content in Barremian [%]	Content in Hauterivian [%]
Muscovite/illite	19 (10-37)	19 (2-36)
Kaolinite	17 (4-27)	12 (2-20)
Smectite	1 (0-3)	3 (2-6)
Quartz	27 (6-49)	18 (4-29)
Feldspar	3 (1-10)	2 (1-4)
Chlorite	6 (2-10)	5 (2-8)
Clay mixed layer	6 (5-10)	2 (0-5)
Gypsum	4 (2-12)	1 (0-2)
Pyrite	6 (3-33)	5 (1-9)
Calcite	5 (1-24)	26 (5-79)
Dolomite	6 (3-10)	6 (2-8)
Siderite	2 (0-14)	6 (0-12)
Goethite	1 (0-3)	10 (0-20)
Apatite	2 (0-3)	0
Amorphous components	15 (1-36)	10 (3-22)
Organic material	2 (1-3)	0.5 (0.4-0.7)

These clay formations are in contact with fresh water as well as with salt water with up to 5 M NaCl and additional higher valent cations such as Ca^{2+} and Mg^{2+} (Klinge et al., 2002; Reinhold et al., 2013). This has to be considered in a possible water intrusion scenario and in the saturation of the host rock. As a consequence of this, the present work focuses not only on low saline but also on very high saline solutions as background electrolytes.

2.3.2 The multi-barrier system

To protect the biosphere and groundwater from radionuclides in the HLW, multiple barriers are scheduled. These include technical barriers as well as the host rock as natural geological barrier. In Figure 5, the potential borehole emplacement for a repository in claystone is shown.

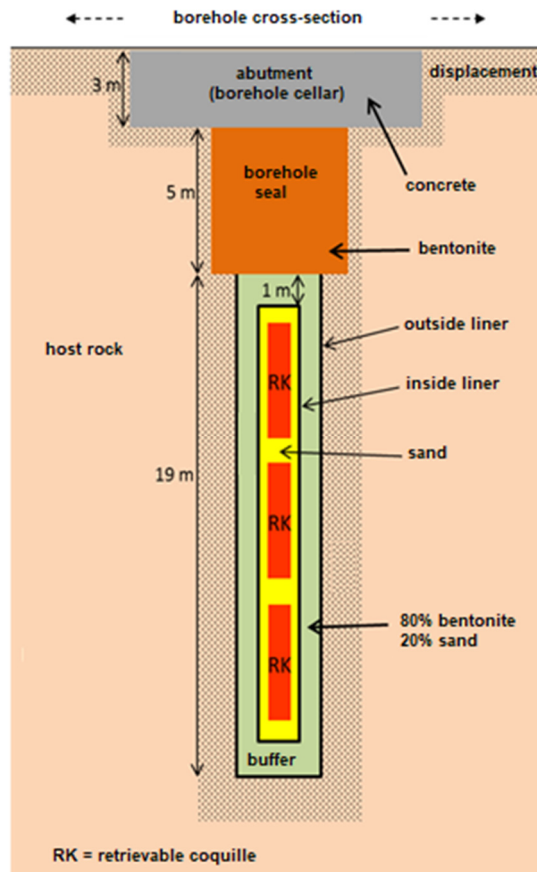


Figure 5. Schematically description of a borehole emplacement for a high-level nuclear waste disposal in northern Germany in claystone as host rock (Lommerzheim and Jobmann, 2015).

The first obstacle for the radionuclide migration are the coquilles which consist of fine-grain structural steel and have a wall thickness of 19.5 - 44.5 mm. These containers should be retrievable and tight for at least 500 years (Lommerzheim and Jobmann, 2015). Steel (and also other) containers are assumed to corrode over time under the conditions occurring in a HLW repository in deep geological formations (Kurstien et al., 2004; Shoesmith, 2006; Bennett and Gens, 2008; Féron et al., 2009; King and Kolář, 2019; Zhang et al., 2019). This can lead to leakages and following a release of radiant material out of the containers. Since some steel

containers are designed to outlast 10,000 years, the postulated 500 years for the coquilles used in Germany can be practicable.

After the containers, the next barrier for the HLW is the inside liner. It should also be stable for 500 years at minimum. Grey cast iron is scheduled as inside liner if the HLW repository would be built in a salt formation and is also considered suitable in claystone, but this has still to be evaluated.

The cavity between inside and outside liner should be filled with a buffer material containing 80% bentonite and 20% sand which is an additional barrier due to the bentonite's capability of adsorbing positively charged species. However, its primary function is to prevent solution movement from the surroundings (pore water from the host rock) towards the containers to avoid an acceleration of the corrosion. Bentonite should also be used as borehole seal to inhibit the advective transport of solutions (Lommerzheim and Jobmann, 2015).

The outside liner is not a barrier since it is perforated to allow the transport of solution into the backfill material. Its function is to endure the ground pressure of the surrounding formations and the capping. After 750 years, it is assumed to be broken due to corrosion (Lommerzheim and Jobmann, 2015).

Another barrier with large influence, although not used in the borehole itself, is concrete. It is going to be used as abutment over the borehole seal and also for the construction of the repository. So, several tons of it will be available to interact with the surroundings or the radionuclides (Lommerzheim and Jobmann, 2015). If the host rock pore water gets into contact with the alkaline concrete, additional cations can get leached out of it and the pH value of the solution increases up to 13 (Berner, 1992; Bateman et al., 1999; Gaucher and Blanc, 2006). Because of this, it is estimated that the pH value of the solution which could interact with the radionuclides will stay above ten for several thousand years. Nevertheless, concrete serves as a barrier as well as adsorption material due to its partly different charged surface (Höglund et al., 1985; Evans, 2008; Arayro et al., 2018).

The outermost barrier against an uncontrolled release of radionuclides is the host rock itself. Its thickness and depth, combined with the low permeability should guarantee that no radiant material will contaminate the ground water or the environment or ever reach humanity in the next one million years. Another great challenge is to keep the knowledge about the upcoming HLW disposals worldwide and the handling of radioactive materials for such a long time.

In the present work, OPA as model clay for a possible host rock and Calcigel (a commercial Ca-bentonite) as buffer and backfill material are investigated for their capacity to adsorb cations under varying conditions.

2.3.3 Fundamentals of ion immobilisation on potential barriers of a disposal

Some of the disposal's barriers in this concept are not only physical barriers against the migration of radionuclides, but they are also able to immobilise some elements via adsorption processes. Clay, bentonite (consisting mainly of the clay mineral montmorillonite) and cement are such potential barriers. The basics of the adsorption processes are explained below.

Adsorption is defined as accumulation of a substance (adsorbate) on a boundary surface between two phases (adsorbent). In the context of a HLW disposal, it implies the attachment of radioactive elements out of an aqueous solution (e.g. the clay pore water) onto the surface of clay, bentonite or cementitious materials. The surface of these materials is charged and ions can intercalate for example in interlayers or adsorb in areas of crystal defects to neutralise the substance to the outside. The reversed process is called desorption. Adsorption is based on electrostatic interactions which can be divided in physisorption and chemisorption depending on their adsorption enthalpy (ΔH_{ads}). Physisorption describes mainly van der Waals interactions with $\Delta H_{\text{ads}} < 50 \text{ kJ mol}^{-1}$, whereas chemisorption resembles a chemical reaction with $\Delta H_{\text{ads}} > 100 \text{ kJ mol}^{-1}$ (Martens-Menzel, 2011). The transitions between both processes are fluid and partly not assignable. Just as the adsorption processes of metal ions on clay are considered to be chemisorption but ΔH_{ads} is found in broad ranges dependent on the specific metals and clay minerals (Bradl, 2004; Gupta and Bhattacharyya, 2006; Unuabonah et al., 2007; Bhattacharyya and Gupta, 2008).

There are different mathematical models to describe the relation between the amount of an adsorbed substance (c_{ads}) and its concentration in solution or partial pressure (c_{eq}), the so-called adsorption isotherm. The simplest one is the linear Henry adsorption isotherm

$$c_{\text{ads}} = K_{\text{H}} \cdot c_{\text{eq}} \quad (1)$$

where K_{H} represents the Henry coefficient and which resembles Henry's law for the solubility of gases in solutions (Henry, 1803). In this equation (1), the amount of adsorbed substance does not affect the adsorption of further substance and the adsorption places are not limited. It is often only valid for very small adsorbate concentrations.

In 1907, Herbert Freundlich presented an empirical adsorption model where the reduced capacity of the adsorbent with increasing adsorbate concentration is taken into account (Freundlich, 1907). The corresponding adsorption isotherm is called Freundlich isotherm

$$c_{\text{ads}} = K_F \cdot c_{\text{eq}}^{1/n} \quad (2)$$

with K_F as Freundlich coefficient and n as Freundlich exponent. Most adsorption processes of small ion concentrations on clay or cementitious materials can be described by this equation (2) (Gupta and Bhattacharyya, 2006; Bhattacharyya and Gupta, 2008; Elbana et al., 2018; Georgescu et al., 2018; Tiruneh et al., 2018). Discrepancies mainly occur if there are more adsorption sites with very different selectivities.

Another popular model was developed by Irving Langmuir (Langmuir, 1918). The adsorption isotherm

$$c_{\text{ads}} = \frac{K_L \cdot c_{\text{eq}}}{1 + K_L \cdot c_{\text{eq}}} \quad (3)$$

with K_L as Langmuir coefficient takes additionally into account that only a monolayer of adsorbate can be bound. Contrary to the Freundlich model, saturation phenomena can be described with this formula which are necessary for high adsorbate concentrations.

There are also other adsorption models considering different phenomena and circumstances such as the Brunauer-Emmett-Teller, the Gibbs and the Temkin isotherms (Gibbs, 1878; Swan and Urquhart, 1926; Brunauer et al., 1938; Emmett and Kummer, 1943).

In the following, the properties and structure of OPA and bentonites, especially Calcigel (a commercial Ca-bentonite), concerning the adsorption of cations are elucidated in more detail.

2.3.4 Opalinus Clay as a model for the host rock

In the context of this work, no sample of lower Cretaceous clay from the Lower Saxony Basin was available. Therefore, OPA is used as reference clay to represent the host rock. It naturally occurs in Switzerland and south Germany. OPA is often used as reference material because its properties are already well investigated by the Swiss National Cooperative for the Disposal of Radioactive Waste. OPA was deposited as a marine segment about 180 million years ago and

is located in the Jurassic section. It contains 40-80% clay minerals and 10% of them are swellable (Van Loon et al., 2003). This swelling capacity leads to high compaction of the material and low permeability for solutions. In the context of a HLW disposal this means an aqueous plume could travel only very slowly through the encapsulating host rock. The diffusion coefficients D_e for e.g. Cs^+ and iodide through OPA were determined as $D_e(\text{Cs}^+) \approx 2 \cdot 10^{-10} \text{ m}^2 \text{ s}^{-1}$ and $D_e(\text{I}^-) \approx 1 \cdot 10^{-11} \text{ m}^2 \text{ s}^{-1}$ from laboratory as well as field data (Van Loon et al., 2004; Wersin et al., 2004). This equals a movement $< 1 \text{ cm}^2$ per year.

Responsible for the clay's swelling ability is the structure of the contained clay minerals. These minerals are so-called sheet silicates. They consist of aqueous aluminium silicates in tetrahedral and octahedral layers. SiO_4 tetrahedrons are corner-linked and AlO_6 octahedrons are edge-linked (Figure 6). The number of sheets depends on the sort of the clay mineral. Kaolinite consists of two sheets, illite and smectite of three and chlorite even of four. The substitution of Si(IV) by Al(III) or Al(III) by Mg(II) leads to an overall negatively charged surface. Due to this, besides water, various cations can intercalate in the clay's interlayers or get complexed on the clay surface. The widening of the interlayers causes the clay to swell. This phenomenon depends on the salinity and composition of the actual clay pore water as well as most adsorption processes on the clay's surface (Thury, 2002; Herbert et al., 2008; Li et al., 2009; Chang et al., 2012; Massat et al., 2016; Liu et al., 2018; He et al., 2019; Soler et al., 2019).

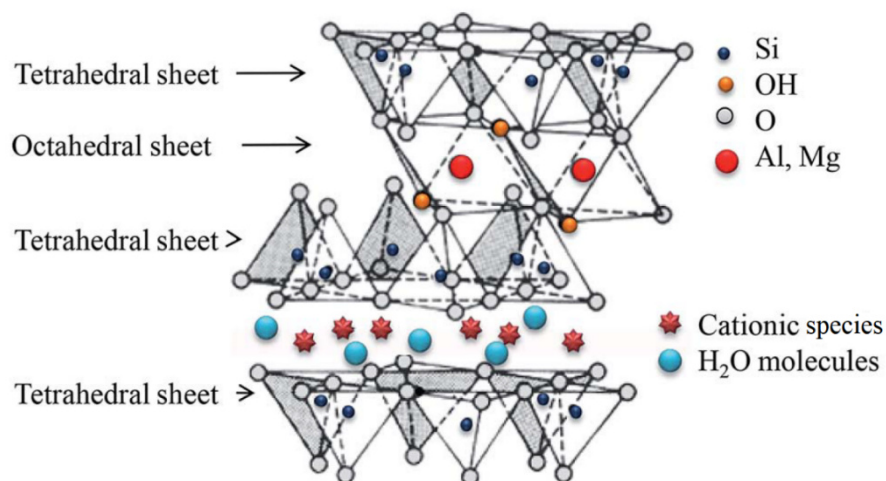


Figure 6. Structure of a 2:1 clay mineral (two tetrahedral and one octahedral sheet) (modified after Ghadiri et al., 2015).

In OPA as well as in the lower Cretaceous clay in the Lower Saxony Basin the main clay minerals are kaolinite and illite. The composition of the OPA sample BHE-24/1 from Mont Terri used in this study is given in table 3 in section 3.1. The natural pore water of OPA consists mainly of NaCl, has an ionic strength of 0.4 M and a neutral pH of 7.6 (see section 3.1, table 1)

(Van Loon et al., 2005; Appelo et al., 2010). Natural clay can be regarded as a colloidal system with a porosity of 8 to 18% (Thury and Bossart, 1999). The specific surface area of OPA BHE-24/1 was determined to $41.3 \text{ m}^2 \text{ g}^{-1}$ (Joseph et al., 2011). Most pores inside the material are interconnected and occupied by water and solutes. The main part of the pores is very small and the embedded pore water is strongly bound to the mineral surface. Only a few pores are large enough to embed also free water (Zhang et al., 2010).

The affinity of cations to the interlayers or surface of the clay depends on their charge and hydrodynamic radius. With increasing charge and decreasing hydrodynamic radius the probability for a cation to adsorb on clay increases (Blum, 2007). Especially, surface complexes between cations and clay depend additionally on the pore water pH (Bradbury and Baeyens, 2011; Baborová et al., 2018). The cationic exchange capacity (CEC) of OPA ranges from 10.2 to $16 \text{ meq } 100\text{g}^{-1}$ (Nagra, 2002).

As in all natural soils, some organic molecules are contained in OPA. These can be small ones such as acetate, lactate or formate or even large humic substances with a maximal total content of 1% mass fraction (Courdouan et al., 2007; Joseph et al., 2011). Such molecules can have an impact on the retention of the cations. Organic compounds may prevent the adsorption due to complexation (Courdouan et al., 2008; Barkleit et al., 2014; Hahn et al., 2017). This leads generally to a mobilisation in solution and following this, to a lower retention, which has to be considered in the safety assessment of a potential HLW disposal.

2.3.5 Bentonite as buffer and backfill material

Bentonites are scheduled as buffer and backfill material in many concepts for HLW storage (Radhakrishna et al., 1989; Güven, 1990; Ishikawa et al., 1990; Madsen, 1998; Ye et al., 2010). They consist of a mixture of different clay minerals and other components. The main clay mineral is montmorillonite. Compared to OPA, the swelling capacity of montmorillonite is even larger (Tournassat et al., 2015). This results in very low permeability, so bentonite is predestined as sealing material. Established applications are for example as borehole seal, binder in cat litter, drying agent and binder for heavy metals in lakes and aquaristics (Harvey and Lagaly, 2013).

The inner surface of bentonites is larger than in other clays which leads to a high adsorption capacity. Bentonites are classified by their natural major interlayer cation such as Na-bentonite

or Ca-bentonite. However, since the cations are exchangeable, the actual major interlayer cation depends on the surrounding solution (Staunton and Roubaud, 1997; Poinssot et al., 1999; Missana et al., 2014a).

In the present work Calcigel (former Montigel), a Ca-bentonite from Bavaria, is investigated. Calcigel consists of 60-70% of montmorillonite (see table 1 in section 3.3), a three-sheet silicate. Its inner surface is with $493 \text{ m}^2 \text{ g}^{-1}$ around then times bigger than this of OPA and its CEC is about $58.7 \text{ meq } 100\text{g}^{-1}$ (Müller-Vonmoss and Kahr, 1983; Clariant, 2015). Calcigel is a “mixture of selected Bavarian raw clays” (Clariant, 2015). In view to the costs of a HLW disposal, this bentonite has not to get imported if chosen as buffer and backfill material (Lommerzheim and Jobmann, 2015). Its suitability was already investigated for the Swiss and the Swedish HLW disposal concepts. They studied e.g. the thermal conductivity, bacterial growth, diffusion coefficients, CEC and swelling pressure under different conditions (Müller-Vonmoss and Kahr, 1983; Madsen, 1998; Herbert and Moog, 2002; Bengtsson and Pedersen, 2017). However, Calcigel’s adsorption properties in the context of a HLW disposal under high saline and hyperalkaline conditions were not studied yet.

The main disadvantages for clay as host rock and bentonite as buffer material for a HLW repository are their low thermal conductivity and their low thermal endurance (Bundesgesellschaft für Geowissenschaften und Rohstoffe, 2007). HLW emits heat in the first hundreds of years of storage and consequently, the surrounding in the near-field will heat up. The exact temperature depends on the barrier’s saturation and total volume of the waste. It is assumed that the near-field heats up to $\sim 100 \text{ }^\circ\text{C}$ (Johnson et al., 2002). The clay near the heat source will dry due to water evaporation and shrink. This leads to a drawing of additional water from the surroundings and the clay swells. Both contrary processes cause a lot of stress for the material which can lead to irreversible deformation and thermal excess pore pressure (Gens et al., 2002, 2009; Monfared et al., 2011).

2.4 Experimental methods and data analysis

2.4.1 Retention experiments

There are different types of experiments which can be performed to investigate the adsorption of a species or ion on an adsorbent. The most intuitive and realistic ones are diffusion experiments. A solution (usually HTO or another solution spiked with analytes) is brought into contact with an excess of solid and whether the time it needs to pass through this solid is measured or the distance it migrated in a set time (Van Loon et al., 2003; Gimmi, 2008). Although the design is very realistic, diffusion experiments are cumbersome and it can last several years to get reliable results.

Contrary to diffusion experiments, batch experiments are more simple, but also highly standardised and easy reproducible. A comparatively small amount of solid gets into contact with an excess of solution. After a set equilibration time, analyte ions are added and after another defined period of time the analyte distribution can be analysed (Lippold et al., 2005; Kautenburger and Beck, 2008; Schmeide and Bernhard, 2010). This type of experiments is conducted in the present work.

Another way to investigate the adsorption behaviour are miniaturised column experiments. With a solid to liquid ratio as realistic as in diffusion experiments and runtimes from minutes to days, they combine the advantages of diffusion and batch experiments. A pre-column for high pressure liquid chromatography (HPLC) is filled with adsorbent and installed in a HPLC apparatus. Analytes can be added directly in the HPLC eluent, which continuously flows through the column or a small amount can be injected via a sample loop (Kautenburger, 2014; Sander, 2017). After the column, the solution or rather its analyte content can be analysed. For this, the coupling to other analytical tools (e.g. ICP-MS) can be beneficial.

The effectiveness of an adsorption process is often described via so-called distribution coefficients (K_d)

$$K_d = \frac{c_{\text{ads}}}{c_{\text{eq}}} \quad (4)$$

which describe the ratio between bounded (c_{ads}) and free amount of the substance (c_{eq}).

Since especially in alkaline solutions, precipitation can also be involved in the immobilisation of the elements, the retention cannot always be described adequately by K_d values. It is proper to use retention coefficients R_d in their place

$$R_d = \frac{c_{im}}{c_{eq}} \quad (5)$$

where c_{im} refers to the amount of the immobilised substance. In relation to ions in solution adsorbing on charged mineral phases, the unit of R_d is normally given in $L\ kg^{-1}$ (or $m^3\ kg^{-1}$ referring to SI units). It gets calculated of the immobilised concentration per kilogram adsorbent in $mol\ kg^{-1}$ and the remaining concentration in solution in $mol\ L^{-1}$. With a known initial analyte concentration and a measured c_{eq} , R_d can easily be calculated for the experimental setups mentioned above.

2.4.2 Elemental quantification via mass spectrometry with inductively coupled plasma

ICP-MS is a powerful analytical tool to quantify most elements in the periodic table quasi simultaneously at trace levels in aqueous solutions or solids. It is used to determine c_{eq} of HLW relevant elements after the batch experiments in the present work.

The first commercial device was introduced in 1983 by Perkin-Elmer SCIEX which could already detect > 90% of the elements down to a detection limit of 0.5-10 $\mu g/L$ (Date, 1983; Hunt, 2008). In the 1970s and 80s, a lot of research and development on this technique was done by Gray and Houk and their co-workers (Gray, 1974, 1975a, 1975b; Houk et al., 1980, 1981; Houk, 1986). At this early stage of development, it was only useful for research applications because only samples prepared in the laboratory could be investigated due to a lot of interferences and unstable measurement conditions, even in cleanrooms. Despite that, combining the detection limit of graphite furnace atomic absorption with the rapid multi-element analysis of inductively coupled plasma optical emission spectrometry, the implementation of ICP-MS was somewhat revolutionary in the analytical chemistry (Thomas, 2001a). Over the last decades, ICP-MS evolved from a complicated research tool only useful for high specific liquid samples to a standard method for widespread analytical questions with even higher detection limits, also in natural samples such as sea water or solids and even in

single cells or nanoparticles (Mitrano et al., 2012; Lee et al., 2014; Mueller et al., 2014; Hein et al., 2017; Qiao and Xu, 2018; Itoh et al., 2018; Lobo et al., 2018; Meyer et al., 2018; Hendriks et al., 2019; Lesniewski et al., 2019; Löhr et al., 2019).

The measurement principle is based on the formation of monocharged cations in the plasma followed by separation through the ion's mass to charge ratio. In the following, it is described in detail based on the Agilent 7500 series. For liquid analysis by default, the sample gets transported via a peristaltic pump, which guarantees a constant flow of liquid, into a nebuliser. A fine aerosol is formed, supported by argon as carrier gas (~1 L/min). Argon gas drags sample droplets from the tip of the nebuliser and carries them into a spray chamber (Figure 7). Here, larger droplets (> 10 µm in diameter) hit a wall and flow to the waste outlet (~99%) (Browner and Boorn, 1984), whereas the really small ones get transported to the plasma torch by the gas stream (Thomas, 2001b).

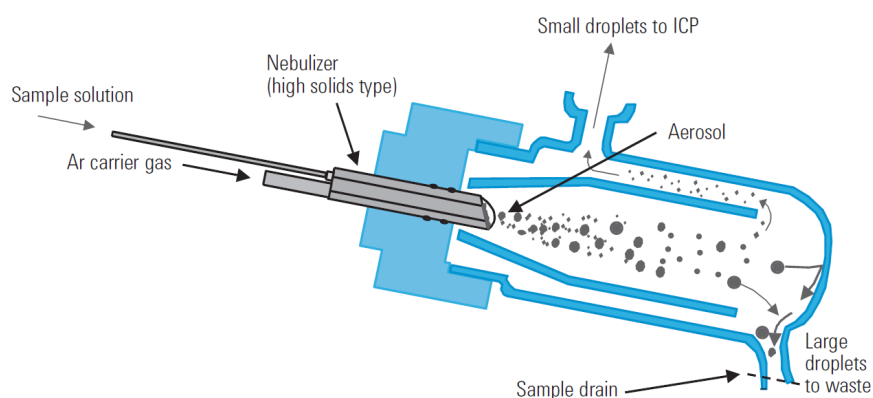


Figure 7. Nebuliser and double pass spray chamber typically used in an Agilent 7500 ICP-MS (Agilent Technologies, 2005).

The plasma torch consists of three concentric quartz tubes (Figure 8). In the outer and largest one, around 12-17 L argon are flowing through every minute. This argon stream is needed to form the plasma. At the top of the torch, a radio frequency coil creates an alternating current. Following this, an intense electromagnetic field is generated in this area. When the argon gas is flowing through the torch, a high-voltage spark splits some electrons from their atoms which were accelerated and causing a chain reaction through collision with other atoms leading to a cloud of separated Ar^+ -ions and their electrons. In the middle tube, another argon stream around 1 L/min is applied, the auxiliary gas, to stabilise the plasma's position relative to the tubes. The sample gets injected through the inner tube together with the Ar carrier gas. As the sample

reaches the plasma, its components get desolvated, evaporated, atomised and at least ionised by former argon electrons to mostly monocharged cations (Thomas, 2001c).

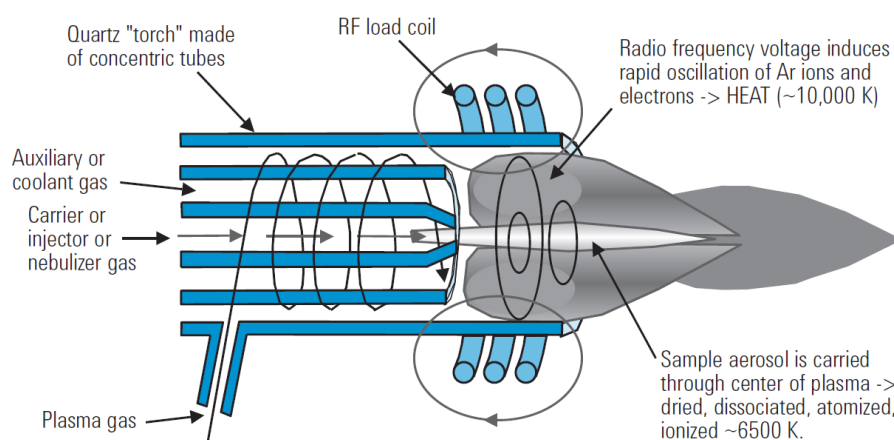


Figure 8. Plasma torch in an Agilent 7500 ICP-MS (Agilent Technologies, 2005).

After the ionisation under atmospheric conditions, the sample has to pass the interface leading to the mass spectrometer analyser in the high vacuum zone. The interface consists of two metallic cones (usually Ni or Pt) with small orifices, whereas the orifice of the first cone, called sampler, is still larger (0.8 – 1.2 mm) than that of the following skimmer cone (0.4 – 0.8 mm). To prohibit overheating by contact with the plasma, the outer part of the sampler cone consists of copper or aluminium which dissipate heat easily and additionally, the interface casing is water-cooled (Thomas, 2001d). After the cones, the sample ions get to the ion optics (Figure 9), whose function is to transport as much of analyte ions to the mass separation device as possible. The optic consists of metallic plates, barrels or cylinders and is under electrical voltage. This is necessary to keep the ion beam focused and get rid of neutral species and photons (Thomas, 2001e).

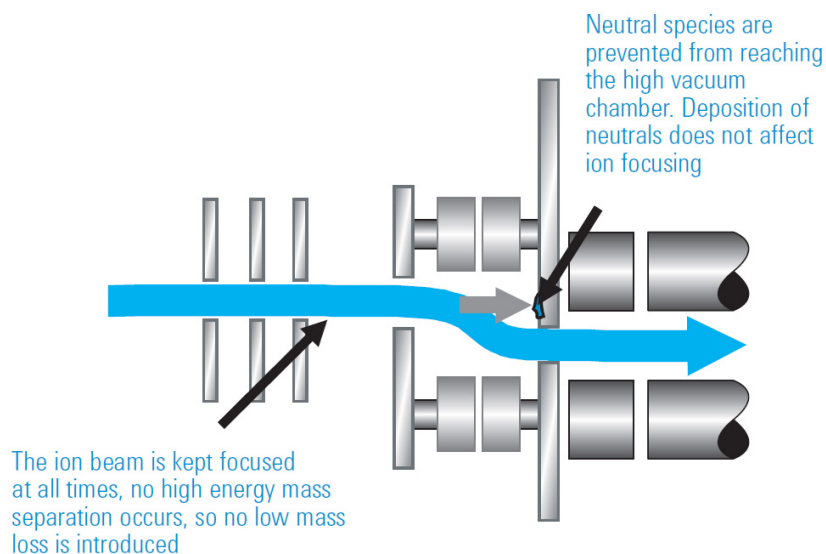


Figure 9. Schematically structure of the ion optic of an Agilent 7500 ICP-MS (Agilent Technologies, 2005).

Before the ion beam finally reaches the mass analyser, a collision or reaction cell is connected upstream to allow also the detection of elements which typically suffer from spectral interferences by so-called molecular ions generated out of the plasma gas or sample components. Examples for these species are $^{40}\text{Ar}^{16}\text{O}^+$ which equals the mass of $^{56}\text{Fe}^+$ and $^{38}\text{ArH}^+$ disturbing the quantification of $^{39}\text{K}^+$. To avoid additional detection of these molecular ions, a cell with a radio frequency multipole (e.g. an octopole) is flooded with hydrogen or helium. The focused ion beam collides with the gas. Molecular ions are larger than normal ions and collide statistically more often with He or H₂. Every collision leads to a loss of kinetic energy. A potential barrier at the entrance of the mass analyser excludes the low energy ions (Thomas, 2002a) and only the focused beam of mainly monocationic, single atomic ions reaches the mass analyser. In most cases, as well as in the Agilent 7500 series, this component is a quadrupole, which means four charged metal rods, arranged quadratic, where the counterparts carry the same charge and the rods in neighbourhood the opposite charge (Figure 10). Over this direct current an alternating current voltage is placed, changing the charge of the paired rods with a variable frequency. This frequency is responsible whether an ion with specific mass to charge ratio can pass or collides with one of the rods and does not reach the following detector (Thomas, 2001f). Typical detectors used in ICP-MS systems are discrete dynode electron multipliers. An ion passing the mass analyser has to follow a curve to hit the first dynode off-axis which minimizes the background noise. The first strike on the dynode unleashes secondary electrons. These are accelerated to the next dynode, where they generate even more electrons and so on. At least, one ion triggers a lot of electrons, generating a pulse

that is captured by the multiplier collector or anode, resulting in a measurement signal (Thomas, 2002b).

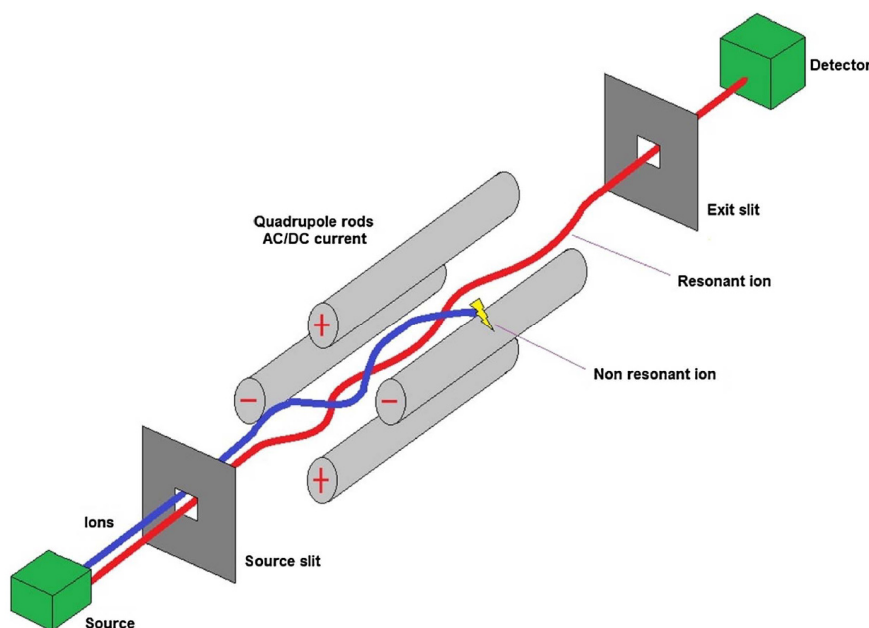


Figure 10. Structure of a quadrupole mass analyser (Santoiemma, 2018).

In the present work and many studies concerning the safety of a HLW disposal, ICP-MS is used as a powerful tool to analyse trace level concentrations of selected elements. In the context of the high saline pore water in northern Germany and the application of the WC, two challenges arose which not allow ICP-MS measurements by default.

The first challenge is the high amount of matrix (up to 5 M NaCl). It leads to suppression of the analyte signal and deposition of salt in the ICP-MS system. The latter accelerates the abrasion of the components significantly. To handle these problems, a new measurement method was implemented. The sample will be injected into the ICP-MS system only for a very short time (10 s). An additional make-up solution (diluted HNO₃) guarantees a constant flow and dilutes the sample fourfold before it gets nebulised. Instead of a stable plateau, where the analyte signal intensities are tapped by default (e.g. as counts per second), a signal peak is obtained (Figure 11). The peak area is proportional to the concentration of the analyte (Hein et al., 2017). With this method, trace concentrations of elements can be detected even in very high saline matrices without additional sample clean up.

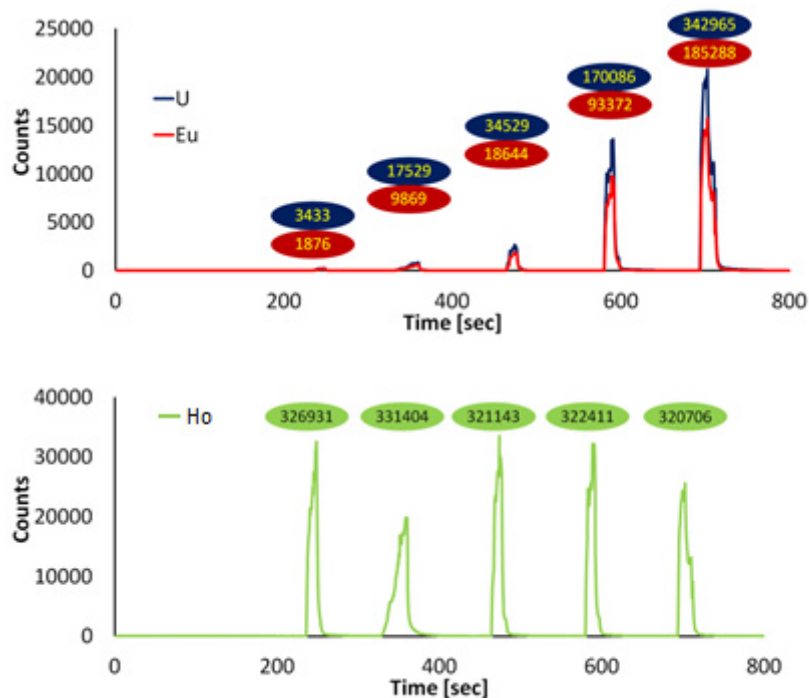


Figure 11. Chromatographic illustration of the transient measurement of the analytes ^{153}Eu (red), ^{238}U (blue) and ^{165}Ho as internal standard (green) with integrated peak areas (Ho concentration $10 \mu\text{g L}^{-1}$, Eu and U concentrations 0.1, 0.5, 1, 5 and $10 \mu\text{g L}^{-1}$) (Hein et al., 2017).

The second challenge is the simultaneous quantification of high valent metals and iodine. Metals are measured via ICP-MS in acidic solutions by default to avoid wall adsorption and precipitation effects. However, iodine forms volatile compounds in acidic environment such as iodine and hydrogen iodide. These compounds adsorb on the spray chamber wall. As a consequence of this, the measurement signal is instable and a memory effect arises (Vanhoe et al., 1993; Al-Ammar et al., 2001). Therefore, iodine measurements by ICP-MS are usually performed in the neutral or alkaline pH range. To optimise the ICP-MS measurement of the whole WC in one sample, a method to determine all WC elements together and simultaneously in acidic solution is presented in section 3.2.

2.5 Geochemical modelling

2.5.1 Theoretical background

In 1962, Garrels and Thompson published a model to calculate the composition of sea water based on dissociation constants and activity coefficients of the involved species for the first time (Garrels and Thompson, 1962). In the following, geochemical modelling based on thermodynamic constants gained popularity and is today a useful tool to confirm experiments and even to predict geochemical processes. In the context of a long-term safety case for a HLW disposal, geochemical modelling can be used to simulate e.g. radionuclide transport, adsorption phenomena, alteration of materials and corrosion of containers (Peña et al., 2008; Zheng et al., 2017; Tournassat et al., 2018; Medved' and Černý, 2019). All this can be done under a broad range of conditions and on long timescales, which is not always possible under laboratory conditions.

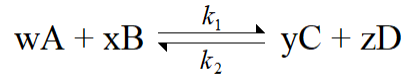
There are different common programs to simulate various issues such as EQ3/EQ6, MINTEQA2, PHREEQC and The Geochemist's Workbench. Every program can face different geochemical questions (Wolery et al., 1988; Allison et al., 1991; Wolery, 1992; Parkhurst and Appelo, 2013; Bethke et al., 2019).

In the present work, PHREEQC (Parkhurst and Appelo, 2013) was used for ion exchange modelling on OPA and Calcigel as well as dissolution and secondary mineral formation of OPA. An exemplary input file for the modelling of the Cs⁺ adsorption on Calcigel is given in figure A1 in section 3.3.

The program can be used for speciation simulations, batch-reactions, one-dimensional transport and inverse geochemical calculations (Parkhurst and Appelo, 2013). It is based on minimisation of the system's Gibbs energy ΔG . As long as $\Delta G < 0$ a reaction takes place and reaches a steady state when $\Delta G = 0$. For the calculation, the formation constant K for every species involved has to be provided. K is the ratio of velocity constants k to form product or starting material in the steady state

$$K = \frac{k_1}{k_2} = \frac{a(C)^y \cdot a(D)^z}{a(A)^w \cdot a(B)^x} \quad (6)$$

with a as activity of the species of a reaction



Since

$$\log K = \frac{-\Delta G}{5.709} \quad (7)$$

at room temperature (25 °C), the amount of every species in a system can be calculated. An algorithm determines the species distribution for which the total Gibbs energy reaches a minimum. To connect the measurable activity of a species with its concentration c

$$a = \gamma \cdot c \quad (8)$$

the activity coefficient γ depended on the ionic strength I of the background electrolyte has to be known. The determination of γ is based on the Debye-Hückel rule

$$\log \gamma = -A \cdot z_i^2 \cdot \sqrt{I} \quad (9)$$

with z as ion charge and A as Debye-Hückel parameter depended on T and the absolute permittivity of the background electrolyte (Debye and Hückel, 1923). Equation 9 is only valid for highly diluted solutions ($I < 0.01$ M). Especially at very high ionic strengths, the calculation of γ is challenging because additional parameters are needed. In PHREEQC, the empirical Davies equation

$$\log \gamma = -A \cdot z_i^2 \cdot \left(\frac{\sqrt{I}}{1 + \sqrt{I}} - 0.3 \cdot I \right) \quad (10)$$

valid for $I < 0.5$ M is used by default (Davies, 1938). This equation (10) is applied for the γ calculations concerning OPA in the present work. For the adsorption experiments in higher saline background electrolytes (≤ 5 M) the specific ion interaction theory (SIT)

$$\log \gamma = -A \cdot z_i^2 \cdot \left(\frac{\sqrt{I}}{1 + B \cdot \sqrt{I}} \right) + \sum_u \varepsilon(i, u) \cdot m_u \quad (11)$$

including B as empirical constant ($1.5 \sqrt{\frac{kg}{mol}}$), m_u as molality of the counterion u and ϵ as ion interaction parameter is used (Brönsted, 1922; Guggenheim, 1935; Scatchard, 1936). For every aqueous species pair (e.g. Na^+ and Cl^- or Cs^+ and Cl^-) in the model, ϵ has to be provided additionally.

Precipitation of solids is considered in PHREEQC via the relation

$$SI = \frac{IAP}{K} \quad (12)$$

where SI references to the saturation index and IAP is the ion activity product of the concerned solid. The K value in equation 12 describes the formation constant of the separated ions, which is commonly known as solubility product (Parkhurst and Appelo, 2013). A solid tends to precipitate if $SI > 1$. $SI = 0$ represents a steady state. When $SI < 1$ and the release of a solid's ions into the solution causes a decrease in ΔG , this solid will dissolve.

K and A depend on the temperature. The constants given in PHREEQC databases are normally valid for $T = 25$ °C. Conversion to higher temperatures can be made via the Van't Hoff equation

$$\log K_1 - \log K_2 = \frac{-\Delta H_0}{R} \cdot \left(\frac{1}{T_1} - \frac{1}{T_2} \right) \quad (13)$$

with ΔH_0 as standard enthalpy. Since ΔH_0 is not available for all minerals involved in the model for OPA, the simulation is limited to 25 °C.

Beside species calculations and mineral behaviour, also adsorption processes can be simulated by using PHREEQC. The surface complexation reactions used in this work are based on the model of Dzombak and Morel (published 1990) for complexation of heavy metal ions on hydrous ferric oxide (Parkhurst and Appelo, 2013). Here, the complete number of sites is divided in strong and weak binding sites. The associated formation constants for the surface-complex are also called selectivity constants.

The cationic exchange gets simulated via a defined amount of an exchanger X^- and the associated $\log K$ to form the compound PX_z with P as an arbitrary cation and z as its charge.

2.5.2 Adsorption models for Eu^{3+} , UO_2^{2+} and Cs^+

In the literature, different models to simulate the adsorption of cations on clay surfaces are known. The theoretical studies for Eu^{3+} , UO_2^{2+} and Cs^+ presented in this work base on such models. They are slightly refined since the experimental conditions such as pH, ionic strength or the used clay varied compared to the literature.

For the modelling of Eu^{3+} and UO_2^{2+} adsorption on OPA a two-site surface complexation model and additional cationic exchange was applied. It is based on Bradbury and Baeyens' 2 site protolysis non-electrostatic surface complexation and cation exchange sorption model (Bradbury and Baeyens, 1997, 2011). They determined the uptake of aqueous metal species by different experiments and found, that it needed at least two surface complexation sites and also cationic exchange to describe the observations (Baeyens and Bradbury, 1997; Bradbury and Baeyens, 2009).

In the case of Cs^+ , there are different proposals in the literature to describe the adsorption behaviour best. The Cs^+ adsorption on clay strongly depends on the initial Cs^+ concentration, which is contributed to very selective and non-selective adsorption sites (Cornell, 1993; Staunton and Roubaud, 1997; Missana et al., 2004). For experiments on OPA respectively on illite, two or three different sites described as surface complexation or cationic exchange are suggested (Brouwer et al., 1983; Poinssot et al., 1999; Bradbury and Baeyens, 2000; Missana et al., 2014b). Whereas on montmorillonite or smectite mainly two surface complexation reactions are implemented to describe the adsorption (Gutierrez and Fuentes, 1996). In this work, a two-site surface complexation model as proposed by Missana *et al.* is used for the simulations on Calcigel (Missana et al., 2014a).

3. Results and Discussion

3.1 Insights into the retention behaviour of europium(III) and uranium(VI) onto Opalinus Clay influenced by pore water composition, temperature, pH and organic compounds

Extended abstract:

OPA was investigated as one reference clay for a potential host rock of a HLW disposal in Germany. The adsorption behaviour of Eu^{3+} and UO_2^{2+} on OPA was determined in a broad pH range (2-12) at different temperatures (25 and 60 °C) in a low saline inert background electrolyte (0.01 M NaOCl_4 , SP) and in OPA reference pore water (PW, $I = 0.4$ M) by laboratory experiments and theoretically by the use of geochemical modelling. On the one hand, the host rock of a HLW will be in contact with the cementitious construction material, which is an alkaline material. This can lead to an increasing pH value of the pore water solution. On the other hand, OPA contains pyrite which gets presumably oxidised in the storage phase of around one million years. During this reaction, protons are generated and the pH value of the surrounding pore water solution can decrease. These contrary processes presuppose the knowledge of the elements' adsorption behaviour at different proton concentrations. Since the HLW generates heat in the first hundreds of years, the phase composition and following this, the adsorption capacity of the host rock can change. So, it is also necessary to investigate the possible interactions at elevated temperatures. Furthermore, the influence of organic matter (lactate and humic acid) as potential complexing agents on the retention behaviour of Eu^{3+} and UO_2^{2+} was investigated.

For Eu^{3+} , higher adsorption was observed at 60 °C than at room temperature over the whole pH range and in both background electrolytes. This is in agreement with the endothermic character of the adsorption process, which was analysed via a Van't Hoff plot ($T = 25, 40$ and 60 °C). At $\text{pH} > 7$ the immobilisation of Eu^{3+} was nearly 100% under the investigated conditions. The developed two-site surface complexation model with additional respect to cationic exchange could only be applied for $T = 25$ °C, due to the lack of enthalpy data for most of the involved mineral phases. It underrates the Eu^{3+} adsorption in the acidic pH range in NaClO_4 . A reason for this could be an overestimated dissolving behaviour of OPA in the model and following this, too many competing cations in solution compared to the experiments. In OPA pore water, the modelling fits almost perfect over the whole pH range.

The adsorption of UO_2^{2+} on OPA increases with increasing pH value until the neutral pH range is reached. Here, the adsorption decreases in both electrolytes and at both temperatures. Around pH 7, a neutral aquo complex $\text{Ca}_2\text{UO}_2(\text{CO}_3)_3$ is formed, which does not adsorb on the negatively charged clay surface. With increasing alkalinity, the uranyl adsorption increases again until nearly 100% are reached at pH 10 or 11 and above, due to the precipitation of different uranium containing minerals. The applied two-site surface complexation model with additional respect to cationic exchange describes the adsorption behaviour in OPA pore water very well. In NaClO_4 , the formation of the neutral complex was overestimated compared to the experiments. This is a consequence of the complete dissolution of calcite contained in OPA in the model, which acts as Ca-source. Additionally, the decreasing of the UO_2^{2+} adsorption is shifted to one higher pH number compared to the laboratory experiments. As it was found for Eu^{3+} before, the adsorption of uranyl on OPA is an endothermic reaction and consequently the adsorption was, in general, higher at 60 °C than at room temperature.

The influence of lactate and humic acid on the adsorption behaviour of Eu^{3+} and UO_2^{2+} was investigated in OPA pore water at its natural pH 7.6. For Eu^{3+} , no influence of lactate could be observed. By addition of humic acid, the retention increases about 20% at an Eu^{3+} concentration of $32.9 \cdot 10^{-6}$ M, where the OPA surface is already saturated. The formed negatively charged complexes could precipitate with additional cations contained in the pore water solution. For uranyl, the effect of the organic matter was only an increasing adsorption at 60 °C in the presence of humic acid at both investigated UO_2^{2+} concentrations. This can also be attributed to precipitation.

An analysis of the formed Eu^{3+} species with humic acid was done via capillary electrophoresis coupled to an ICP-MS. Here, only a weakly bound Eu^{3+} containing organic matter species could be detected.

Ralf Kautenburger is the corresponding author and he had the supervision during the experiments. He planned, designed and wrote the publication. Kristina Brix was also involved in writing the publication and revised the manuscript before publicising. She developed an ion exchange model to simulate the sorption edge experiments and carried out the modelling of the data. Christina Hein carried out the experiments, analysed the samples and interpreted the results. She also revised the manuscript before the publicising.

These results have been published in *Applied Geochemistry*.

Kautenburger, R., Brix, K., Hein, C., 2019, *Appl. Geochem.* 109, 104404.

<https://doi.org/10.1016/j.apgeochem.2019.104404>

Copyright (2019) Elsevier.

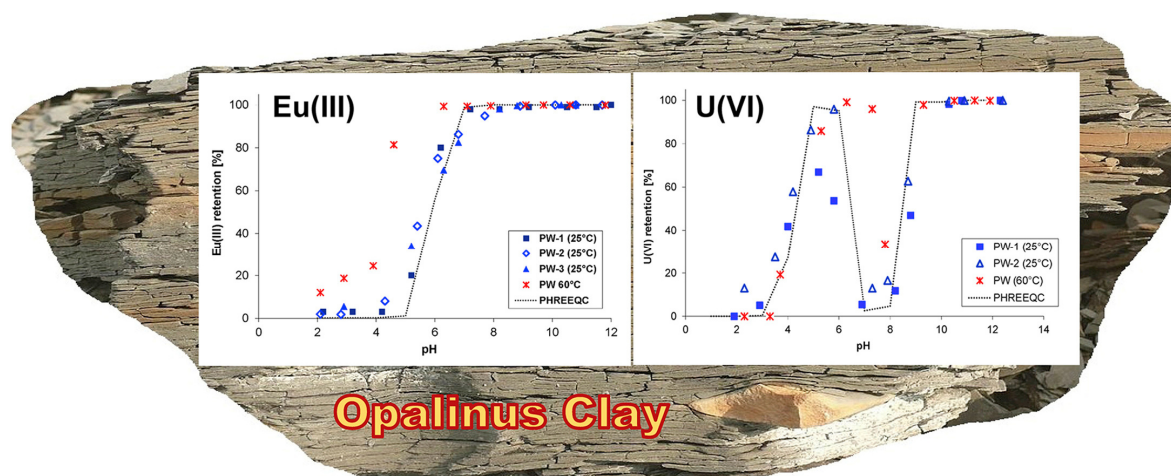


Figure 12. Adsorption edges of Eu(III) and U(VI) on Opalinus Clay in front of a piece of Opalinus Clay (Graphical abstract of Insights into the retention behaviour of europium(III) and uranium(VI) onto Opalinus Clay influenced by pore water composition, temperature, pH and organic compounds).



Contents lists available at ScienceDirect

Applied Geochemistry

journal homepage: www.elsevier.com/locate/apgeochem

Insights into the retention behaviour of europium(III) and uranium(VI) onto Opalinus Clay influenced by pore water composition, temperature, pH and organic compounds



Ralf Kautenburger*, Kristina Brix, Christina Hein

WASTE Group, Inorganic Chemistry, Saarland University, Campus C4 1, 66123, Saarbrücken, Germany

ARTICLE INFO

Editorial handling by Thomas Gimmi

Keywords:

Europium(III)
 Natural organic matter (NOM)
 Opalinus clay
 PHREEQC modelling
 Retention
 Uranium(VI)
 HLW disposal
 Sorption edges
 Temperature

ABSTRACT

In the scientific community, a consensus exists to store high-level radioactive waste (HLW) in deep geological formations for several hundred thousand years to protect humanity and the environment. After a container damage followed by the release of HLW components, the retention of the radionuclides can be affected by diverse chemical reactions in the geosphere. In this study, geochemical effects possibly influencing the retention of the radionuclides were investigated. Therefore, the retention behaviour of U(VI) and Eu(III) (as homologue for trivalent actinides) onto Opalinus Clay (OPA) as a potential host rock for a HLW disposal was analysed at different geochemical conditions. For these experiments, a wide range of metal concentrations in presence and absence of natural clay organic matter (NOM) (lactate or humic acid) in different types of background electrolytes (0.01 mol L^{-1} sodium perchlorate and 0.4 mol L^{-1} synthetic OPA pore water) were investigated. Inductively coupled plasma mass spectrometry (ICP-MS) was used as a high specific and very sensitive method for elemental trace analysis. For the speciation of Eu^{3+} -NOM-complexes, a method with high separation performance, capillary electrophoresis, was hyphenated with ICP-MS. The performed batch experiments simulate a potential water intrusion into the waste disposal. The retention (determined as $\log K_d$ values) of the metal ions strongly depends on the pH value, the presence of competing cations, temperature and NOM. At a pH value of pH 7.6 in synthetic OPA pore water, which is relevant for a disposal in OPA formations, the sorption of Eu(III) onto OPA (4 g L^{-1}) is significantly higher ($\log K_d = 3.35 \pm 0.04$ at 25°C and 4.85 ± 0.08 at 60°C) than the retention of uranyl ($\log K_d = 2.17 \pm 0.21$ at 25°C and 2.86 ± 0.01 at 60°C) due to the formation of an uncharged aqueous calcium-uranyl-carbonate-complex ($\text{Ca}_2\text{UO}_2(\text{CO}_3)_3(\text{aq})$) which does not sorb onto OPA. Modelling metal retention data onto OPA with PHREEQC reveals a very good agreement with most measurement results. At elevated temperatures, PHREEQC modelling could not be performed due to lack of data, especially for possible secondary minerals. The observed increased K_d values at elevated temperature revealed in this study might be assumed advantageous for the safe storage of HLW in a future repository.

1. Introduction

The safe disposal of high-level radioactive waste (HLW) in deep geological formations is assumed to be the best way of providing adequate protection for humans and the environment. For the long-term isolation of HLW, low permeability and high sorption capacity of the geological barrier are very important. Different rock formations to host a repository play a major role in different concepts for HLW storage (Bradbury and Baeyens, 2003; Ericsson, 1999; Hoth et al., 2007; Hummel and Schneider, 2005; Nagra, 2002). Clay formations could be part of the repository's natural barrier protecting the environment from the possibility of radionuclide contamination (Altmann, 2008; Madsen,

1998; McCombie and Smith, 2005). The long-lived actinides uranium, neptunium, plutonium, americium and curium determine the radio-toxicity of the waste for a long time period and are of special interest for long-term safety considerations (Kersting et al., 1999; Morss, 1986).

The mobility of radionuclides in the geosphere can be affected by a wide variety of parameters such as temperature, pH value, composition of the pore water (PW) or natural clay organic matter (NOM) like humic matter or small clay organic molecules such as acetate or lactate (Chautard et al., 2015; Courdouan et al., 2007, 2008; Joseph et al., 2013b; Kautenburger and Beck, 2008). Humic matter includes a large and heterogeneous group of metal complexing macromolecules of different molecular weight and charge density, with complex and

* Corresponding author. WASTE group, Inorganic Chemistry, Saarland University, Campus C 4 1, 66123, Saarbrücken, Germany
 E-mail address: r.kautenburger@mx.uni-saarland.de (R. Kautenburger).

<https://doi.org/10.1016/j.apgeochem.2019.104404>

Received 13 December 2018; Received in revised form 25 July 2019; Accepted 15 August 2019

Available online 15 August 2019

0883-2927/ © 2019 Elsevier Ltd. All rights reserved.

difficultly identifiable structures (Piccolo, 2002), whereas clay organic matter such as lactate can form small and mobile metal-NOM complexes. Most studies on metal mobility in clay are performed at room temperature and low ionic strength of the used aqueous solution or in inert background electrolytes. However, due to the heat, released from HLW, the surrounding of the containments will heat up to temperatures of 60–100 °C. Consequently, the host rock's properties and according to this, the retention behaviour of the radionuclides released by a damaged waste container (Bauer et al., 2005) can be altered. Furthermore PW with high ionic strength (which is e.g. the case for many potential geological sites in Germany) contains especially bi- or higher valent cations which can compete for the same binding sites on clay as the radionuclides.

One aim of our study was to elucidate the interaction of metal ions with NOM such as humic acid (HA) or lactate influencing their retention onto OPA as a potential host rock for a prospective HLW repository. Most studies dealing with the interaction between metal ions and clay are focused on experiments using only one pure clay mineral such as kaolinite (Kautenburger and Beck, 2010; Křepelová et al., 2006; Verma and Mohapatra, 2016), illite (Bradbury and Baeyens, 2011; Marques Fernandes et al., 2015) or montmorillonite (Norrfors et al., 2016; Tournassat et al., 2018) with a well-defined composition and structure so that the interaction of metal ions with the clay became relatively ordinary to determine and the modelling of the behaviour could usefully be carried out.

Nearly all sorption studies for U(VI) retention onto clay rock formations such as OPA are performed only at one constant pH value (Appelo et al., 2010; Fröhlich et al., 2012; Joseph et al., 2011) or in a relatively small pH range mostly from 3 to 8 or up to a maximum of pH 10. Additionally, mostly inert background electrolytes such as sodium chloride or perchlorate were used (Comarmond et al., 2016; Hartmann et al., 2008; Joseph et al., 2013a). At these conditions, sorption experiments can be easily performed but are far from relevant conditions for a HLW disposal in clay. In a potential HLW disposal, a great part of the technical barrier consists of cementitious material, due to the alteration of concrete in contact with PW an equilibrium pH range between 10 and 12 will be reached. For these conditions almost no results on the retention behaviour of metal ions are available, especially in the presence of PW with high ionic strength due to leaching processes of the technical, geotechnical as well as natural barriers. Due to the pyrite content in the OPA for example, protons can be released during the surface oxidation process of pyrite which can cause a decreasing of the pH range (Bonnisel-Gissingner et al., 1998). It is rarely researched how the contrary pH processes interact under natural conditions in a disposal (temperature, bacteria and redox components like copper canisters) (King, 2013), therefore knowing the sorption behaviour over a large pH range is also of fundamental interest.

Typically used methods for the determination of metal-organic species combine different chemical separation techniques, e.g. extraction methods, ion exchange, ultrafiltration or precipitation, with sensitive detection methods such as nuclear magnetic resonance spectroscopy, soft X-ray spectromicroscopy (STXM) or mass spectrometry (Hahn et al., 2017; Kim et al., 2005; McDonald et al., 2004; Plaschke et al., 2004; Wröbel et al., 2003). For quantitative elemental speciation analysis some separation techniques like high performance liquid chromatography (HPLC), ion- (IC) or gas chromatography (GC) have been used in combination with element-selective detectors like inductively coupled plasma (ICP), optical emission (OES) and mass spectrometry (MS) or atomic absorption spectroscopy (AAS) (Harrison and Rapsomanikis, 1989; Popp et al., 2010; Vanhaecke and Degryse, 2012). Within the present study capillary electrophoresis (CE) was hyphenated via a homemade interface to inductively coupled plasma-mass spectrometry (ICP-MS). This established and optimised CE-ICP-MS-system was used to investigate the speciation of metal ions with NOM (Hein et al., 2014, 2017; Kautenburger et al., 2014, 2017; Michalke, 2016; Möser et al., 2012; Timerbaev, 2010).

Herein, we present results for the binary system metal (Eu(III) and U(VI)) - clay (OPA), and also results for the ternary system consisting of the used metals and OPA in the presence of NOM (humic acid or lactate) under varying experimental conditions. With highly standardised laboratory experiments (batch techniques) (Kautenburger and Beck, 2008) we investigated the retention (sorption experiments) of the lanthanide europium, and the actinide uranium as U(VI) (as uranyl ion) onto OPA to get a basic understanding for the complex binary and ternary system. Especially, the influence of geochemical parameters such as temperature (25–60 °C), pH value (2–12), ionic strength (0.01 or 0.4 mol L⁻¹) or the presence of different competing metal cations on the metal mobility in the absence (binary system) or presence of NOM are investigated (Hein et al., 2017). The log K_d values of the metals have been determined for their interaction with OPA. From temperature depended sorption data of Eu(III) and U(VI), thermodynamic parameters (sorption enthalpy ΔH and sorption entropy ΔS) were calculated. PHREEQC modelling was performed to investigate the correspondence of the measured data with theoretical calculations for the complex mineral mixture of the natural OPA. In addition, CE-ICP-MS speciation (Hein et al., 2014; Kautenburger et al., 2006, 2017) was used to analyse the retention of Eu(III) in the presence of NOM in the ternary system. This herein presented work is based on results from the BMWi (German Federal Ministry for Economic Affairs and Energy) research project (grant no. 02E10196) "Migration of Lanthanides and Uranium in Natural Clay Formations - From Mineral Suspensions to Compact Clays" (Kautenburger et al., 2012).

2. Experimental

2.1. Materials

2.1.1. Chemicals and standards

All chemicals for the preparation of the used background solutions (see also Table 1) were of p.a. quality or better (analytical quality, e.g. suprapure or emsure) and were obtained from Merck (Darmstadt, Germany). Milli-Q (Millipore Gradient A10, Merck, Darmstadt, Germany) deionised water (18.2 M Ω cm) was used to prepare all solutions. The single element standards of Cs, Eu, U, Ca and Ho were CertiPUR® ICP-elemental solution standards (1000 mg L⁻¹) obtained from Merck (Darmstadt, Germany). For dilution of the elemental standards 0.01 M NaClO₄ (SP) was used. For adjusting the pH value, perchloric acid (70%, p.a.) and NaOH (30%, p.a.) from Merck (Darmstadt, Germany) were applied. The humic acid (AHA) used in the experiments is commercially available from Aldrich (St. Louis, USA; AHA sodium salt) and was purified as described in the literature (Kim et al., 1990). Lactate was purchased from Aldrich (St. Louis, USA; No. 490040, sodium L-lactate-3-¹³C solution). For the CE experiments, an electrolyte buffer of 0.1 mol L⁻¹ acetic acid and 0.01 mol L⁻¹ sodium acetate solution was used. Argon 5.0 (99.999%, Praxair Deutschland GmbH, Düsseldorf, Germany) was used as plasma gas for the ICP-MS (see Table 2).

Table 1
Chemical composition and properties of the used PW according to Pearson (1998)

Compound	M [g mol ⁻¹]	Conc. [g L ⁻¹]
NaCl	58.44	12.38
Na ₂ SO ₄	142.04	2.00
NaHCO ₃	84.01	0.04
KCl	74.55	0.12
MgCl ₂ ·6H ₂ O	203.30	3.46
CaCl ₂ ·2H ₂ O	147.02	3.79
SrCl ₂ ·6H ₂ O	266.62	0.14
Ionic strength	0.4 mol L ⁻¹	
pH value	7.6	

Table 2
Operating parameters of the CE System and the ICP-MS.

CE	Beckman Coulter P/ACE® MDQ
Capillary	fused silica (Polymicro Technologies)
Capillary dimensions/ Temperature	74 µm ID, 362 mm o.d., 80 cm length/25 °C
CE electrolyte buffer	0.1 mol L ⁻¹ acetic acid, 0.01 mol L ⁻¹ sodium acetate, pH 3.7
Internal Standard (IS) CE buffer	200 ppb (1.5·10 ⁻⁶ mol L ⁻¹) Cs
DC-voltage/current	+ 30 kV/16–18 µA
Interface	homemade
Spray-chamber	Cinnabar cyclonic, chilled at 4 °C, 20 mL volume
Nebuliser	MicroMist 50 µl, type AR35-1-FM005E, 2.8 bar
Make-up fluid	2% HNO ₃ , 2.4·10 ⁻⁵ mol L ⁻¹ (4 ppb) Ho (IS), 112 µl min ⁻¹
ICP-MS	Agilent 7500cx
RF-power	1600 W
Cooling/auxiliary gas	15.0/0.9 L min ⁻¹
Dwell times/Repetition	300 ms per mass/3 times
Samples	
Ca, Cs, Eu, Ho, U ICP- standards	CertiPUR® (Merck), diluted in 10 mM HClO ₄
Analysed isotopes	⁴⁴ Ca, ¹³³ Cs, ¹⁵³ Eu, ¹⁶⁵ Ho, ²³⁸ U
NOM	Purified AHA (Aldrich H1,675-2, technical grade), Lactate (Aldrich 490040, sodium L-lactate-3- ¹³ C solution, 45–55% (w/w) in H ₂ O)
Ion strength:	0.01 mol L ⁻¹ (sodium perchlorate; SP) 0.4 mol L ⁻¹ (OPA pore water; PW)
pH-range	2–12

2.1.2. OPA and PW

The solid phase used in this study was OPA, which was obtained from a drill core (BHE-24/1) from the Mont Terri rock laboratory (Switzerland). A detailed characterisation of BHE-24/1 is given by Joseph et al. (2011). The core sample was stored in containers with 0.5 bar Ar overpressure. The aerobic clay homogenate was obtained by milling the clay to a fine-grained powder with a particle size smaller than 500 µm. The ungrounded OPA represents a well characterised clay with a cation exchange capacity (CEC) ranging from 10.2 to 16.0 meq/100 g (Nagra, 2002), the CEC of the used clay sample BHE-24/1 was determined to 10.5 ± 0.5 meq/100 g by the use of the compulsive exchange method (Sumner et al., 1994). The milled clay used in our study was characterised by X-ray diffraction (XRD) phase analysis (Siemens D5000, OED) followed by data interpretation with the TOPAS software (version 2.1, Bruker AXS, Delft, The Netherlands). For a better simulation of the natural conditions, a synthetic PW referring to the natural PW of OPA was prepared according to Pearson (1998) and used in our experiments. The chemical composition is shown in Table 1.

2.2. Methods

The experiments were carried out under ambient atmosphere (pCO₂ = 10^{-3.5} bar) at room temperature (25 °C) or at elevated temperatures (40 or 60 °C). The experiments were performed in centrifuge tubes (VWR PP-SuperClear 15 ml, VWR International GmbH, Darmstadt, Germany) which have low metal adsorption properties. The determined wall sorption for Eu(III) and U(VI) is less than 5% (for metal concentrations > 100 ng L⁻¹) in the analysed pH-range.

2.2.1. Batch experiments

For all sorption experiments an equivalent amount of 4 g L⁻¹ OPA was used (each experiment was made by weighing 40 mg OPA into a tube filled up with the adequate solution to a final volume of 10 ml). After 72 h preconditioning the clay with 9 ml of the corresponding background solution (0.01 mol L⁻¹ NaClO₄ to buffer the ionic strength or 0.4 mol L⁻¹ PW), the remaining components (metal standard stock solution and in the ternary system NOM) were added. The pH was adjusted by addition of diluted HClO₄ or NaOH (suprapure, Merck,

Darmstadt, Germany) to values between 2 and 12, according to the experiments. Depending on the pH value, a readjusting was necessary several times. After reaching a stable pH value, the tube was filled up to 10 mL with background solution. The samples were mixed for at least 72 h end over end in a tube rotator, which could be tempered from 20 to 100 °C (Stuart SB3 Tube Rotator, Cole-Parmer Ltd, UK) with all components present to reach a state of balance. The samples were prepared at 25 and 60 °C for preconditioning and sorption step, respectively. Afterwards the tubes were centrifuged at 12800 g (10000 rpm) for 10 min. Samples were taken from the supernatant solutions. Diluted and acidified solutions (pH value was adjusted to pH < 1 with HNO₃ suprapure) were prepared with an internal standard (10 mg L⁻¹ Ho stock solution) to determine the metal content in the solution by ICP-MS.

2.2.2. Sorption experiments

The sorption experiments at different temperature in the binary system were performed with 1.97·10⁻⁶ mol L⁻¹ Eu(III) (0.3 mg L⁻¹) or 0.42·10⁻⁶ mol L⁻¹ uranyl (0.1 mg L⁻¹) in the appropriate solution at pH 5 and 7.6 under identical conditions, respectively. In this process, possible differences in sorption or desorption behaviour between the metal ions can be observed adequately. In all cases, an ionic strength of 0.01 mol L⁻¹ when using NaClO₄ (SP) or 0.4 mol L⁻¹ in PW was present in the solutions. Additionally, in preliminary experiments the evaporation of the samples during the preparation time was studied and is negligible, when the samples were sealed with parafilm.

The sorption edges were determined at pH values ranging from 2 to 12 (pH ± 0.1) with a metal concentration of 0.42·10⁻⁶ mol L⁻¹ (U (VI)) or 1.97·10⁻⁶ mol L⁻¹ (Eu(III)) with 0.01 mol L⁻¹ sodium chloride solution and PW as background solutions. The correct pH value was adjusted by ultra-pure HClO₄ and NaOH (0.1 or 1.0 mol L⁻¹). The batch sorption experiments in the ternary system were prepared in synthetic PW in a final volume of 10 mL at the natural equilibrium pH value of 7.6. After the preconditioning Eu(III) concentrations of 3.29·10⁻⁶ mol L⁻¹ (0.5 mg L⁻¹) and 32.9·10⁻⁶ mol L⁻¹ (5 mg L⁻¹), as well as U(VI) concentrations of 2.10·10⁻⁶ mol L⁻¹ (0.5 mg L⁻¹) and 10.5·10⁻⁶ mol L⁻¹ (2.5 mg L⁻¹) were added. Additionally, 25 mg L⁻¹ NOM (AHA or lactate) were added before the equilibration, too. Afterwards all samples were treated like it is described in section 2.2.1.

As the initial metal concentration [Me]_{init} is known and the non-adsorbed metal [Me]_{eq} is measured, it is possible to calculate the amount of adsorbed metal [Me]_{clay}. Filtering (e.g. ultrafiltration) of the samples was not performed due to some drawbacks (for example low metal recovery rates due to filter adsorption and disturbed sorption/desorption equilibrium) which were found out in a previous study (Kautenburger and Beck, 2007). The retention of the metal ions onto OPA in percent and the distribution coefficient (K_d) were determined by using the following equations:

$$\text{Retention [\%]} = 100 \% \times \left(1 - \frac{[\text{Me}]_{\text{eq}}}{[\text{Me}]_{\text{init}}} \right) \quad (1)$$

$$K_d = \frac{[\text{Me}]_{\text{clay}}}{[\text{Me}]_{\text{eq}}} \quad (2)$$

with concentrations given in mol L⁻¹. The distribution coefficient K_d (in L·kg⁻¹) is given by the amount of sorbed metal [Me]_{clay} onto clay (in mol·kg⁻¹) divided by equilibrium concentration [Me]_{eq} (in mol L⁻¹).

2.2.3. Van't Hoff plot

To specify sorption as a thermodynamic process it is necessary to discuss enthalpy (ΔH) and entropy (ΔS) values. These can be determined from a Van't Hoff plot. In order to calculate such thermodynamic parameters, we performed a set of sorption experiments at three different temperatures (25, 40 and 60 °C) for U(VI) and Eu(III) onto OPA, respectively. The procedure is the same as for the sorption experiments described above. The calculated ln K_d values were plotted

against $1/T$ and with the linear relation of the values using the following equation:

$$\ln K_d = -\frac{\Delta H}{RT} + \frac{\Delta S}{R} \quad (3)$$

the slope m of the graph is $-\frac{\Delta H}{R}$ and the intercept b is $\frac{\Delta S}{R}$, where R represents the ideal gas constant ($8314 \frac{J}{mol \cdot K}$). With this mathematical correlation, a calculation of enthalpy and entropy is possible.

2.2.4. Speciation of Eu(III) in the ternary system

For the speciation of Eu(III) via CE-ICP-MS, sample preparation was similar to the sorption experiments in the ternary system. Due to the relatively high salinity of PW (0.4 mol L^{-1}), CE-ICP-MS measurements were not possible and therefore, the supernatant after the sorption experiments with PW could not be used for CE-ICP-MS measurements. Therefore, samples with $3.29 \cdot 10^{-6} \text{ mol L}^{-1}$ Eu(III) (0.5 mg L^{-1}) and 25 mg L^{-1} HA in 0.01 mol L^{-1} NaClO_4 at pH 5 and 7.6 were prepared. After the equilibration time and the phase separation, the samples were filtered ($0.45 \mu\text{m}$ syringe filter, Minisart, Sartorius, Germany). Afterwards the Eu(III) speciation in the supernatant was carried out with CE-ICP-MS as described subsequently (section 2.3.2.).

2.3. Instrumentation

2.3.1. ICP-MS

An Agilent 7500cx ICP-MS (Santa Clara, USA) with collision cell was used for the isotope measurements. Detailed analytical conditions are given in Table 2 and in the literature (Hein et al., 2014; Kautenburger et al., 2017; Möser et al., 2012). As internal standard ^{165}Ho was used in all experiments to correct for instrumental instability. All samples were measured by ICP-MS in triplicate (RSD values are in the range of 0.3–3.9%).

2.3.2. CE-ICP-MS

Capillary electrophoresis (CE, Beckman Coulter P/ACE MDQ) was hyphenated by a homemade interface to ICP-MS to obtain a high sensitivity for the speciation of Eu(III) with AHA. To couple CE to ICP-MS a fused-silica CE-capillary was fitted into a MicroMist 50 μl nebuliser with a Cinnabar cyclonic spray chamber (chilled to 4°C). A make-up fluid including $2.4 \cdot 10^{-8} \text{ mol L}^{-1}$ (4 ppb) Ho as internal standard was combined with the flow from the capillary (where Cs is used as CE flow marker) within the interface to obtain a flow rate high enough to maintain a continuous nebulisation. Best results for the Eu(III) calibration and separation of the different Eu-AHA species were obtained with a CE electrolyte buffer consisting of 0.1 mol L^{-1} acetic acid and 0.01 mol L^{-1} sodium acetate. In this buffer solution $1.5 \cdot 10^{-6} \text{ mol L}^{-1}$ Cs were added to control the flow of the background electrolyte (BGE) from the CE-capillary towards the ICP-MS. The Cs signal of each CE run shows three typical so-called system Eigenpeaks whose meaning is explained elsewhere (Kautenburger et al., 2014). In the optimised CE-ICP-MS-system a DC-voltage of 30 kV and additionally a pressure of 3 psi (20.7 kPa) was applied to obtain the best separation conditions for the uncomplexed and NOM complexed Eu(III). Detailed analytical conditions are given in Table 2.

2.4. Modelling

The geochemical computer code PHREEQC Interactive v3.4 (Parkhurst and Appelo, 2013) in combination with Nuclear Energy Agency (OECD/NEA, 2007) thermodynamic database was used for calculation and modelling of Eu(III) and U(VI) speciation and retention onto OPA. Electrostatic surface complexation models (containing electrical double layer correction terms in the mass law for adsorption reactions) for illite were selected from existing literature (Table S2 in the supporting information) to describe our experimental data for Eu(III)

Table 3

Mineral analyses (range of nine samples) of OPA for shaly facies (Pearson et al., 2003) in comparison to XRD main phase analysis ($n = 5$) of the used OPA sample BHE-24/1 from Mont Terri.

Mineral	OPA Range ($n = 9$) [wt%] (Pearson et al., 2003)	Mont Terri BHE-24/1 Average \pm SD ^a [wt%] This work
Kaolinite-Serpentine	15–33 ^b	36.5 ± 2.7
Illite	16–40	25.1 ± 1.3
Illite/Smectite	5–20	
Chlorite	4–20	< 5
Silica	6–24	22.9 ± 1.1
Calcite	5–28	13.2 ± 1.2
Dolomite/Ankerite	0.2–2	nd ^c
Siderite	1–4	nd
K-feldspar	1–3.1	< 4
Pyrite	0.6–2	1.5 ± 0.2
Organic carbon	< 0.1–1.5	nd

^a SD: standard deviation (1 σ).

^b Determined as kaolinite.

^c Not detected.

and U(VI) retention onto OPA (Bradbury and Baeyens, 2011). A component-additivity approach was then used, based on minerals shown in Table 3 and including atmospheric gases such as oxygen and carbon dioxide, with respect to secondary minerals formed due to different pH values, to predict Eu(III) and U(VI) retention behaviour onto OPA. According to Davis and Kent (1990) a reference surface site density of 2.31 sites/nm² was used for calculation. For the complex mineral mixture in OPA, the PHREEQC code can simulate metal retention to different mineral components while also providing their specific surface charges.

3. Results and discussion

3.1. Characterisation of the used OPA

The XRD phase analysis results of the used OPA followed by data interpretation with TOPAS software are given in Table 3. Kaolinite, illite, silica and calcite could be determined as main phases with amounts in the range of 13.2–25.1%, respectively, while only 1.5% pyrite is present. Illite and illite/smectite mixed layers were determined as sum to be $25.1 \pm 1.3\%$. Chlorite and Feldspar could not be found. These determined values are in a good agreement with the mineralogical composition from shaly facies of OPA from Mont Terri (Pearson et al., 2003) as well as XRD data from similar OPA (Nagra, 2002; Van Loon and Jakob, 2005).

3.2. Analysis of the binary system metal – clay

3.2.1. Sorption experiments onto OPA in SP and PW

3.2.1.1. Influence of the preconditioning and sorption temperature on Eu(III) sorption. The sorption experiments initially started at 25°C in SP with an ionic strength of 0.01 mol L^{-1} and in PW ($I = 0.4 \text{ mol L}^{-1}$), respectively. The $\log K_d$ values for pH values of 5 and 7.6 are given in Table 4. At pH 7.6 a considerably higher retention for Eu(III) onto OPA in SP as well as in PW can be determined in comparison to pH 5. For both pH values at 25°C the Eu(III) sorption in SP solution is significantly higher ($\log K_d = 4.81 \pm 0.19$ at pH 7.6 and 2.71 ± 0.17 at pH 5) than in PW ($\log K_d = 3.47 \pm 0.04$ at pH 7.6 and 1.96 ± 0.11 at pH 5) probably due to the competing cations in the PW which displace the lanthanides from the binding sites on OPA.

As known from the literature (Bradbury et al., 2005; Tertre et al., 2006) the sorption of Eu(III) (present as Eu^{3+} as the sole significant species) onto clay minerals at lower pH values is dominated by outer-sphere complexes especially via a cation exchange mechanism on the

Table 4

Log K_d values ($L \cdot kg^{-1}$) and standard deviations (\pm SD) of Eu(III) ($1.97 \cdot 10^{-6} \text{ mol L}^{-1}$) sorption onto OPA in SP and PW at pH 5 or 7.6 and 25 °C or 60 °C. The first temperature refers to the preconditioning, the second to the sorption experiment.

Eu(III)	SP pH 7.6			PW pH 7.6			SP pH 5			PW pH 5		
Temp.	log K_d	+SD	-SD									
25/25 °C	4.81	0.13	0.19	3.35	0.03	0.04	2.71	0.11	0.17	1.96	0.05	0.11
60/60 °C	5.94	0.07	0.08	4.85	0.07	0.08	4.50	0.25	0.63	2.64	0.07	0.09
60/25 °C	5.56	0.09	0.11	3.76	0.06	0.07	3.26	0.05	0.07	2.07	0.09	0.13

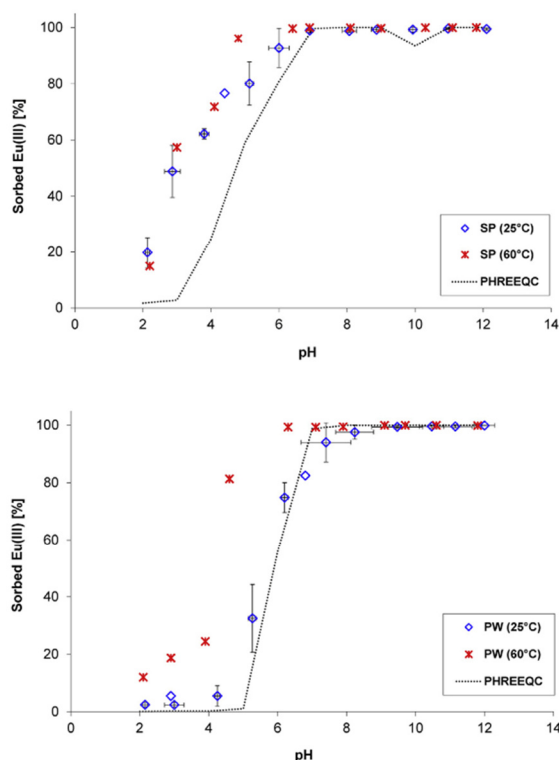


Fig. 1. Sorption edges of Eu(III) ($1.97 \cdot 10^{-6} \text{ mol L}^{-1}$) onto OPA at two different temperatures (25 or 60 °C) in SP and PW compared to the PHREEQC modelled sorption edges at 25 °C. Average values and error bars (\pm SD) from repeated experiments at 25 °C.

permanently charged surface sites (planar sites) whereas with increasing pH values the formation of inner-sphere Eu(III) surface complexes begin to become more important. Due to the stronger competitive effect of cations, particularly in the lower pH region, the sorption edge at higher ionic strength is shifted to higher pH values (pH 5–6) as seen in Fig. 1 for PW in comparison to SP (pH 4–5). These results are in a good agreement with those obtained by other studies using time-resolved laser fluorescence spectroscopy (TRLFS) for the sorption of Eu(III) onto different single clay minerals such as smectite and kaolinite (Stumpf et al., 2002) or illite and montmorillonite (Schnurr et al., 2015).

To check the influence of higher temperature on the sorption of Eu(III) onto OPA, we repeated these sorption experiments (as described in section 2.2.1 and 2.2.2) at elevated preconditioning and sorption temperature (60 °C). The sorption differences especially at pH 7.6 between 25 and 60 °C are shown by the log K_d values (Table 4) of the different sorption experiments where the increasing sorption at higher temperature is clearly visible. Also at pH 5 and 60 °C, a higher sorption can

be observed in comparison to 25 °C. In PW (pH 5) the sorption increases from log $K_d = 1.96 \pm 0.11$ at 25 °C to log $K_d = 2.64 \pm 0.09$ at 60 °C. In SP (pH 5) the sorption increases from log $K_d = 2.71 \pm 0.17$ at 25 °C to log $K_d = 4.50 \pm 0.63$ at 60 °C. These observations could be an effect of a structural modification of the clay, due to a higher amount of negatively charged OPA surface, modification of the metal speciation or a temperature effect of the sorption (endothermic reaction) (Schott et al., 2012). At pH 7.6 the calculated log K_d values for Eu(III) sorption onto OPA are more than one order of magnitude higher for all examined conditions. In PW (pH 7.6) the sorption increases from log $K_d = 3.35 \pm 0.04$ at 25 °C to log $K_d = 4.85 \pm 0.08$ at 60 °C and is in good agreement with the values determined by Schott et al. (2012) where the log K_d values increased from 4.77 ± 0.046 (25 °C) to 5.54 ± 0.06 (50 °C). In SP (pH 7.6) the sorption increases from log $K_d = 4.81 \pm 0.19$ at 25 °C to log $K_d = 5.94 \pm 0.08$ at 60 °C. These results for pH 7.6 show the same trend as presented by Tertre et al. for Eu(III) onto the single clay mineral montmorillonite (Tertre et al., 2005, 2006). The log K_d values of Tertre et al. increase from 4.6 (25 °C) to 5.4 (80 °C) in 0.025 mol L^{-1} SP and from 3.6 (25 °C) to 5.1 (80 °C) in another PW with an ionic strength of 0.5 mol L^{-1} , and are (within the estimated uncertainty of about ± 0.4 log unit) in good agreement with the log K_d values of our results.

To gain more insight into this finding it was analysed whether the increased sorption process at higher temperature is reversible. We therefore preconditioned the samples at 60 °C, and let the sorption process take place at 25 °C. As a result of the preconditioning step of 60 °C a higher sorption of Eu(III) on OPA compared to 25 °C preconditioning can be observed. For example, in PW (pH 7.6 and 25 °C) the sorption increases from log $K_d = 3.35 \pm 0.04$ at 25 °C preconditioning to log $K_d = 3.76 \pm 0.07$ for preconditioning at 60 °C. In SP (pH 7.6 and 25 °C) the sorption of Eu(III) onto OPA increases from log $K_d = 4.81 \pm 0.19$ at 25 °C preconditioning to log $K_d = 5.56 \pm 0.11$ at a preconditioning temperature of 60 °C. This result shows a partial reversibility of the effect of preconditioning at high temperatures on sorption. At higher temperature the clay surface is evidently modified by the solution and new potential negatively charged binding sites occur where Eu(III) can sorb additionally (Tertre et al., 2006).

3.2.1.2. Influence of pH and temperature on sorption edges of Eu(III). The previous results show the influence of two pH values 5 and 7.6 and temperature on the Eu(III) retention onto OPA. In the next step, the influence of both parameters on metal retention over a wide pH range (2–12) is compared in SP and PW as background solutions. The experiments in this section are performed at 25 °C in three independent series. Regarding the sorption edges of Eu(III) onto OPA in SP at pH from 2 to 12 (Fig. 1) the retention is very high (95–100%) for pH > 7, but decreases noticeably from 94% (pH 7) to only around 20% at pH 2. At low pH, protons and cations from clay dissolution compete with the Eu(III) cations for sorption sites and interfere with their retention. Additionally, the used pH values are partially under the pH_{pzc} (pH at which the surface charge of the clay switches from positive to negative) of OPA. At pH < pH_{pzc} a positively charged clay surface is available which leads to an electrostatic repulsion of the cations. The main clay minerals in OPA are kaolinite with a pH_{pzc} of 4–5 and illite

with a pH_{pzc} of 2.5 (Ismadji et al., 2015). With pH values under 5 we can assume that the negative surface charge of the OPA decreases with the increasing amount of protons and other cations until a positive charged surface is available which leads to a repulsion of Eu(III). These effects are slightly overestimated by PHREEQC modelling of the Eu(III) sorption in this pH region, perhaps due to the complex dissolution characteristics of the OPA minerals and additionally due to the different sorption capacities of the heterogeneous mineral mixture in OPA. Cations originally present in the PW further compete with the Eu(III) cations. The sorption in PW (Fig. 1) already decreases at pH values lower than 7–8 and then primarily at 25 °C even with a steeper decline than in the SP case. At very low pH values (< pH 4) virtually no sorption is observable especially at 25 °C. These experimental results can be modelled significantly better by the use of PHREEQC due to the active involvement of the higher PW ionic strength into the model parameters.

As a result, the modelled sorption edge of Eu(III) in PW is consistent with the experimental results with both shifted from pH 4–6 in SP background solution to pH 5–6 in PW. However, to the best of our knowledge, the Eu(III) sorption edge onto OPA at elevated temperature (60 °C) cannot be adequately modelled by PHREEQC with the actually available data sets. Especially in PW for pH < 7 higher temperatures favour higher Eu(III) sorption due to the fact that the sorption onto OPA is an endothermic reaction as shown via Van't Hoff plot (section 3.2.1.4.). Therefore, at 60 °C a significantly higher Eu(III) sorption compared to 25 °C onto OPA can be observed. This effect can be caused by a structural change of the clay minerals at higher temperature resulting in an increase in the layer charge as determined for smectite (Bauer et al., 2005).

At higher temperature, an additional increase of the Eu(III) sorption onto a montmorillonite fraction of MX80 bentonite could be observed at higher ionic strength in the background solution (Tertre et al., 2005), which is in good agreement with our results found for PW in comparison to SP. At pH > 7 a high retention of Eu(III) onto OPA could be observed (> 95%) in all cases. In this pH range are only relatively small differences in the retention behaviour (retention of Eu(III) decreased from about 99% in SP to about 95% in PW) between SP and PW can be observed. The retention is dominated by precipitation of $Eu_2(CO_3)_3 \cdot 3H_2O$ and $NaEu(CO_3)_2 \cdot 5H_2O$ according to the modelled data. However, the $\log K_d$ values (Table 4) reflect the decreasing sorption in the presence of competing cations from the PW well ($I = 0.4 \text{ mol L}^{-1}$) compared to 0.01 mol L^{-1} SP (e.g. at pH 7.6 the $\log K_d$ decreased from 4.81 ± 0.19 in SP to 3.35 ± 0.04 in PW for 25 °C).

3.2.1.3. Influence of pH and temperature on sorption edges of U(VI). The experiments in this section are performed at 25 °C in two independent series. In comparison to the sorption edges of Eu(III) the results for the uranyl species U(VI) are very different. For U(VI) a first sorption maximum can be observed between pH 4 and 6, and a second one between pH 9 and 11 as seen in Fig. 2. In the near-neutral pH range (pH 6–9) the uranyl sorption shows a minimum due to the formation of a neutral aquo complex $Ca_2UO_2(CO_3)_3(aq)$ (Endrizzi and Rao, 2014; Wu et al., 2016) which does not sorb onto OPA. In SP the formation of the $Ca_2UO_2(CO_3)_3(aq)$ complex depends on the amount of dissolved calcite (a component of OPA), whereby leaching experiments of OPA with MilliQ water revealed Ca^{2+} concentrations about $2\text{--}3 \cdot 10^{-3} \text{ mol L}^{-1}$ in the neutral pH range (Kautenburger, 2011). In PW a higher amount of the $Ca_2UO_2(CO_3)_3(aq)$ complex is formed due to the excess of calcium ions (about 0.04 mol L^{-1} , 0.026 mol L^{-1} of which originated from the PW composition) in PW. This is in agreement with the species distribution observed in PHREEQC model, where $3 \cdot 10^{-10} \text{ mol L}^{-1}$ of $Ca_2UO_2(CO_3)_3(aq)$ are formed in SP. However, in PW about $2 \cdot 10^{-7} \text{ mol L}^{-1}$ of the neutral complex was predicted, due to the high amount of Ca^{2+} in the medium. As a consequence, the U(VI) sorption onto OPA at pH 7.6 in PW ($\log K_d = 1.38 \pm 0.34$) is considerably lower in comparison to SP ($\log K_d = 2.17 \pm 0.21$) as also shown in

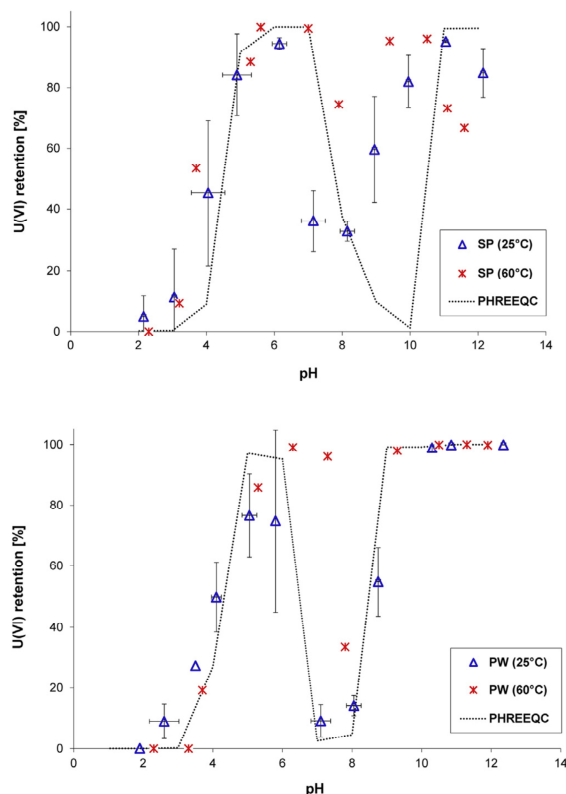


Fig. 2. Sorption edges of U(VI) ($0.42 \cdot 10^{-6} \text{ mol L}^{-1}$) onto OPA at two different temperatures (25 or 60 °C) in SP compared to PW compared to the PHREEQC modelled sorption edges at 25 °C. Average values and error bars (\pm SD) from repeated experiments at 25 °C.

Table 5

$\log K_d$ values ($L \cdot kg^{-1}$) and standard deviations (\pm SD) of U(VI) ($0.42 \cdot 10^{-6} \text{ mol L}^{-1}$) sorption onto OPA in SP and PW at 7.6 and 25 °C or 60 °C. The first temperature refers to preconditioning, the second to the sorption experiment. The $\log K_d$ values in brackets are deduced from a diffusion experiments under similar conditions (Joseph et al., 2013a).

U(VI)	SP pH 7.6			PW pH 7.6		
Temp.	$\log K_d$	+SD	-SD	$\log K_d$	+SD	-SD
25/25 °C	2,17	0,14	0,21	1,38 (1.40)	0,19 (0.05)	0,34 (0.06)
60/60 °C	2,86	0,01	0,01	2,10 (2.40)	0,11 (0.08)	0,16 (0.10)

Table 5.

Furthermore, the uranyl ion forms negatively charged complexes with carbonate (e.g. $UO_2(CO_3)_3^{4-}$ as dominating species at pH > 8) and hydroxide (e.g. $(UO_2)_2CO_3(OH)_3^-$ in the near-neutral pH range) in solution. At pH 4–6 these complexes can be neutralised and precipitated by cations present in the PW in addition to the cation exchange reaction of uranyl on the permanently charged surface sites. In the near-neutral pH range where $Ca_2UO_2(CO_3)_3(aq)$ is the dominating species in solution it was assumed in the literature that $Ca_2UO_2(CO_3)_3(aq)$ also adsorbs to some extent on the mineral surface (Hartmann et al., 2008; Joseph et al., 2011). At pH > 9 sorption of U(VI) increases again by the formation of ternary hydroxo surface complexes on the clay mineral fraction of OPA (Hartmann et al., 2008).

With increasing temperature, the sorption increases over a wide pH range especially in the neutral pH region in both background solutions.

This increasing sorption at 60 °C could be an effect of a structural change of the clay surface and/or of the uranyl speciation. For example, the metal aquo complex ($\text{Ca}_2\text{UO}_2(\text{CO}_3)_3(\text{aq})$) may be less stable at higher temperatures. The comparison of the modelled U(VI) retention on OPA especially in the PW background solution at 25 °C shows a very good agreement with the measured U(VI) retention values. For evaluated temperatures as e.g. the used 60 °C in this study the PHREEQC model parameters must be adapted to better reflect the experimentally determined retention data. Altogether modelling metal retention onto real clay samples as complex mixtures of many different types of minerals by the use of PHREEQC is a promising approach to predict the retention behaviour of Eu(III) as well as U(VI) onto clay formations such as OPA.

The U(VI) sorption and the $\log K_d$ values (Table 5) increase at higher temperatures in both background solutions (from 2.17 ± 0.21 at 25 °C to 2.86 ± 0.01 at 60 °C in SP as well as from 1.38 ± 0.34 to 2.10 ± 0.16 in PW, respectively). The determined values for U(VI) sorption onto OPA in SP are in the same range as the sorption data for uranium onto OPA ($\log R_d$ between 2.0 and 2.5 L kg^{-1}), which were determined by Hartmann et al. (2008). The $\log K_d$ values for U(VI) in PW are in very good agreement with the calculated $\log K_d$ values of diffusion experiments in compacted OPA under otherwise comparable conditions (Joseph et al., 2013a) as shown in Table 5. In PW a higher amount of the ternary ($\text{Ca}_2\text{UO}_2(\text{CO}_3)_3(\text{aq})$) complex is formed in comparison to SP which could be attributed to the additional calcium concentration present in the PW (Hartmann et al., 2008; Joseph et al., 2013a). The sorption values of U(VI) are significant lower in comparison to those of Eu(III) but they are in the same order of magnitude as determined in other studies (Amayri et al., 2016; Joseph et al., 2011).

3.2.1.4. Calculation of thermodynamic values via Van't Hoff plot. To validate the results of the sorption experiments, thermodynamic parameters (sorption enthalpy and entropy) for the Eu(III) and U(VI) sorption onto OPA are calculated via a Van't Hoff plot (see section 2.2.3) where sorption data at 25, 40 and 60 °C were used. In Fig. 3 the Van't Hoff plots of the sorption of Eu(III) and uranyl (U(VI)) in PW at pH 7.6 are shown.

As a result, for Eu(III), a sorption enthalpy of $71 \pm 2 \text{ kJ mol}^{-1}$ and an entropy of $259 \pm 5 \text{ J K}^{-1} \cdot \text{mol}^{-1}$ were calculated. These values are in a good agreement with the findings of a study by Schott et al. ($\Delta H = 52 \pm 4 \text{ kJ mol}^{-1}$, $\Delta S = 267 \pm 12 \text{ J K}^{-1} \cdot \text{mol}^{-1}$) (Schott et al., 2012). The values for uranium are with $\Delta H = 93 \pm 3 \text{ kJ mol}^{-1}$ and $\Delta S = 273 \pm 8 \text{ J K}^{-1} \cdot \text{mol}^{-1}$ in a similar range. These values are similar to those reported for Np(V) sorption onto OPA ($\Delta H = 80 \pm 16 \text{ kJ mol}^{-1}$ and $\Delta S = 278 \pm 48 \text{ J K}^{-1} \cdot \text{mol}^{-1}$) (Fröhlich et al., 2012). The endothermic sorption reaction of both metal ions can be explained by an increase of the negative OPA surface charge as shown for Na-montmorillonite (Tertre et al., 2006) or changes in the

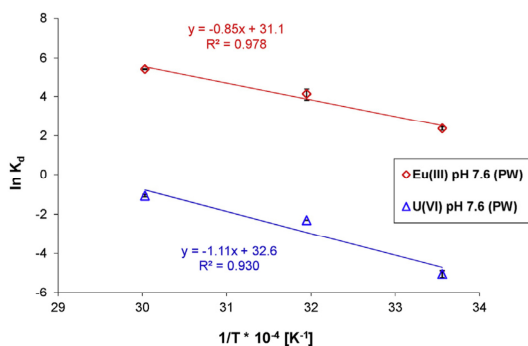


Fig. 3. Linear fit of the Van't Hoff plot of the sorption of Eu(III) and U(VI) onto OPA in PW at a pH value of 7.6 (298, 313 and 333 K).

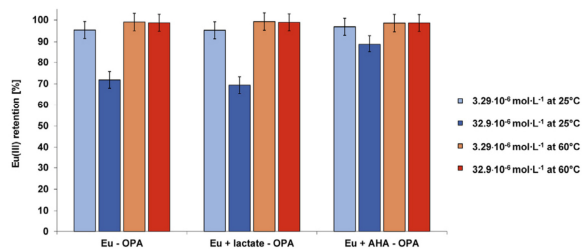


Fig. 4. Retention of $3.29 \cdot 10^{-6} \text{ mol L}^{-1}$ (0.5 mg L^{-1}) and $32.9 \cdot 10^{-6} \text{ mol L}^{-1}$ (5.0 mg L^{-1}) Eu(III) onto OPA in PW ($I = 0.4 \text{ mol L}^{-1}$, pH 7.6) at different temperatures (25 and 60 °C) in the presence or absence of NOM (lactate, AHA). Maximum uncertainty of 3.9% is assumed for all measurements.

hydration shell of the metal ions as described for Cm(III) (Lindqvist-Reis et al., 2005).

3.3. Analysis of the ternary system metal – clay – NOM

3.3.1. Sorption experiments in the ternary system

For the experiments in the ternary system we used the equilibrium pH value of OPA PW (pH 7.6) and PW as background solution. So, conditions close to nature were selected with both parameters.

In Fig. 4 the sorption of $3.29 \cdot 10^{-6} \text{ mol L}^{-1}$ and $32.9 \cdot 10^{-6} \text{ mol L}^{-1}$ Eu(III) at different temperatures (25 and 60 °C) and with different organic compounds (lactate, AHA) is shown ($\log K_d$ values are given in Table S5). With $3.29 \cdot 10^{-6} \text{ mol L}^{-1}$ of Eu(III) no significant differences between lactate and AHA could be observed and also no relevant effect of NOM on the Eu(III) sorption onto OPA could be found. This result is in contrast to the findings of Schott et al. (2012) where the presence of small ligands (citrate and tartrate) decreased the Eu(III) ($2 \cdot 10^{-9} \text{ mol L}^{-1}$) sorption significantly from 95% to 44% in the presence of 5 mM citrate or at least to 53% in the presence of 5 mM tartrate at 25 °C, respectively (Schott et al., 2012). The different results are probably due to the different conditions used, in particular the ratio of Eu(III)/NOM. In our study, the Eu(III)/NOM ratio is 0.02 and 0.2, respectively, in contrast to the ratio of $4 \cdot 10^{-7}$ (Schott et al., 2012). It can be assumed that the influence of NOM on the retention correlates with the Eu(III)/NOM complex stability as the formation constants $\log \beta_{110}$ of the 1 : 1 complexes demonstrate: Eu(III)-lactate: 2.51 ± 0.13 (Barkleit et al., 2014), Eu-tartrate: 4.2 ± 0.3 (Acker et al., 2011), Eu-citrate: 7.5 ± 0.2 (Heller et al., 2011). Hence, a significant influence of lactate on the Eu(III) retention onto OPA is not expected due to the comparable low complex stability, and with the small excess of lactate used in our experiments. For Eu(III) complexation with humic acids from different sources a comparison of the complex stability is rather difficult as it consists of a complex mixture of different substances. In previous studies a complex stability $\log \beta$ (assuming a 1:1 complex) in the range of about 5–7 could be calculated (Hahn et al., 2017; Kautenburger et al., 2014, 2017). Regarding the experiments at increasing temperature (25 → 60 °C), the sorption increases insignificantly.

At higher europium concentration ($32.9 \cdot 10^{-6} \text{ mol L}^{-1}$) some differences compared to 25 °C can be observed. At 25 °C, the sorption is significantly reduced compared to the lower concentration. A considerably higher amount (nearly up to 25%) of the binding sites of the clay is occupied by Eu(III), further sorption is limited due to the restricted loading capacity ($\text{CEC}_{\text{OPA(BHE-24/1)}} = 10.5 \pm 0.5 \text{ meq/100 g}$) of the clay. The humic acid in the ternary system contributes to an increase in the retention behaviour of the metal ions. In SP solution negatively charged europium humate complexes would be formed. In PW the contained cations neutralise the humates and the europium-humate compounds precipitate. The mobilisation of europium decreases in comparison to the results in the binary system or in

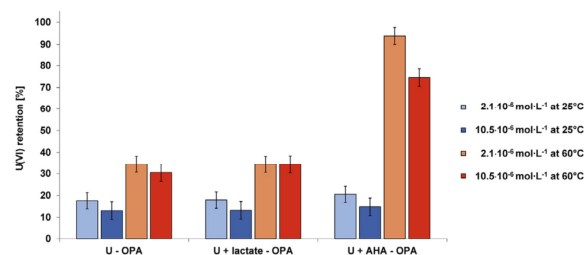


Fig. 5. Retention of $2.1 \cdot 10^{-6} \text{ mol L}^{-1}$ (0.5 mg L^{-1}) and $10.5 \cdot 10^{-6} \text{ mol L}^{-1}$ (2.5 mg L^{-1}) U(VI) onto OPA in PW ($I = 0.4 \text{ mol L}^{-1}$, $\text{pH} = 7.6$) at different temperatures (25 and 60 °C) in the presence or absence of NOM (lactate, AHA). Maximum uncertainty of 3.7% is assumed for all measurements.

comparison to the results with lactate. At 60 °C no differences between the organic compounds are visible. The sorption in the binary and ternary systems is almost complete, the presence of AHA does not contribute to an increase of sorption.

The results with uranyl are very different compared with the results with Eu(III). Fig. 5 shows the results of the sorption experiments with uranyl at 25 and 60 °C in the presence of lactate as well as of AHA compared to the binary system in the absence of NOM (log K_d values are given in Table S5). At 25 °C the retention of the uranyl cations is very low. Eu(III) is sorbed up to 69% and more, uranium only between 10 and 20%. This effect can be explained by the formation of the neutral ($\text{Ca}_2\text{UO}_2(\text{CO}_3)_3(\text{aq})$) complex, which does not adsorb onto OPA, so U(VI) stays mobile in solution. No differences can be seen between the binary and ternary system and the different organic compounds. The formation of the aquo-complex is dominant. These findings are in a good agreement with other studies of U(VI) retention onto OPA in the presence or absence of HA where the presence of HA in the pH region from 7.5 to 10 has also no significant influence on the U(VI) sorption onto OPA (Joseph et al., 2011, 2013a). The authors also attributed this finding to the neutral ($\text{Ca}_2\text{UO}_2(\text{CO}_3)_3(\text{aq})$) complex which dominates the U(VI) speciation in this pH region.

At higher temperature (60 °C), especially in the presence of humic acid, the sorption increases strongly in comparison to the sorption in the presence of lactate or without organic compounds. With humic acid and for uranium concentrations of $2.1 \cdot 10^{-6} \text{ mol L}^{-1}$ the sorption increases from 34% to 94%, with $10.5 \cdot 10^{-6} \text{ mol L}^{-1}$ of uranium the sorption increases from 30% (absence of organics) to 34% (presence of lactate) and 75% in the presence of humic acid. Some explanations are possible. The speciation of uranyl in PW has probably changed with increasing temperature, the neutral aquatic complex may not be stable at higher temperatures or the uranyl forms a complex with AHA and precipitates due to the high concentration of the PW cations. Additionally, humic acids show a strong reduction behaviour (Peretyazhko and Sposito, 2006) in dependence of pH and ionic strength and are known to reduce hexavalent actinides such as NpO_2^{2+} and PuO_2^{2+} (Ivanov et al., 2012). At room temperature and atmospheric conditions in most experiments no reduction of U(VI) to U(IV) is observed (Markich, 2002) but it is not completely ruled out that a reduction of U(VI) with HA at 60 °C is possible. The reduced U(IV) would precipitate as UO_2 (Mühr-Ebert et al., 2019) and pretend a higher sorption in presence of HA at 60 °C.

3.3.2. Speciation of the Eu(III)-humate complexes in presence of OPA

The influence of NOM on the sorption of europium onto OPA was analysed in section 3.3.1. These results illustrate differences in the sorption behaviour but the exact Eu(III)-humate species are unknown. By the use of CE-ICP-MS speciation technique the determination of these species in solution is possible. In Fig. 6 the electropherograms of the Eu(III)-humate speciation in presence of OPA are presented. In comparison with the experiments without clay (Kautenburger et al.,

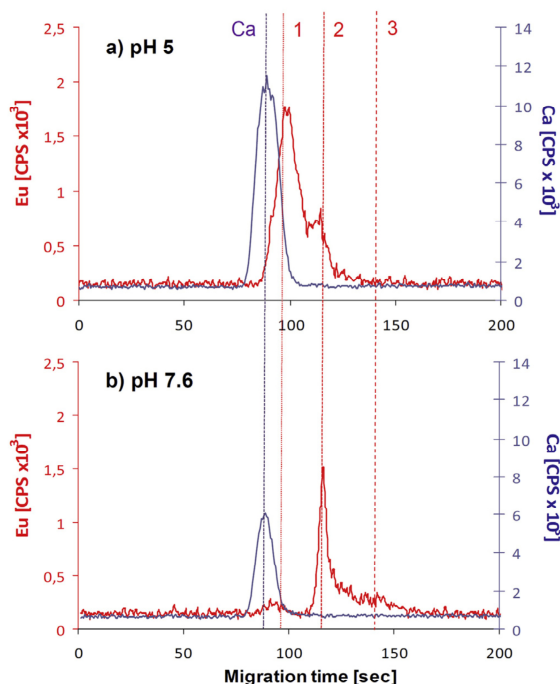


Fig. 6. Comparison of the CE-ICP-MS electropherograms in the ternary system with Eu(III) ($3.29 \cdot 10^{-6} \text{ mol L}^{-1}$), AHA (25 mg L^{-1}) and OPA (4 g L^{-1}) in SP (^{153}Eu signal red, ^{44}Ca signal blue); a) at pH 5; b) at pH 7.6. ^{44}Ca signal is added as migration time reference marker. Auxiliary lines are added for better comparing of the species in both electropherograms. (For interpretation of the references to colour in this figure legend, the reader is referred to the Web version of this article.)

2014, 2017) less than 10% of europium was recovered caused by the high sorption of Eu(III) onto the clay. There are some differences between the experiments at pH 5 and 7.6. At pH 5 mainly two Eu(III) species are visible. The first fraction (denoted as 1 in Fig. 6) is the non-NOM-complexed Eu(III) which is complexed by acetate during the CE separation (a detailed description is given in a previous study (Kautenburger et al., 2006)). During the CE separation and due to the applied voltage (30 kV) the Eu(III) dissociates out of the humate complex and migrates as Eu(III)-acetate complex slower to the cathode than the “free” europium. The second fraction (denoted as 2) represents the weakly NOM bound Eu(III). The existence of strong binding sites (denoted as 3) for Eu(III) cannot be verified in this case. When adjusting the pH, some minerals, such as calcite, dissolved. The released cations (e.g. Ca(II)) neutralise the negatively charged Eu(III)-humate species in the background solution followed by the precipitation of $\text{Ca(II)-Eu(III)-humate}$. Eu(III) is no more detectable by CE-ICP-MS.

In comparison to pH 5 the Eu(III) speciation has changed at pH 7.6. The first Eu(III) fraction (1) is very small, almost not visible. The second fraction (2) shows here the largest peak whereas from fraction 3 (AHA strong bonding sites for Eu(III)) trace levels can be detected at most. For pH 7.6, the recovery of the whole europium species in the solution decreased to only 3%. The different speciation of Eu(III) with AHA at pH 7.6 compared to pH 5 could possibly be caused by a structural change of the AHA at pH 5, e.g. due to a higher degree of protonation. This was also observed in previous CE-ICP-MS studies (Kautenburger and Beck, 2007; Kautenburger et al., 2014) where complex stability constants (log β) for Eu(III) and AHA in the pH region of 3–10 were determined. In the range between pH 5–10 the calculated log β values are in the same order of magnitude (6.06 ± 0.05), and only in the

acidic pH range ≤ 3 a relevant decrease of the Eu(III) complexation by AHA could be observed. But in this study, in the presence of OPA also other cations such as Ca^{2+} from clay dissolution or anions such as carbonates and hydroxides in addition to the AHA are available to interact with Eu(III). At pH 7.6, the concentration of non-AHA-complexed Eu(III) (1) as well as the Ca^{2+} concentration in solution decreases significantly from pH 5 to 7.6 most probably due to the precipitation as a ternary species such as Ca(II)-Eu(III)-humate or -carbonate.

4. Conclusions

In order to gain more insights into the complex system consisting of OPA, metal ions and NOM in our experiments ICP-MS was used for elemental trace analysis. For the retention experiments of the metals onto OPA batch experiments are performed to study the influence of different geochemical parameters (pH, ionic strength, temperature and NOM) in clay as a potential host rock for a HLW disposal. For the speciation of Eu(III) with AHA in solution, capillary electrophoresis was hyphenated with ICP-MS.

Retention measurements by the use of the batch technique are performed to estimate $\log K_d$ values for different geochemical conditions. The retention of the metal ions strongly depends on the pH value, the presence of competing cations, temperature and NOM. At a pH value of pH 7.6, which is the equilibrium pH value of the OPA PW, the sorption of Eu(III) is nearly complete in contrast to the sorption of the uranyl ion due to the formation of an uncharged aqueous calcium-uranyl-carbonate-complex ($\text{Ca}_2\text{UO}_2(\text{CO}_3)_3(\text{aq})$) which does not sorb onto OPA. These findings are confirmed by modelling the data with PHREEQC. Overall, modelling metal retention data onto the natural OPA as a complex mixture of different mineral phases proved to be a promising approach which should be further developed by adding more experimental data into the databases. The positive effect of higher temperature on metal sorption onto OPA may be helpful in the storage of high-level radioactive waste. In our experiments with higher temperatures up to 60 °C, the retention of the analysed metals onto OPA increases strongly.

The presence of NOM in the sorption experiments with OPA in PW shows a differentiated picture. The presence of lactate shows no significant influence on the metal retention in OPA whereas humic acid in the ternary system contributes to an increase in the retention behaviour of both metal ions. For Eu(III) it is notably at 25 °C (for 60 °C the Eu(III) retention is complete in all experiments), and especially for U(VI) at 60 °C (from about 30% to more than 75%). The OPA pore water contains cations, which neutralise the negatively charged metal-humates. The metal-humate compounds precipitate, particularly at higher temperatures (60 °C). The metal speciation in the ternary system analysed by CE-ICP-MS shows that in solution only a very low amount (< 3%) of the initial Eu(III) concentration can be recovered due to the high sorption capacity of OPA for Eu(III) in combination with the precipitation e.g. as a ternary species. Particularly at pH 7.6, the CE-ICP-MS speciation showed that the remaining dissolved Eu(III) exists only as negatively charged Eu(III)-humate complexes.

Acknowledgement

This work was carried out within the BMWi (German Federal Ministry for Economic Affairs and Energy, Germany) project "Migration of Lanthanides and Uranium in Natural Clay Formations - From Mineral Suspensions to Compact Clays". The authors therefore thank the BMWi for financial support (grant no. 02E10196, 02E10991 and 02E11415D) and our project partners for the kind collaboration.

Appendix A. Supplementary data

Supplementary data to this article can be found online at <https://doi.org/10.1016/j.apgeochem.2019.104404>.

References

- Acker, M., Müller, M., Barkleit, A., Taut, S., 2011. UV-Vis study of complexation of trivalent Am, Eu and Nd by tartaric acid at low metal concentrations. In: HZDR-IRC Annual Report 2010. Helmholtz-Zentrum Dresden-Rossendorf.
- Altmann, S., 2008. 'Geochemical research: a key building block for nuclear waste disposal safety cases. J. Contam. Hydrol. 102, 174–179.
- Amayri, S., Fröhlich, D.R., Kaplan, U., Trautmann, N., Reich, T., 2016. Distribution coefficients for the sorption of Th, U, Np, Pu, and Am on opalinus clay. Radiochim. Acta 104, 33–40.
- Appelo, C.A.J., Van Loon, L.R., Wersin, P., 2010. Multicomponent diffusion of a suite of tracers (HTO, Cl, Br, I, Na, Sr, Cs) in a single sample of Opalinus Clay. Geochem. Cosmochim. Acta 74, 1201–1219.
- Barkleit, A., Kretschmar, J., Tsushima, S., Acker, M., 2014. Americium (III) and europium (III) complex formation with lactate at elevated temperatures studied by spectroscopy and quantum chemical calculations. Dalton Trans. 43, 11221–11232.
- Bauer, A., Rabung, T., Claret, F., Schäfer, T., Buckau, G., Fanghänel, T., 2005. Influence of temperature on sorption of europium onto smectite: the role of organic contaminants. Appl. Clay Sci. 30, 1–10.
- Bonnissel-Gissing, P., Alnot, M., Ehrhardt, J.-J., Behra, P., 1998. Surface oxidation of pyrite as a function of pH. Environ. Sci. Technol. 32, 2839–2845.
- Bradbury, M., Baeyens, B., 2003. Far Field Sorption Data Bases for Performance Assessment of a High-Level Radioactive Waste Repository in an Undisturbed Opalinus Clay Host Rock. Paul Scherrer Institut.
- Bradbury, M., Baeyens, B., Geckeis, H., Rabung, T., 2005. Sorption of Eu (III)/Cm (III) on Ca-montmorillonite and Na-illite. Part 2: surface complexation modelling. Geochem. Cosmochim. Acta 69, 5403–5412.
- Bradbury, M.H., Baeyens, B., 2011. Predictive sorption modelling of Ni(II), Co(II), Eu (III), Th(IV) and U(VI) on MX-80 bentonite and Opalinus Clay: a "bottom-up" approach. Appl. Clay Sci. 52, 27–33.
- Chautard, C., Ritt, A., De Windt, L., Libert, M., Stammose, D., 2015. Characterization of low-molecular-weight organic acids isolated from the Toarcian argillite pore water (Tournemire site, France). Compt. Rendus Geosci. 347, 77–83.
- Comarmond, M.J., Stuedtner, R., Stockmann, M., Heim, K., Müller, K., Brendler, V., Payne, T.E., Foersterdorf, H., 2016. The sorption processes of U(VI) onto SiO_2 in the presence of phosphate: from binary surface species to precipitation. Environ. Sci. Technol. 50, 11610–11618.
- Courdouan, A., Christl, I., Meylan, S., Wersin, P., Kretschmar, R., 2007. Characterization of dissolved organic matter in anoxic rock extracts and in situ pore water of the Opalinus Clay. Appl. Geochem. 22, 2926–2939.
- Courdouan, A., Christl, I., Rabung, T., Wersin, P., Kretschmar, R., 2008. Proton and divalent metal cation binding by dissolved organic matter in the opalinus clay and the callovo-oxfordian formation. Environ. Sci. Technol. 42, 5985–5991.
- Davis, J.A., Kent, D.B., 1990. Mineral-water interface geochemistry. In: Hochella, M.F., White, A.F. (Eds.), Reviews in Mineralogy. Mineralogical Society of America, Washington, DC, pp. 177–260.
- Endrizzi, F., Rao, L., 2014. Chemical speciation of uranium (VI) in marine environments: complexation of calcium and magnesium ions with $[(\text{UO}_2)(\text{CO}_3)_3]^{4-}$ and the effect on the extraction of uranium from seawater. Chem. Eur. J. 20, 14499–14506.
- Ericsson, L.O., 1999. Geoscientific R&D for high level radioactive waste disposal in Sweden — current status and future plans. Eng. Geol. 52, 305–317.
- Fröhlich, D.R., Amayri, S., Drebert, J., Reich, T., 2012. Influence of temperature and background electrolyte on the sorption of neptunium(V) on Opalinus Clay. Appl. Clay Sci. 69, 43–49.
- Hahn, R., Hein, C., Sander, J.M., Kautenburger, R., 2017. Complexation of europium and uranium with natural organic matter (NOM) in highly saline water matrices analysed by ultrafiltration and inductively coupled plasma mass spectrometry (ICP-MS). Appl. Geochem. 78, 241–249.
- Harrison, R.M., Rapsomanikis, S., 1989. Environmental Analysis Using Chromatography Interfaced with Atomic Spectroscopy. E. Horwood.
- Hartmann, E., Geckeis, H., Rabung, T., Lützenkirchen, J., Fanghänel, T., 2008. Sorption of radionuclides onto natural clay rocks. Radiochim. Acta Int. J. Chem. Aspect. Nucl. Sci. Technol. 96, 699–707.
- Hein, C., Sander, J.M., Kautenburger, R., 2014. Speciation via hyphenation metal speciation in geological and environmental samples by CE-ICP-MS. J. Anal. Bioanal. Tech. 5 (6), 1000225.
- Hein, C., Sander, J.M., Kautenburger, R., 2017. New approach of a transient ICP-MS measurement method for samples with high salinity. Talanta 164, 477–482.
- Heller, A., Barkleit, A., Foersterdorf, H., Bernhard, G., 2011. Luminescence and absorption spectroscopic study on the complexation of europium(III) with citric acid. In: HZDR-IRC Annual Report 2010. Helmholtz-Zentrum Dresden-Rossendorf.
- Hoth, P., Wirth, H., Reinhold, K., Bräuer, V., Krull, P., Feldrappe, H., 2007. In: Rohstoffe, B.F.G.u. (Ed.), Untersuchung und Bewertung von Tongesteinsformationen. Endlagerung radioaktiver Abfälle in tiefen geologischen Formationen Deutschlands, Berlin/Hannover.
- Hummel, W., Schneider, J.W., 2005. Safety of nuclear waste repositories. Chimia Int. J. Chem. 59, 909–915.
- Ismadji, S., Soetaredjo, F.E., Ayucitra, A., 2015. Clay Materials for Environmental Remediation. Springer.
- Ivanov, P., Griffiths, T., Bryan, N.D., Bozhikov, G., Dmitriev, S., 2012. The effect of humic acid on uranyl sorption onto bentonite at trace uranium levels. Journal of Environmental Monitoring 14 (11), 2968–2975.
- Joseph, C., Schmeide, K., Sachs, S., Brendler, V., Geipel, G., Bernhard, G., 2011. Sorption of uranium(VI) onto Opalinus Clay in the absence and presence of humic acid in Opalinus Clay pore water. Chem. Geol. 284, 240–250.

- Joseph, C., Stockmann, M., Schmeide, K., Sachs, S., Brendler, V., Bernhard, G., 2013a. Sorption of U(VI) onto opalinus clay: effects of pH and humic acid. *Appl. Geochem.* 36, 104–117.
- Joseph, C., Van Loon, L.R., Jakob, A., Steudtner, R., Schmeide, K., Sachs, S., Bernhard, G., 2013b. Diffusion of U(VI) in opalinus clay: influence of temperature and humic acid. *Geochem. Cosmochim. Acta* 109, 74–89.
- Kautenburger, R., 2011. Batch is bad? Leaching of Opalinus clay samples and ICP-MS determination of extracted elements. *J. Anal. At. Spectrom.* 26, 2089–2092.
- Kautenburger, R., Beck, H.P., 2007. Complexation studies with lanthanides and humic acid analyzed by ultrafiltration and capillary electrophoresis-inductively coupled plasma mass spectrometry. *J. Chromatogr. A* 1159, 75–80.
- Kautenburger, R., Beck, H.P., 2008. Waste disposal in clay formations: influence of humic acid on the migration of heavy-metal pollutants. *ChemSusChem* 1, 295–297.
- Kautenburger, R., Beck, H.P., 2010. Influence of geochemical parameters on the sorption and desorption behaviour of europium and gadolinium onto kaolinite. *J. Environ. Monit.* 12, 1295–1301.
- Kautenburger, R., Hein, C., Sander, J.M., Beck, H.P., 2014. Influence of metal loading and humic acid functional groups on the complexation behavior of trivalent lanthanides analyzed by CE-ICP-MS. *Anal. Chim. Acta* 816, 50–59.
- Kautenburger, R., Möser, C., Beck, H.P., 2012. Migration of lanthanides and uranium in natural clay formations - from mineral Suspensions to Compact clays. In: Marquardt, C. (Ed.), *Interaction and Transport of Actinides in Natural Clay Rock with Consideration of Humic Substances and Clay Organic Compounds*, KIT-7633. KIT Scientific Publishing, pp. 806.
- Kautenburger, R., Nowotka, K., Beck, H.P., 2006. Online analysis of europium and gadolinium species complexed or uncomplexed with humic acid by capillary electrophoresis-inductively coupled plasma mass spectrometry. *Anal. Bioanal. Chem.* 384, 1416–1422.
- Kautenburger, R., Sander, J.M., Hein, C., 2017. Europium (III) and Uranium (VI) complexation by natural organic matter (NOM): effect of source. *Electrophoresis* 38, 930–937.
- Kersting, A., Efur, D., Finnegan, D., Rokop, D., Smith, D., Thompson, J., 1999. Migration of plutonium in ground water at the Nevada Test Site. *Nature* 397, 56–59.
- Kim, H.-J., Baek, K., Kim, B.-K., Yang, J.-W., 2005. Humic substance-enhanced ultrafiltration for removal of cobalt. *J. Hazard Mater.* 122, 31–36.
- Kim, J.-I., Buckau, G., Li, G., Duschner, H., Psarros, N., 1990. Characterization of humic and fulvic acids from Gorleben groundwater. *Fresenius J. Anal. Chem.* 338, 245–252.
- King, F., 2013. Container materials for the storage and disposal of nuclear waste. *Corrosion* 69, 986–1011.
- Křepelová, A., Sachs, S., Bernhard, G., 2006. Uranium (VI) sorption onto kaolinite in the presence and absence of humic acid. *Radiochim. Acta* 94, 825–833.
- Lindqvist-Reis, P., Klenze, R., Schubert, G., Fanghänel, T., 2005. Hydration of Cm³⁺ in aqueous solution from 20 to 200 °C. A time-resolved laser fluorescence spectroscopy study. *J. Phys. Chem. B* 109, 3077–3083.
- Madsen, F., 1998. Clay mineralogical investigations related to nuclear waste disposal. *Clay Miner.* 33, 109–129.
- Markich, S.J., 2002. Uranium speciation and bioavailability in aquatic systems: an overview. *The Scientific World Journal* 2, 707–729.
- Marques Fernandes, M., Vér, N., Baeyens, B., 2015. Predicting the uptake of Cs, Co, Ni, Eu, Th and U on argillaceous rocks using sorption models for illite. *Appl. Geochem.* 59, 189–199.
- McCombie, C., Smith, P., 2005. Multibarrier systems in geological disposal programmes. In: *Proceedings-10th International Conference on Environmental Remediation and Radioactive Waste Management*. ICEM, pp. 1634–1639.
- McDonald, S., Bishop, A.G., Prenzler, P.D., Robards, K., 2004. Analytical chemistry of freshwater humic substances. *Anal. Chim. Acta* 527, 105–124.
- Michalke, B., 2016. Capillary electrophoresis-inductively coupled plasma mass spectrometry. *Capill. Electrophor.: Methods Protoc.* 167–180.
- Morss, L., 1986. In: Katz, J.J., Seaborg, G.T., Morss, L.R. (Eds.), *The Chemistry of the Actinide Elements*, vol. 2 Chapman & Hall, London.
- Möser, C., Kautenburger, R., Philipp Beck, H., 2012. Complexation of europium and uranium by humic acids analyzed by capillary electrophoresis-inductively coupled plasma mass spectrometry. *Electrophoresis* 33, 1482–1487.
- Mülr-Ebert, E.L., Wagner, F., Walther, C., 2019. Speciation of uranium: Compilation of a thermodynamic database and its experimental evaluation using different analytical techniques. *Applied geochemistry* 100, 213–222.
- Nagra, 2002. Projekt Opalinuston-Synthese der geowissenschaftlichen Untersuchungsergebnisse, Entsorgungsnachweis für abgebrannte Brennelemente, verglaste hochaktive sowie langlebige mittelaktive Abfälle. Nagra Wettingen, Switzerland.
- Norrfors, K.K., Marsac, R., Bouby, M., Heck, S., Wold, S., Lützenkirchen, J., Schäfer, T., 2016. Montmorillonite colloids: II. Colloidal size dependency on radionuclide adsorption. *Appl. Clay Sci.* 123, 292–303.
- OECD/NEA, 2007. *Chemical Thermodynamics of Solid Solutions of Interest in Radioactive Waste Management*, Chemical Thermodynamics. OECD Publishing, Paris. <https://doi.org/10.1787/9789264033191-en>.
- Parkhurst, D.L., Appelo, C., 2013. Description of Input and Examples For Phreeqc Version 3: A Computer Program for Speciation, Batch-Reaction, One-Dimensional Transport, and Inverse Geochemical Calculations. US Geological Survey.
- Pearson, F., 1998. Opalinus Clay Experimental Water: A1 Type, Version 980318. Paul Scherrer Institut, Villigen, Switzerland.
- Pearson, F., Arcos, D., Bath, A., Boisson, J., Fernández, A., Gaebler, H., Gaucher, E., Gauschi, A., Griffault, L., Hernan, P., 2003. Mont Terri project-Geochemistry of Water in the Opalinus Clay Formation at the Mont Terri Rock Laboratory-Synthesis Report. Federal Office for Water and Geology, FOWG.
- Peretyazhko, T., Sposito, G., 2006. Reducing capacity of terrestrial humic acids. *Geoderma* 137 (1–2), 140–146.
- Piccolo, A., 2002. The supramolecular structure of humic substances: a novel understanding of humus chemistry and implications in soil science. In: *Advances in Agronomy*. Academic Press, pp. 57–134.
- Plaschke, M., Rothe, J., Denecke, M.A., Fanghänel, T., 2004. Soft X-ray spectromicroscopy of humic acid europium (III) complexation by comparison to model substances. *J. Electron. Spectrosc. Relat. Phenom.* 135, 53–62.
- Popp, M., Hann, S., Koellensperger, G., 2010. Environmental application of elemental speciation analysis based on liquid or gas chromatography hyphenated to inductively coupled plasma mass spectrometry—a review. *Anal. Chim. Acta* 668, 114–129.
- Schnurr, A., Marsac, R., Rabung, T., Lützenkirchen, J., Geckeis, H., 2015. Sorption of Cm (III) and Eu (III) onto clay minerals under saline conditions: batch adsorption, laser-fluorescence spectroscopy and modeling. *Geochem. Cosmochim. Acta* 151, 192–202.
- Schott, J., Acker, M., Barkleit, A., Brendler, V., Taut, S., Bernhard, G., 2012. The influence of temperature and small organic ligands on the sorption of Eu (III) on Opalinus Clay. *Radiochim. Acta Int. J. Chem. Aspect. Nucl. Sci. Technol.* 100, 315–324.
- Stumpf, T., Bauer, A., Coppin, F., Fanghänel, T., Kim, J.-I., 2002. Inner-sphere, outer-sphere and ternary surface complexes: a TRIFS study of the sorption process of Eu (III) onto smectite and kaolinite. *Radiochim. Acta* 90, 345–349.
- Sumner, M.E., de Ramos, L., Kukier, U., 1994. Compulsive exchange method for determining soil exchange capacities: proposed time and labor saving modifications. *Commun. Soil Sci. Plant Anal.* 25, 567–572.
- Tertre, E., Berger, G., Castet, S., Loubet, M., Giffaut, E., 2005. Experimental sorption of Ni²⁺, Cs⁺ and Ln³⁺ onto a montmorillonite up to 150 °C. *Geochem. Cosmochim. Acta* 69, 4937–4948.
- Tertre, E., Berger, G., Simoni, E., Castet, S., Giffaut, E., Loubet, M., Catalette, H., 2006. Europium retention onto clay minerals from 25 to 150 °C: experimental measurements, spectroscopic features and sorption modelling. *Geochem. Cosmochim. Acta* 70, 4563–4578.
- Timerbaev, A.R., 2010. Inorganic species analysis by CE – an overview for 2007–2008. *Electrophoresis* 31, 192–204.
- Tournassat, C., Tinnacher, R.M., Grangeon, S., Davis, J.A., 2018. Modeling uranium(VI) adsorption onto montmorillonite under varying carbonate concentrations: a surface complexation model accounting for the spillover effect on surface potential. *Geochem. Cosmochim. Acta* 220, 291–308.
- Van Loon, L., Jakob, A., 2005. Evidence for a second transport porosity for the diffusion of tritiated water (HTO) in a sedimentary rock (Opalinus clay-OPA): application of through-and out-diffusion techniques. *Transp. Porous Media* 61, 193–214.
- Vanhaecke, F., Degryse, P., 2012. *Isotopic Analysis: Fundamentals and Applications Using ICP-MS*. John Wiley & Sons.
- Verma, P.K., Mohapatra, P.K., 2016. Effect of different complexing ligands on europium uptake from aqueous phase by kaolinite: batch sorption and fluorescence studies. *RSC Adv.* 6, 84464–84471.
- Wrobel, K., Sadi, B.B., Wrobel, K., Castillo, J.R., Caruso, J.A., 2003. Effect of metal ions on the molecular weight distribution of humic substances derived from municipal compost: ultrafiltration and size exclusion chromatography with spectrophotometric and inductively coupled plasma-MS detection. *Anal. Chem.* 75, 761–767.
- Wu, W., Priest, C., Zhou, J., Peng, C., Liu, H., Jiang, D.-e., 2016. Solvation of the Ca₂UO₂(CO₃)₂ complex in seawater from classical molecular dynamics. *J. Phys. Chem. B* 120, 7227–7233.

SUPPORTING INFORMATION

Insights into the retention behaviour of europium (III) and uranium (VI) onto Opalinus Clay influenced by pore water composition, temperature, pH and organic compounds

Ralf Kautenburger*, Kristina Brix, Christina Hein

WASTe group, Inorganic Chemistry, Saarland University,
Campus C4 1, 66123 Saarbrücken, Germany

*Corresponding author. Tel.: +49 681 302 2171; fax: +49 681 302 70655

E-mail address: r.kautenburger@mx.uni-saarland.de (R. Kautenburger)

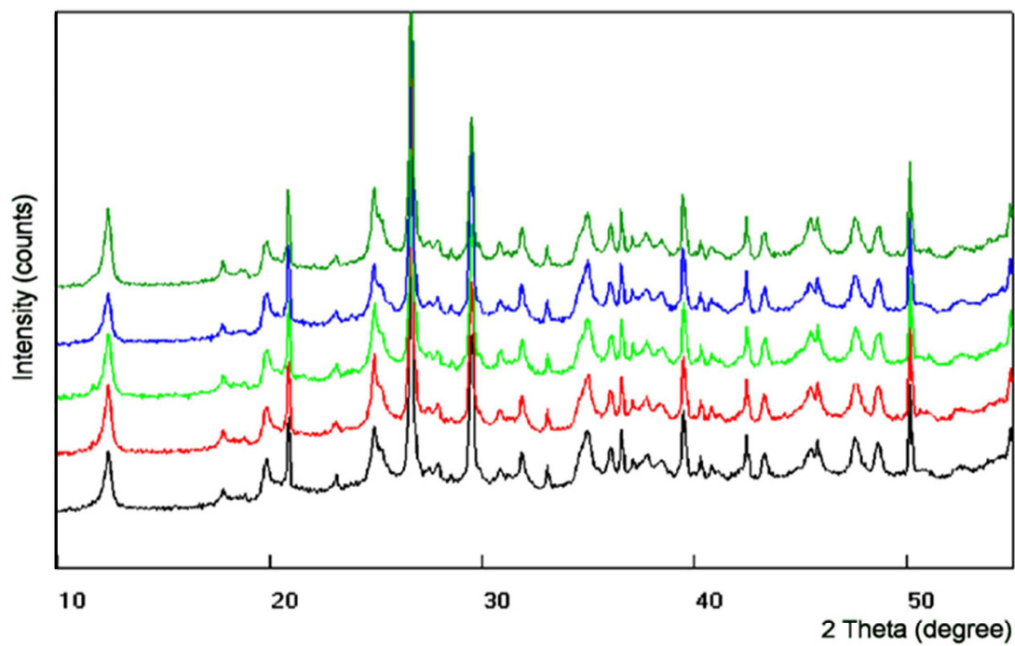
Address:

PD Dr. Ralf Kautenburger

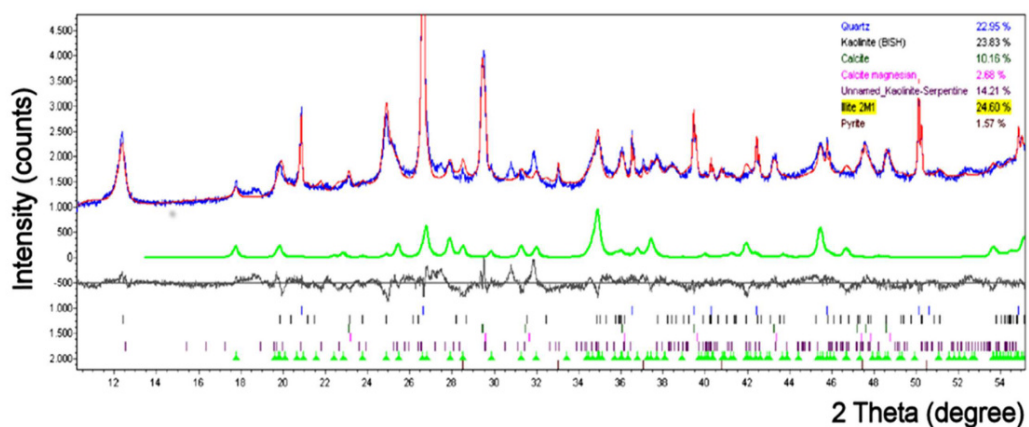
WASTe group, Inorganic Chemistry

Saarland University, Campus C 4 1

66123 Saarbrücken, Germany



A



B

Fig. S1

Powder XRD main analysis of five clay samples (A) and Rietveld refinement (TOPAS 2.1, Bruker AXS) of the OPA (B).

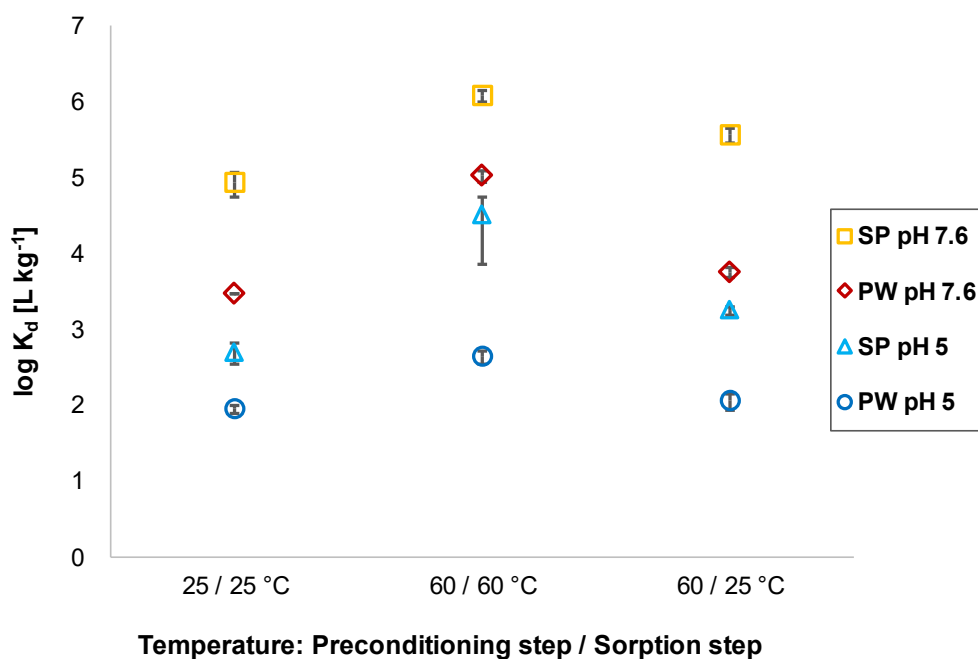


Fig. S2.

Log K_d values of the Eu(III) sorption onto OPA at pH 5 or 7.6 and 25 or 60°C in PW and SP. The first temperature refers to the preconditioning, the second to the sorption experiment.

Table S1

K_d values ($L \cdot kg^{-1}$) and standard deviations ($\pm SD$) of Eu(III) ($1.97 \cdot 10^{-6} \text{ mol} \cdot L^{-1}$) sorption onto OPA in SP and PW at pH 5 or 7.6 and 25°C or 60°C. The first temperature refers to the preconditioning, the second to the sorption experiment.

Temperature	SP pH 7.6	PW pH 7.6	SP pH5	PW pH5
25 / 25 °C	65000±15500	22560±71	507±160	91±11
60 / 60 °C	865000±12700	71000±9100	31800±24400	438±80
60 / 25 °C	362000±79500	5790±877	1800±238	116±28

Table S2

Parameters for calculations of Eu(III) / U(VI) sorption onto OPA. The Davies Equation was used for activity corrections in all cases.

Surface complexation or exchange reaction	logK
$\equiv\text{S}^{\text{S}}\text{OH} + \text{Eu}^{3+} \leftrightarrow \equiv\text{S}^{\text{S}}\text{OEu}^{2+} + \text{H}^+$	1.9
$\equiv\text{S}^{\text{S}}\text{OH} + \text{Eu}^{3+} + \text{H}_2\text{O} \leftrightarrow \equiv\text{S}^{\text{S}}\text{OEuOH}^+ + 2 \text{H}^+$	-4.6
$\equiv\text{S}^{\text{S}}\text{OH} + \text{Eu}^{3+} + 2\text{H}_2\text{O} \leftrightarrow \equiv\text{S}^{\text{S}}\text{OEu}(\text{OH})_2 + 3 \text{H}^+$	-12.8
$\equiv\text{S}^{\text{S}}\text{OH} + \text{Eu}^{3+} + 3\text{H}_2\text{O} \leftrightarrow \equiv\text{S}^{\text{S}}\text{OEu}(\text{OH})_3^- + 4 \text{H}^+$	-24.0
$\equiv\text{S}^{\text{W}}\text{OH} + \text{Eu}^{3+} \leftrightarrow \equiv\text{S}^{\text{W}}\text{OEu}^{2+} + \text{H}^+$	0.3
$\equiv\text{S}^{\text{W}}\text{OH} + \text{Eu}^{3+} + \text{H}_2\text{O} \leftrightarrow \equiv\text{S}^{\text{W}}\text{OEuOH}^+ + 2 \text{H}^+$	-6.2
$\equiv\text{S}^{\text{S}}\text{OH} + \text{UO}_2^{2+} \leftrightarrow \equiv\text{S}^{\text{S}}\text{OUO}_2^+ + \text{H}^+$	2.0
$\equiv\text{S}^{\text{S}}\text{OH} + \text{UO}_2^{2+} + \text{H}_2\text{O} \leftrightarrow \equiv\text{S}^{\text{S}}\text{OUO}_2\text{OH} + 2 \text{H}^+$	-3.5
$\equiv\text{S}^{\text{S}}\text{OH} + \text{UO}_2^{2+} + 2\text{H}_2\text{O} \leftrightarrow \equiv\text{S}^{\text{S}}\text{OUO}_2(\text{OH})_2^- + 3 \text{H}^+$	-10.6
$\equiv\text{S}^{\text{S}}\text{OH} + \text{UO}_2^{2+} + 3\text{H}_2\text{O} \leftrightarrow \equiv\text{S}^{\text{S}}\text{OUO}_2(\text{OH})_3^{2-} + 4 \text{H}^+$	-19
$\equiv\text{S}^{\text{W}}\text{OH} + \text{UO}_2^{2+} \leftrightarrow \equiv\text{S}^{\text{W}}\text{OUO}_2^+ + \text{H}^+$	0.1
$\equiv\text{S}^{\text{W}}\text{OH} + \text{UO}_2^{2+} + \text{H}_2\text{O} \leftrightarrow \equiv\text{S}^{\text{W}}\text{OUO}_2\text{OH} + 2 \text{H}^+$	-5.3
$3 \text{NaX} + \text{Eu}^{3+} \leftrightarrow \text{EuX}_3 + 3 \text{Na}^+$	1.9
$2 \text{NaX} + \text{UO}_2^{2+} \leftrightarrow \text{UO}_2\text{X}_2 + 2 \text{Na}^+$	0.65

Table S3

Average $\log K_d$ values for the sorption edges of Eu(III) ($n=3$; $1.97 \cdot 10^{-6} \text{ mol} \cdot \text{L}^{-1}$) and U(VI) ($n=2$; $4.2 \cdot 10^{-7} \text{ mol} \cdot \text{L}^{-1}$) onto OPA in porewater (PW) and sodium perchlorate (SP) at 25 °C (calculated errors: $\text{pH} \pm 0.2$ log units and $\log K_d \pm 0.3$ log units).

pH	Eu(III)	Eu(III)	U(VI)	U(VI)
	SP	PW	SP	PW
2	1.8	1.0	1.4	1.6
3	2.4	1.6	1.9	1.7
4	2.7	2.0	2.3	2.4
5	3.0	2.4	3.1	2.9
6	3.5	3.1	3.6	2.9
7	4.4	3.6	2.1	1.4
8	4.3	4.0	2.1	1.6
9	4.5	4.6	2.6	2.5
10	4.5	4.8	3.1	4.3
11	4.8	4.8	3.7	5.2
12	4.7	5.6	3.1	5.4

The sorption edges experiments are performed for U(VI) in two and for Eu(III) in three independent series. The analytical uncertainty for pH is calculated to be ± 0.2 log units, and for the sorption edges the uncertainty increases at low metal ion concentrations (especially Eu(III)) left in solution at high pH where $> 90\%$ of Eu(III) is sorbed and this leads to an uncertainty of $\log K_d$ values of about ± 0.3 log units. Uncertainty for each pH value is shown in Fig. 1 for Eu(III) and in Fig. 2 for U(VI).

Table S4

K_d values and standard deviations ($L \cdot kg^{-1}$) of U(VI) ($4.2 \cdot 10^{-7} \text{ mol} \cdot L^{-1}$) onto OPA in porewater (PW) and sodium perchlorate (SP) at pH 7.6 and 25/60°C.

U(VI)	K_d value PW [$L \cdot kg^{-1}$]	K_d value SP [$L \cdot kg^{-1}$]
25°C	24±13	149±57
60°C	126±38	730±4

Table S5

Log K_d values for the sorption of $3.29 \cdot 10^{-6} \text{ mol} \cdot L^{-1}$ ($0.5 \text{ mg} \cdot L^{-1}$) and $32.9 \cdot 10^{-6} \text{ mol} \cdot L^{-1}$ ($5.0 \text{ mg} \cdot L^{-1}$) Eu(III), and $2.1 \cdot 10^{-6} \text{ mol} \cdot L^{-1}$ ($0.5 \text{ mg} \cdot L^{-1}$) and $10.5 \cdot 10^{-6} \text{ mol} \cdot L^{-1}$ ($2.5 \text{ mg} \cdot L^{-1}$) U(VI) onto OPA in PW ($I = 0.4 \text{ mol} \cdot L^{-1}$, pH 7.6) at different temperatures (25 and 60°C) in the presence or absence of NOM (lactate, AHA), respectively. Maximum measurement error is < 4%, uncertainty of ±0.3 log units is estimated for all experiments.

Log K_d (25°C)	Log K_d (60°C)		
	Absence of NOM	Presence of lactate	Presence of AHA
Eu(III)			
$3.29 \cdot 10^{-6} \text{ mol} \cdot L^{-1}$	3.7	3.7	3.9
$32.9 \cdot 10^{-6} \text{ mol} \cdot L^{-1}$	2.8	2.8	3.3
U(VI)			
$2.1 \cdot 10^{-6} \text{ mol} \cdot L^{-1}$	1.7	1.7	1.8
$10.5 \cdot 10^{-6} \text{ mol} \cdot L^{-1}$	1.6	1.6	1.6

3.2 Simultaneous quantification of iodine and high valent metals via ICP-MS under acidic conditions in complex matrices

Extended abstract:

A new method was developed to quantify iodine in acidic solutions via ICP-MS. Iodine gets quantified in alkaline media by default because the high volatile compounds I_2 and HI, which are favoured in acidic media, adsorb in the area of the spray chamber. This leads to an unstable measurement signal and memory effects. A precise quantification is not possible under these conditions. In alkaline solutions, high valent metals like Eu^{3+} precipitate as hydroxides or carbonates. As a consequence, the simultaneous measurement of iodine and such metals via ICP-MS was not practicable without using additional complexing agents for the high valent metals. In very complex matrices such as artificial cement pore water (ACW, ≈ 3 M), the complexation of all cations is practically impossible.

In natural solutions, the iodine species are mainly free iodide or iodate as well as organic molecules containing iodine. Only iodide forms volatile I_2 and HI in the presence of acid. A suitable method to avoid this is to oxidise iodide to iodate before the acidic ICP-MS sample preparation. NaOCl was found to be an appropriate oxidation agent. The reaction time can be varied between 1-72 h at minimum. Afterwards, acid can be added and the samples are stable for at least 5 d.

The recovery of iodide oxidised with NaOCl to iodate was determined in deionised water depended on the internal standard (Br-79, In-115, Te-125, Ho-165) used for the compensation of measurements fluctuations. With Br-79 the iodide concentration was always overestimated (126-290% recovery). A recovery near 100% for all investigated iodide concentrations (0.3-90 $\mu\text{g L}^{-1}$) could be obtained with a signal correction to the other three elements. Nevertheless, the best recoveries in the whole iodide concentration range were obtained by using Ho-165 as internal standard.

Iodide and Eu^{3+} or the whole WC were quantified in low and high saline solutions (Milli-Q water, ACW, 5 M NaCl) at neutral and alkaline pH (12.5) of the equilibration medium to test the robustness of the method. During the oxidation step, all used elements were present in solution. The recovery of all elements was 91-105% with a relative standard deviation $\leq 5\%$ under all investigated conditions for element concentrations ranging from 15 to 90 $\mu\text{g L}^{-1}$. No interference of NaOCl on the recovery of the metals could be observed. The oxidation of iodide

to iodate with NaOCl is a robust and inexpensive method to determine iodine in the presence of high valent metals via ICP-MS as long as no speciation analytic is required.

Kristina Brix planned, designed and wrote the publication. She planned and carried out the experiments, analysed the samples and interpreted the results. Christina Hein and Jonas Michael Sander were involved in the planning and discussion of the experiments and revised the manuscript before publicising. Ralf Kautenburger is the corresponding author. He had supervision during the experiments and writing. He was also involved in discussing the results, design and writing of the publication and he revised the manuscript before publicising.

These results have been published in *Talanta*.

Brix, K., Hein, C., Sander, J.M., Kautenburger, R., 2017, *Talanta* 167, 532-536.

<http://dx.doi.org/10.1016/j.talanta.2017.02.056>

Copyright (2017) Elsevier.

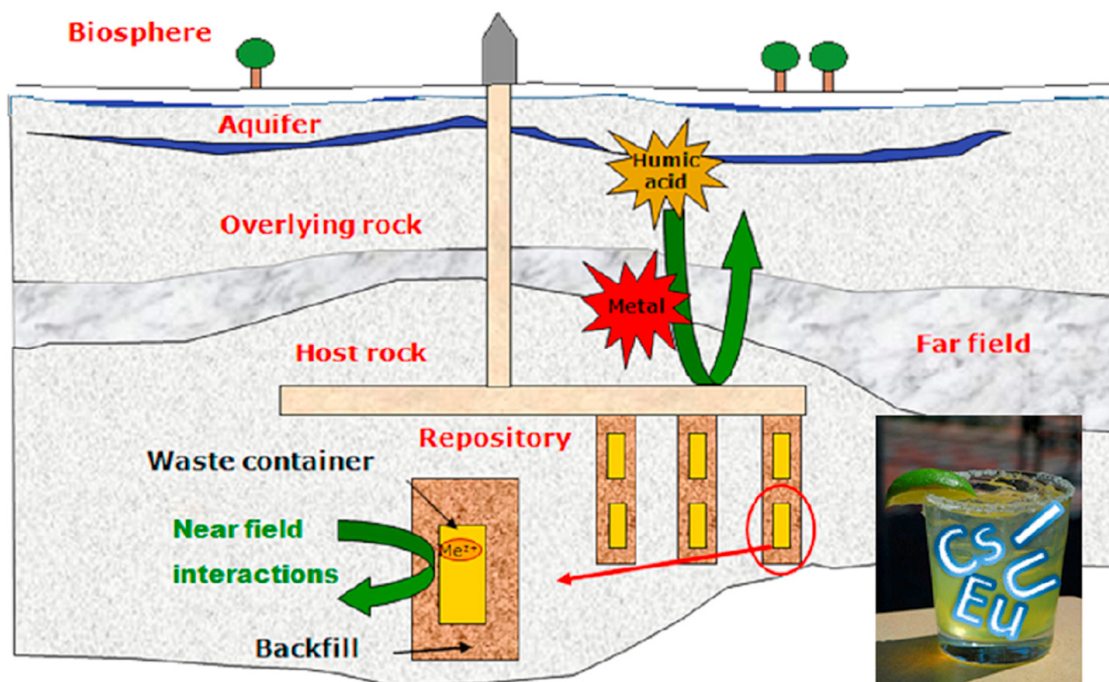


Figure 13. Schematic representation of a potential high-level nuclear waste disposal with the so-called waste cocktail (Graphical abstract of Simultaneous quantification of iodine and high valent metals via ICP-MS under acidic conditions in complex matrices).



Contents lists available at ScienceDirect

Talanta

journal homepage: www.elsevier.com/locate/talanta

Simultaneous quantification of iodine and high valent metals via ICP-MS under acidic conditions in complex matrices



Kristina Brix, Christina Hein, Jonas Michael Sander, Ralf Kautenburger*

WASTe Group, Institute of Inorganic Solid State Chemistry, Saarland University, Campus Dudweiler, Am Markt Zeile 5, D-66125 Saarbrücken, Germany

ARTICLE INFO

Keywords:

ICP-MS
Iodine
Sodium hypochlorite
Simultaneous determination
Artificial cement pore water
High level nuclear waste disposal

ABSTRACT

The determination of iodine as a main fission product (especially the isotopes I-129 and I-131) of stored HLW in a disposal beside its distribution as a natural ingredient of many different products like milk, food and seawater is a matter of particular interest. The simultaneous ICP-MS determination of iodine as iodide together with other elements (especially higher valent metal ions) relevant for HLW is analytically very problematic. A reliable ICP-MS quantification of iodide must be performed at neutral or alkaline conditions in contrast to the analysis of metal ions which are determined in acidic pH ranges. Herein, we present a method to solve this problem by changing the iodine speciation resulting in an ICP-MS determination of iodide as iodate. The oxidation from iodide to iodate with sodium hypochlorite at room temperature is a fast and convenient method with flexible reaction time, from one hour up to three days, thus eliminating the disadvantages of quantifying iodine species via ICP-MS. In the analysed concentration range of iodine (0.1–100 $\mu\text{g L}^{-1}$) we obtain likely quantitative recovery rates for iodine between 91% and 102% as well as relatively low RSD values (0.3–4.0%). As an additional result, it is possible to measure different other element species in parallel together with the generated iodate, even high valent metals (europium and uranium beside caesium) at recovery rates in the same order of magnitude (93–104%). In addition, the oxidation process operates above pH 7 thus offering a wide pH range for sample preparation. Even analytes in complex matrices, like 5 M saline (NaCl) solution or artificial cement pore water (ACW) can be quantified with this robust sample preparation method.

1. Introduction

The proper quantification of iodine is necessary in many different products and matrices. It can be naturally found in food, like milk, but also in seawater. Likewise, its isotope I-131 is also a main fission product of uranium-235 which occurs in radioactive waste. Radioiodine I-131 and I-129 have half-lives of 8 d and 1.57×10^7 years, respectively. Due to its high volatility and mobility, which is related to its anionic nature in ground water as iodide, radioiodine can contaminate sea and fields within a long-ranged area upon its release. As a consequence, consumption of contaminated products often leads to thyroid cancer due to the selective accumulation in the thyroid gland in the human body [1].

To ensure the safety of a high level nuclear waste disposal (HLW) for over hundred thousands of years, it is necessary to know the critical processes and distribution of hazardous elements among the environmental geological formation. For the estimation of relevant geochemical parameters like K_d values that are used in geochemical modelling

experiments [2–6], sorption experiments using (natural) clay minerals are necessary. Therefore, the rapid as well as reproducible quantification of iodine in parallel with other elements relevant for HLW especially uranium, europium as homologue of americium and caesium as another main fission product of uranium is needed.

There are many possible analytical techniques to determine the content of iodine in different samples for example X-ray fluorescence spectrometry [7–9], neutron activation analysis [8,10–12] and colorimetric and catalytic methods [13,14]. However, one of the most reliable techniques is inductively coupled plasma mass spectrometry (ICP-MS) because of its rapid measurements and its ability for quasi-simultaneous multi-element detection. Acid sample digestion, which is used for ICP-MS by default, leads to formation of HI and in presence of oxygen from the atmosphere also I_2 which readily adsorbs in the spray chamber producing an unstable signal and memory effects [13–18]. Therefore, iodine is typically measured by ICP-MS under alkaline conditions where ammonia solution is added to form non-volatile NH_4I . This is a suitable method to determine iodine content in milk,

Abbreviations: ACW, Artificial cement pore water; HLW, High level radioactive waste; HMI, High matrix introduction system; IS, Internal standard; LOD, Limit of detection; LOQ, Limit of quantification; RSD, Relative standard deviation

* Corresponding author.

E-mail address: r.kautenburger@mx.uni-saarland.de (R. Kautenburger).

<http://dx.doi.org/10.1016/j.talanta.2017.02.056>

Received 20 December 2016; Received in revised form 22 February 2017; Accepted 25 February 2017
0039-9140/ © 2017 Elsevier B.V. All rights reserved.

food and water [9,19–25]. However, to investigate the safety of a nuclear waste disposal alkaline sample digestion cannot be used for multiple element analysis because the relevant high valent metals (e.g. europium used as chemical analogue for trivalent actinides) precipitate leading to underestimation and deposition in sample tubes and the instrument. As a consequence, it is necessary to measure all samples twice (one alkaline stage for iodine determination and a separate acidic stage for all metals) or to transform the volatile iodide into a non-volatile species such as iodate, which is stable under acidic conditions.

The oxidation of iodide to iodate with H_2O_2 or HClO_4 only takes place in the lower pH range [26,27]. To avoid the loss of intermediately formed HI or I_2 the reaction has to be performed in gastight vessels. Additionally, high temperatures, reaction times about four hours and sometimes high pressure are required for the quantitative oxidation. Altogether, the pre-treatment of the samples is complex and time consuming.

Another possibility to form non-volatile iodate is the oxidation of iodide with NaOCl at neutral pH and room temperature [28]. In this work we present this oxidation as an easy sample preparation step for ICP-MS measurements of iodine in parallel together with high valent metals under acidic measuring conditions, where no additional equipment or rude reaction conditions are needed. We investigate the recovery of iodide quantitatively oxidised to iodate, also in presence of europium, uranium and caesium, in Milli-Q water and high saline matrices like 5 M NaCl solution. Furthermore, the oxidation also takes place at higher pH values up to pH 12.5. This enables investigations in high saline and alkaline artificial cement pore water (ACW) which is a relevant matrix related to the technical barrier (consisting to a large amount of cement and, over time, of cement corrosion products) of a high level nuclear waste disposal. Vanhoe et al. described the oxidation of iodide with NaOCl and some other oxidising agents as not quantitative and hence being not suitable to prevent a memory effect or to form a stable signal in ICP-MS [29]. However, our relevant iodine concentrations range from $0.1 \mu\text{g L}^{-1}$ to $100 \mu\text{g L}^{-1}$ whereas Vanhoe et al. used 1.3 mg L^{-1} of iodine as their smallest concentration. In consideration of this, the discrepancy to our results can be attributed to the difference in concentration range or different reaction conditions, which are not directly mentioned in the study of Vanhoe et al. [29].

Apart from all these analytical aspects, iodine chemistry in the environment is very complex [30]. The iodine is likely to be present in the nature with multiple forms including different organic iodine species [31]. For example, iodine-humic acid species are non-volatile compounds in which iodine can be quantified without former oxidation. However, in potential deep geological host rock formations, like granite, salt or clay, the presence of organic and therefore organic iodine species (for example bacteria mediated methylation of iodine) can be neglected.

2. Experimental

2.1. Chemicals and standards

All solutions were prepared with Milli-Q deionised water (18.2 M Ω cm). For the preparation of 5 M NaCl solution and the artificial cement pore water (ACW) NaCl with Emsure[®] quality purchased from Merck KGaA (Darmstadt, Germany) was used. Additionally, $\text{CaCl}_2 \cdot 2\text{H}_2\text{O}$ and $\text{SrCl}_2 \cdot 6\text{H}_2\text{O}$ with Emsure[®] quality, KCl and Na_2SO_4 with p.a. quality (pro analysi) purchased from Merck KGaA (Darmstadt, Germany) and Al , Fe and Ba as AAS-standard solutions purchased from Bernd Kraft GmbH (Duisburg, Germany) were used. As 1000 mg L^{-1} stock standard solution, single element ICP-standards of I , Eu (10 g L^{-1} stock standard solution), U , Cs , In , Te , Br and Ho with Certipur[®] quality were used. The pH values were adjusted with NaOH (30%, suprapure). As plasma gas Argon 5.0 (Praxair, Germany) was used. NaOCl (8%, p.a.) for the oxidation was purchased from AppliChem GmbH (Darmstadt, Germany). To realise the acidic measurement conditions, HNO_3 (69%,

suprapur) from Carl Roth GmbH+Co. KG (Karlsruhe, Germany) was used.

2.2. Sample and ACW preparation

For all samples 1.0 mL of medium was pipetted into a 10 mL tube. Then the necessary amount of ICP-standard for each element was added to receive concentrations from 0.1 to $100 \mu\text{g L}^{-1}$ in total volume of 10 mL. The tubes were filled with medium up to 3.32 mL and $10 \mu\text{L}$ of 0.6% sodium hypochlorite solution were added. The mixture was left for 1–72 h for the oxidation from iodide to iodate to take place, then 6.36 mL Milli-Q water, 300 μL nitric acid and $10 \mu\text{L}$ internal standard (10 mg L^{-1}) were added. Each sample was independently prepared and measured three times. Analogously, solutions for calibration were prepared applying the same procedure and exactly the same reaction time as the related samples due to the influence of reaction time on the iodate concentration.

The ACW contains 2.46 M NaCl , 32.4 mM $\text{CaCl}_2 \cdot 2\text{H}_2\text{O}$, 20 mM Na_2SO_4 , 5.1 mM KCl , 0.06 mM $\text{SrCl}_2 \cdot 6\text{H}_2\text{O}$, 0.008 mM Fe , 0.005 mM Ba and 0.004 mM Al which were added stepwise to argon flushed Milli-Q water. Due to the flushing, the content of carbon dioxide in the water gets minimised, which prevents the precipitation of carbonates during the following pH adjustment at 12.5 with NaOH .

2.3. The ICP-MS system

A commercial ICP-MS from Agilent (7500cx, Santa Clara, USA) with a Cetac auto sampler (ASX 500) and a high matrix introduction system for higher salt concentrations (HMI, Agilent) was used in this work. The ICP Mass Hunter workstation software (vers. B01.01, Agilent) has been utilised as analysis software. For samples with low salinity, a default method with 1550 W RF-Power, auxiliary gas flow of 1.15 L min^{-1} , $3 \times 100 \text{ ms}$ dwell time and three times of repetition has been used. Samples with high saline matrix were measured with the transient method. Normally, the analysis of environmental samples with a total dissolved salt content of more than 1% results in excessive deposits on cones and ion guiding components. In consequence of this, the highly saline matrix has to be diluted several tens or hundred times thus decreasing the analyte concentration below the respective limits of detection (LOD). The transient method enables the quantification of elements in up to 5 M saline solution without dilution or sample clean-up steps by decreasing the sample uptake time to only 10 s. Data processing is based on peak area contrary to the default method, where the signal height (measured over a longer time period of about 120 s) is used for quantification. For the transient measurements the obtained peak area is directly proportional to the element concentration and with a calibration by linear regression the concentration of the analyte can be calculated. The detailed setup and conditions of this method are described elsewhere [32].

While for the present study the determination of the stable I-127 is the subject of our investigation, in the context of a final disposal the determination of the radioactive I-129 will be of interest. As a consequence, an isotopic interference with Xe-129 (natural abundance of 26.4%) arises which is present as impurity in argon used as plasma gas. Either this interference can be removed by introducing a correction factor based on the measurement of the X-131 signal [31]. Alternatively, a reaction cell system applying oxygen as reaction gas leads to removal of the Xe-129 background from the analysis [33,34].

3. Results and discussion

3.1. Comparison of different potential internal standards for iodine

Holmium can be used as internal standard (IS) for the determination of the metals caesium, europium and uranium, via ICP-MS, due to its monoisotopic occurrence (100% Ho-165), rarity in nature and

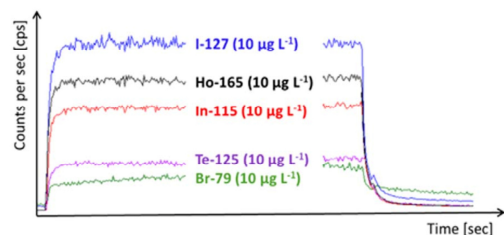


Fig. 1. Signal intensity and stability of the tested IS compared to the I-127 signal.

consequential stable measurement signal. Compared to this, it is difficult to define the best IS for iodine which has naturally an anionic character and undergoes the oxidation to iodate. Preferably, the IS would also be an anion with similar ionisation energy to iodine and undergoing oxidation by NaOCl to a species similar to iodate. Considering this, bromine is a potential candidate since it occurs as anionic bromide with an ionisation energy close to iodine. Unfortunately, NaOCl is not a strong enough oxidation agent to oxidise bromide to bromate. Other candidates known from literature as IS for iodine are tellurium and indium [24,27], whose oxidation energies are similar to holmium and slightly smaller than that of iodine and bromine. Hence, holmium, indium, tellurium and bromine are tested as potential internal standards for iodine. Their signal stability as well as the recovery and reproducibility of iodine corrected to the relative element was determined.

In Fig. 1 the ICP-MS signals for all tested elements (especially the signal rise and drop showing the nebulisation stability as well as the spray chamber transfer and wash out rate) are shown. As result, iodine, holmium and indium show a very similar signal pattern consisting of a sharp signal rise and drop and a stable signal over time. In contrast, bromine as well as tellurium show a time dependent increase of the signal intensity as well as for bromine an incomplete wash out behaviour can be observed thus indicating a memory effect.

In Table 1 the recoveries of iodine corrected to the current internal standard are shown. Bromide as internal standard always leads to an overestimation of iodine concentrations from 125% to 290% and the values also have large uncertainties with relative standard deviations (RSD) up to 11%. Good recoveries and acceptable RSD values can be reached with indium and tellurium at concentrations of 25 $\mu\text{g L}^{-1}$ iodine and higher.

Te-125 has a relatively low ionisation efficiency and only exists naturally by 7.1%. As a consequence, small fluctuation of the tellurium signal implies huge alterations on the recovery of iodine. However, In-115 has a sufficient signal intensity, but there can be an overlap with the signal of Sn-115, which can occur as contamination for example in parts of the ACW and after clay leaching. Only when normalised to holmium, the iodine concentrations were properly determined also at smaller concentrations. The relative standard deviations are also very satisfying with uncertainties of less than 5%, except for the smallest

Table 1
Recovery rates of iodine corrected to Br, In, Te and Ho as internal standards (all values given in percent).

c [$\mu\text{g L}^{-1}$]	^{79}Br	^{115}In	^{125}Te	^{165}Ho
0.3	290 ± 30	25 ± 8	60 ± 8	95 ± 7
1	162 ± 15	80 ± 9	88 ± 9	96 ± 2
5	136 ± 16	107 ± 19	107 ± 20	96 ± 2
15	127 ± 14	108 ± 12	107 ± 11	100 ± 1
25	126 ± 1	101 ± 2	99 ± 2	100 ± 0.3
40	133 ± 4	105 ± 6	104 ± 6	98 ± 1
65	137 ± 8	103 ± 0.3	103 ± 1	99 ± 1
80	136 ± 3	103 ± 1	102 ± 1	100 ± 0.3
90	164 ± 12	104 ± 2	103 ± 1	102 ± 5

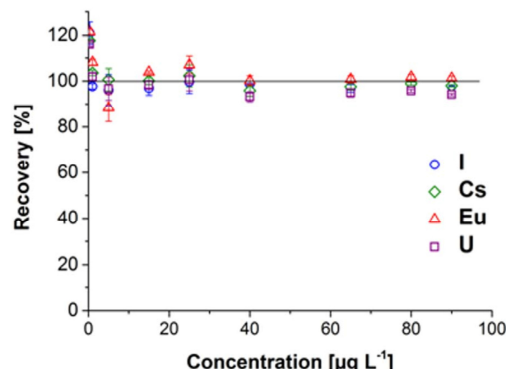


Fig. 2. Recovery of iodine, caesium, europium and uranium in Milli-Q water (normalised by the holmium intensity) at pH 7.

iodine concentration of 0.3 $\mu\text{g L}^{-1}$ where it is about 7%. As a consequence of this holmium is used as internal standard for iodine in all further measurements. The limit of detection (LOD) for the default measurements was determined as $\text{LOD} = |x_B| + 3 \cdot s_B$ (mean of the blank $|x_B|$ and the standard deviation of the blank s_B , $n=15$) with 48 ng L^{-1} . The limit of quantification (LOQ) corresponds to 112 ng L^{-1} with $\text{LOQ} = |x_B| + 10 \cdot s_B$.

3.2. Influence of pH value and addition of other elements in Milli-Q water

The recovery rates of the generated iodate were investigated at two different pH values: the neutral one and pH 12.5. At higher pH values the oxidation potential of sodium hypochlorite decreases, but as the electrochemical potential of iodide/iodate decreases too, the reaction still takes place. pH values below 7 are not recommended because of the formation of volatile hydrogen iodide before the oxidation takes place. Under acidic conditions iodide and iodate again would disproportionate to form an irreproducible amount of gaseous iodine. Fig. 2 shows an overview of all recovery rates for the analysed elements at a neutral pH range. With the exception of the two lowest concentration used (0.3 and 1.0 $\mu\text{g L}^{-1}$, respectively) all other tested recovery rates are close to 100% showing the applicability of the here presented method analysing iodine together with other HLW relevant elements. In Table 2 the accurate recovery rates for several iodine concentrations in Milli-Q water in presence of uranium, europium and caesium are shown. As mentioned above, iodine has a very good recovery rate (96–100%) at concentrations of 1 $\mu\text{g L}^{-1}$ and higher.

At iodine concentration of 15 $\mu\text{g L}^{-1}$ and higher the RSD is about 5% at most. These results are similar to those without presence of other elements. Caesium, europium and uranium show good recoveries at concentrations of 1 $\mu\text{g L}^{-1}$ and higher, except for 5 $\mu\text{g L}^{-1}$ europium (Table 2, italicised) which is considered as outlier. The RSD of all three

Table 2
Recovery of iodine, caesium, europium and uranium in Milli-Q water corrected to holmium at neutral pH (all values given in percent).

c [$\mu\text{g L}^{-1}$]	^{127}I	^{133}Cs	^{153}Eu	^{238}U
0.3	121 ± 5	118 ± 1	122 ± 1	116 ± 1
1	98 ± 1	104 ± 1	108 ± 1	102 ± 2
5	96 ± 7	101 ± 5	88 ± 6.0	97 ± 5
15	97 ± 3	100 ± 2	104 ± 0.5	98 ± 2
25	100 ± 5	102 ± 5	107 ± 4	101 ± 5
40	99 ± 0.4	96 ± 2	100 ± 2	93 ± 2
65	97 ± 2	98 ± 1	101 ± 2	95 ± 2
80	99 ± 1	99 ± 1	102 ± 1	96 ± 1
90	98 ± 0.1	98 ± 0.5	101 ± 1	94 ± 1

Table 3

Recovery of iodine and europium in Milli-Q water corrected to holmium at pH=12.5 (all values given in percent).

c [$\mu\text{g L}^{-1}$]	^{127}I	^{153}Eu
0.3	91 ± 2	94 ± 1
5	97 ± 4	98 ± 7
15	94 ± 1	101 ± 3
50	99 ± 0.4	101 ± 1
90	101 ± 0.4	102 ± 0.4

elements is about 5% at maximum. These results indicate that both the oxidation and presence of sodium hypochlorite have no significant influence on the recovery of the elements and they are measurable simultaneously.

At higher pH values the electrochemical potentials of OCl^-/Cl_2 and IO_3^-/I^- decrease both, hence the recovery of iodine-127 has to be investigated in Milli-Q water at pH 12.5. Furthermore, europium precipitates as europium(III)hydroxide in alkaline solution, so its recoveries were determined simultaneously with those of iodine. The recoveries of iodine and europium are shown in Table 3. Both elements were underestimated at the lowest concentration ($c = 0.3 \mu\text{g L}^{-1}$). At concentrations of $5 \mu\text{g L}^{-1}$ and above the recovery rates increases and RSD decreases by trend. This indicates that the oxidation still takes place and the pH value has no significant influence on the recovery of iodine and europium.

3.3. Influence of salinity in combination with alkaline solutions

The recovery rates of different elements after treatment with sodium hypochlorite were investigated at different concentrations not only in Milli-Q water but also in higher saline matrices. Most natural samples have very complex matrices (seawater, ACW). In this work 5 M saline solution (NaCl) at different pH values and ACW were examined. Therefore, the transient measuring method was used. According to this, LOD and LOQ were determined again, with values of $0.55 \mu\text{g L}^{-1}$ (LOD) and $0.9 \mu\text{g L}^{-1}$ (LOQ), which represent higher values compared to this resulting from the default method. This fact can be explained by the distinctively smaller amount of sample reaching the ICP-MS system.

In 5 M saline solution (Table 4) the recovery of iodine is overestimated at the smallest investigated concentration of $5 \mu\text{g L}^{-1}$ (114%) and has a high RSD of 14%. At higher concentrations the recovery is almost 100% and the RSD decreases to 4% at most. For europium, the recovery is near 100% for every investigated concentration with acceptable RSD values. In summary, high saline solutions like 5 M NaCl do not disturb or slow down the oxidation reaction.

At high alkaline pH values (Table 5), the only significant change in 5 M saline solution in relation to the neutral pH measurement, is that europium is overestimated at the lowest concentration, too. This indicates the robustness of the oxidation not only against the increasing of the pH value, but also against high salinity in the same solution.

Finally, we investigated the recovery and standard deviation of all mentioned elements simultaneously in ACW, which is a really complex, alkaline matrix with high salinity. In Table 6 the results are shown.

Table 4

Recovery of iodine and europium in 5 M NaCl solution with neutral pH (all values given in percent).

c [$\mu\text{g L}^{-1}$]	^{127}I	^{153}Eu
5	114 ± 14	101 ± 7
15	102 ± 4	99 ± 1
25	100 ± 0.2	104 ± 1
40	99 ± 2	98 ± 3
90	99 ± 0.2	99 ± 0.2

Table 5

Recovery of iodine and europium in 5 M saline solution, pH=12.5 (all values given in percent).

c [$\mu\text{g L}^{-1}$]	^{127}I	^{153}Eu
5	118 ± 14	127 ± 2
15	102 ± 3	103 ± 6
25	101 ± 2	99 ± 2
40	100 ± 1	97 ± 0.4

Table 6

Recovery of iodine, caesium, europium and uranium in artificial cement pore water, pH=12.5 (all values given in percent).

c [$\mu\text{g L}^{-1}$]	^{127}I	^{133}Cs	^{153}Eu	^{238}U
5	119 ± 2	106 ± 1	104 ± 0.4	110 ± 0.4
15	97 ± 6	105 ± 1	102 ± 0.4	101 ± 0.4
25	95 ± 1	102 ± 1	99 ± 3	98 ± 0.3
40	98 ± 5	100 ± 3	101 ± 1	94 ± 3
65	99 ± 1	101 ± 2	101 ± 2	94 ± 1
80	102 ± 0.3	101 ± 2	101 ± 2	93 ± 2
90	102 ± 0.2	100 ± 1	101 ± 0.2	94 ± 1

Caesium and europium have acceptable recoveries and good standard deviations for every determined concentration. At a concentration of $25 \mu\text{g L}^{-1}$ for caesium and $15 \mu\text{g L}^{-1}$ for europium and above the results are close to 100% with variations of 3% at most. For most of the investigated iodine concentrations similar results to caesium and europium were obtained. At the smallest investigated concentration iodine gets overestimated about almost 20% and the maximum RSD=6% is slightly larger compared to the other elements. In comparison with the lighter elements, uranium tends to get underestimated at higher concentrations even with good RSD of 3% or less. Further investigations and the results shown in Table 3 indicate that this is a most likely time depended effect, caused by the ACW matrix and is not influenced by addition of iodine and or sodium hypochlorite. The origin of this underestimation of uranium in ACW is topic of current research.

In summary, the oxidation still takes place in ACW, which is an alkaline, complex and high saline matrix. It is possible to measure iodine and high valent metals simultaneously via ICP-MS under acidic conditions with satisfying results and small standard deviation.

In Fig. 3 the recovery rates of selected iodine concentrations at different conditions can be seen. It is remarkable, that the iodine concentration is overestimated at $5 \mu\text{g L}^{-1}$ in all measurements using the transient method for high saline matrices. This can be explained by the 10- to 20-fold lower sample uptake during the transient method and in consequence of this, the higher LOQ. For all other concentrations, the recovery rates are between 94–102%. Although, our samples are partially very complex and undergo an oxidation with sodium hypochlorite, the presented recovery rates are in the order of magnitude of default ICP-MS measurements for all investigated elements. This shows that the presented method of measuring iodine under acidic conditions via ICP-MS is not only an easy and flexible one, but also delivers good and reproducible results compared to single element measurements.

4. Conclusions

The quantification of iodine as a natural occurring ingredient of many different products like milk, food and seawater as well as a main fission product (especially I-131) of stored HLW in a disposal is a matter of particular interest. In the framework of a long term risk assessment of a future HLW disposal a reproducible quantification of iodine together with other elements relevant for HLW is needed. The problem of an ICP-MS quantification of iodide which has to be

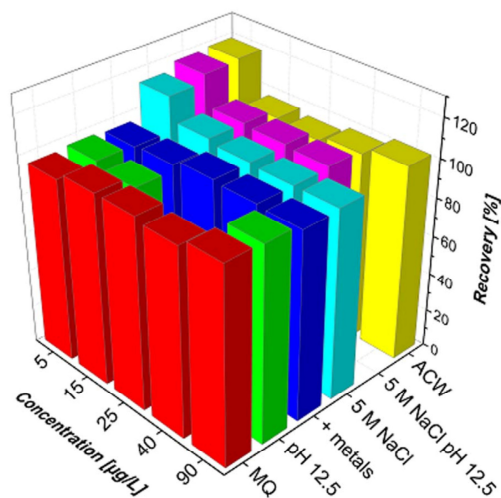


Fig. 3. Recovery schema for selected concentrations of iodine under all investigated conditions.

measured at neutral or alkaline conditions in contrast to the analysis of metal ions which are determined in acid pH ranges can be solved by changing the iodine speciation resulting in the determination of iodide as iodate. The oxidation from iodide to iodate with sodium hypochlorite at room temperature is a fast and easy method with flexible reaction time, from one hour up to three days, to eliminate the disadvantages of quantifying iodine species via ICP-MS. It is possible to measure various other element species in parallel together with the generated iodate, even high valent metals, which precipitate in ammoniac solution. In addition, the oxidation process operates above pH 7 thus offering a wide range for sample preparation. Even analytes in complex matrices, like 5 M saline solution or ACW, can be quantified with this robust sample preparation method. The recovery rates obtained in this work, differ not significantly from those of the single elements in Milli-Q water and are nearly hundred percent all along, with RSD of 3% or smaller for almost every investigated concentration. In a nutshell, the robust method presented in this work can be applied to successfully quantify iodine as iodate alongside high valent metal ions even in complex and high saline matrices using an acidic ICP-MS sample preparation method.

Acknowledgements

We would like to thank the German Federal Ministry of Economics and Energy (BMWi), represented by the Project Management Agency Karlsruhe (PTKA-WTE) for funding (projects: 02E10991 and 02E11415D) and our project partners for the kind collaboration.

References

- [1] J. Malone, J. Unger, F. Delange, R. Lagasse, J.E. Dumont, Thyroid consequences of Chernobyl accident in the countries of the European Community, *J. Endocrinol. Invest.* 14 (1991) 701–717.
- [2] E.C. Gaucher, C. Tournassat, F.J. Pearson, P. Blanc, C. Crouzet, C. Lerouge, S. Altmann, A robust model for pore-water chemistry of clayrock, *Geochim. Cosmochim. Acta* 73 (2009) 6470–6487.
- [3] E. Tertre, A. Hofmann, G. Berger, Rare Earth Element sorption by basaltic rock: experimental data and modeling results using the "generalised composite approach", *Geochim. Cosmochim. Acta* 72 (2008) 1043–1056.
- [4] F.Z. El Aamrani, L. Duro, J. de Pablo, J. Bruno, Experimental study and modeling of the sorption of uranium(VI) onto olivine-rock, *Appl. Geochem.* 17 (2002) 399–408.
- [5] E. Tertre, G. Berger, E. Simoni, S. Castet, E. Giffaut, M. Loubet, H. Catalette, Europium retention onto clay minerals from 25 to 150 °C: experimental measurements, spectroscopic features and sorption modelling, *Geochim. Cosmochim. Acta* 70 (2006) 4563–4578.
- [6] R. Kautenburger, H.P. Beck, Influence of geochemical parameters on the sorption and desorption behaviour of europium and gadolinium onto kaolinite, *J. Environ. Monit.* 12 (2010) 1295–1301.
- [7] E.A. Crecellus, Determination of total iodine in milk by X-Ray fluorescence spectrometry and iodide electrode, *Anal. Chem.* 47 (1975) 2034–2035.
- [8] J. Pavel, M. Fille, U. Frey, Determination of iodine in biological materials and in some standard reference materials by X-ray fluorescence spectrometry, *Fresenius J. Anal. Chem.* 331 (1988) 51–54.
- [9] H. Baumann, Rapid and sensitive determination of iodine in fresh milk and milk powder by inductively coupled plasma – mass spectrometry (ICP-MS), *Fresenius J. Anal. Chem.* 338 (1990) 809–812.
- [10] B.R. Norman, V. Iyengar, The application of preirradiation combustion and neutron activation analysis technique for the determination of iodine in food and environmental reference materials, *Biol. Trace Elem. Res* 63 (1998) 221–229.
- [11] D.J. Morgan, A. Black, G.R. Mitchell, The determination of inorganic iodide in urine by neutron-activation analysis, *Analyst* (1969) 740–743.
- [12] H.L. Rook, The determination of iodine in biological and environmental standard reference materials, *J. Radioanal. Chem.* 39 (1977) 351–358.
- [13] R.E.D. Moxon, E.J. Dixon, Semi-automatic method for the determination of total iodine in food, *Analyst* 105 (1980) 344–352.
- [14] K. Rodgers, D.B. Poole, The estimation of iodine in biological materials: a modification of the method of Ellis & Duncan, *Biochem. J.* 70 (1958) 463–471.
- [15] Y. Gélinas, A. Krushevska, R.M. Barnes, Determination of total iodine in nutritional biological samples by ICP-MS following their combustion with an oxygen stream, *Anal. Chem.* 70 (1998) 1021–1025 70 (1998) 1021–1025.
- [16] P.A. Fecher, I. Goldmann, A. Nagengast, Determination of iodine in food samples by inductively coupled plasma mass spectrometry after alkaline extraction, *J. Anal. At. Spectrom.* 13 (1998) 977–982.
- [17] P. Schramel, S. Hasse, Iodine determination in biological materials by ICP-MS, *Microchim. Acta* 116 (1994) 205–209.
- [18] A. Al-Ammar, E. Reitznerová, R.M. Barnes, Thorium and iodine memory effects in inductively-coupled plasma mass spectrometry, *Fresenius J. Anal. Chem.* 370 (2001) 479–482.
- [19] H.J. Reid, A.A. Bashammakh, P.S. Goodall, M.R. Landon, C. O'Connor, B.L. Sharp, Determination of iodine and molybdenum in milk by quadrupole ICP-MS, *Talanta* 75 (2008) 189–197.
- [20] H. Shi, C. Adams, Rapid IC-ICP/MS method for simultaneous analysis of iodoacetic acids, bromoacetic acids, bromate, and other related halogenated compounds in water, *Talanta* 79 (2009) 523–527.
- [21] V. Hansen, P. Yi, X. Hou, A. Aldahan, P. Roos, G. Possnert, Iodide and iodate (^{129}I and ^{127}I) in surface water of the Baltic Sea, Kattegat and Skagerrak, *Sci. Total Environ.* 412–413 (2011) 296–303.
- [22] T.K.D. Nguyen, R. Ludwig, Quantitative determination of bromine and iodine in food samples using ICP-MS, *Anal. Sci.* 30 (2014) 1089–1092.
- [23] V.C. Costa, R.S. Picoloto, C.A. Hartwig, P.A. Mello, E.M.M. Flores, M.F. Mesko, Feasibility of ultra-trace determination of bromine and iodine in honey by ICP-MS using high sample mass in microwave-induced combustion, *Anal. Bioanal. Chem.* 407 (2015) 7957–7964.
- [24] K. Judprasong, N. Jongjaithe, V. Chavasi, Comparison of methods for iodine analysis in foods, *Food Chem.* 193 (2016) 12–17.
- [25] A. Daroui, L. Tosch, M. Gorny, R. Michel, I. Goroncy, J. Herrmann, H. Nies, H.-A. Synal, V. Alfimov, C. Walther, Iodine-129, iodine-127 and cesium-137 in seawater from the North Sea and the Baltic Sea, *J. Environ. Radioact.* 162–163 (2016) 289–299.
- [26] E.H. Larsen, M.B. Ludwigsen, Determination of iodine in food-related certified reference materials using wet ashing and detection by inductively coupled plasma mass spectrometry, *J. Anal. At. Spectrom.* 12 (1997) 435–439.
- [27] K. Fujisaki, H. Matsumoto, Y. Shimokawa, K. Kiyotaki, Simultaneous quantification of iodine and other elements in infant formula by ICP-MS following an acid digestion with nitric acid and hydrogen peroxide, *Anal. Sci.* (2016).
- [28] K. Takayanagi, The oxidation of iodide to iodate for the polarographic determination of total iodine in natural waters, *Talanta* 33 (5) (1986) 451–454.
- [29] H. Vanhoef, F. Van Allemeersch, Effect of solvent type on the determination of total iodine in milk powder and human serum by inductively coupled plasma mass spectrometry, *Analyst* 118 (1993) 1015–1019.
- [30] X. Hou, V. Hansen, A. Aldahan, G. Possnert, O.C. Lind, G. Lujaneni, A review on speciation of iodine-129 in the environmental and biological samples, *Anal. Chim. Acta* 632 (2009) 181–196.
- [31] H.E. Bowley, S.D. Young, E.L. Ander, N.M.J. Crout, M.J. Watts, E.H. Bailey, Iodine binding to humic acid, *Chemosphere* 157 (2016) 208–214.
- [32] C. Hein, J.M. Sander, R. Kautenburger, New approach of a transient ICP-MS measurement method for samples with high salinity, *Talanta* 164 (2017) 477–482.
- [33] A.V. Izmer, S.F. Boulyga, J.S. Becker, Determination of $^{129}\text{I}/^{127}\text{I}$ isotope ratios in liquid solutions and environmental soil samples by ICP-MS with hexapole collision cell, *J. Anal. At. Spectrom.* 18 (2003) 1339–1345.
- [34] K. Nakano, Y. Shikamori, N. Sugiyama, S. Kakuta, Agilent Application Note, 2013, 5990-8171EN.

3.3 Adsorption of caesium on raw Ca-bentonite in high saline solutions: Influence of concentration, mineral composition, other radionuclides and modelling

Extended abstract:

Calcigel was investigated as potential buffer and backfill material for a HLW disposal. Its retention capacity for Cs^+ was determined under varying conditions by laboratory experiments as well as theoretically by the use of geochemical modelling. In the repository, the bentonite will be in contact with cementitious materials which lead to increasing alkalinity of the pore water. Therefore, the experiments were carried out under hyperalkaline conditions (pH 12.5-13). In the model region northern Germany, the host rock pore water can consist of up to 5 M NaCl and it can also interact with the cement. So, beside NaCl with different ionic strengths (0.1, 1, 5 M, pH 13) an ACW ($I \approx 3$ M, pH 12.5) was used as background electrolyte for the adsorption experiments. For the first time, the adsorption of Cs^+ on bentonite was investigated combining such hyperalkaline and high saline conditions.

The Cs^+ adsorption behaviour depended on the initial Cs^+ concentration (5 nM-250 μM) is non-linear. This contributes to the two different adsorption sites for Cs^+ on clays containing mainly montmorillonite such as Calcigel. In accordance with the results for background electrolytes with low ionic strength in the literature, the retention of Cs^+ decreases with increasing ionic strength even in very high saline solutions. The adsorption decreased also with increasing Cs^+ concentration but even in 5 M NaCl at the highest Cs^+ concentration (250 μM) the retention was still around 10%. Since much more bentonite as adsorbent will be used in a HLW disposal compared to these experiments, suitable retention of Cs^+ is also in very high saline solutions very likely.

Besides these experiments, a two-site surface complexation model was developed. With this model it was possible to determine the values of the Cs^+ , K^+ and Ca^{2+} adsorption parameters for Calcigel. The selectivity constants for both binding sites are higher in the case of Cs^+ and lower for the investigated competing ions (K^+ , Ca^{2+}) compared to the literature determined in background electrolytes with lower ionic strength (0.1 M at maximum). This indicates, that the models developed for adsorption experiments in low saline background electrolytes are not absolutely transferable to high saline solutions.

To determine the influence of the inhomogeneity of raw Calcigel, the adsorption of Cs^+ was also investigated on pure Na-montmorillonite in 0.1 M NaCl and ACW, respectively. In the

lower saline solution, the Cs^+ adsorption on Na-montmorillonite did not depend much on the initial Cs^+ concentration and was better reproducible than on Calcigel. In ACW, almost no differences between the two adsorbent materials were visible. There, the influence of the various competing ions in the background electrolyte is bigger than the influence of Calcigel's inhomogeneity.

To simulate realistic conditions in a HLW disposal, the adsorption of Cs^+ on Calcigel was additionally investigated in the presence of Eu^{3+} , UO_2^{2+} and I^- as representatives of other elements contained in HLW. In 0.1 and 1 M NaCl, no differences compared to the single elements experiments could be observed. At higher salinity (ACW, 5 M NaCl), differences occur at the highest and lowest initial Cs^+ concentration. For 5 nM Cs^+ , the retention decreased in ACW and increased in 5 M NaCl in the WC experiments. Since the Cs^+ background of leached Cs^+ out of Calcigel is about 21 nM, this can be contributed to measurement uncertainties. Contrary to this, the Cs^+ retention decreased at 250 μM Cs^+ in both solutions. This effect is also implied in 1 M NaCl. Here, further investigations at higher concentrations or with other additional HLW relevant elements are necessary.

Kristina Brix is the corresponding author and planned, designed and wrote the publication. She carried out all experiments concerning the Ca-bentonite, analysed the samples and interpreted the results. The development of an appropriate ion exchange model and the modelling of the data were also done by Kristina Brix. Christina Hein was involved in planning the experiments and discussion of the results. She also revised the manuscript before publicising. Aaron Haben carried out the experiments concerning Na-montmorillonite and analysed the samples. The interpretation and discussion of the Na-montmorillonite results were done by Aaron Haben under the supervision of Ralf Kautenburger, Christina Hein and Kristina Brix. Ralf Kautenburger had supervision during all the experiments and writing. He was also involved in the discussion of the results as well as design and writing of the publication. He revised the manuscript before publicising.

These results have been published in *Applied Clay Science*.

Brix, K., Hein, C., Haben, A., Kautenburger, R., 2019, *Appl. Clay Sci.* 182, 105275.

<https://doi.org/10.1016/j.clay.2019.105275>

Copyright (2019) Elsevier.

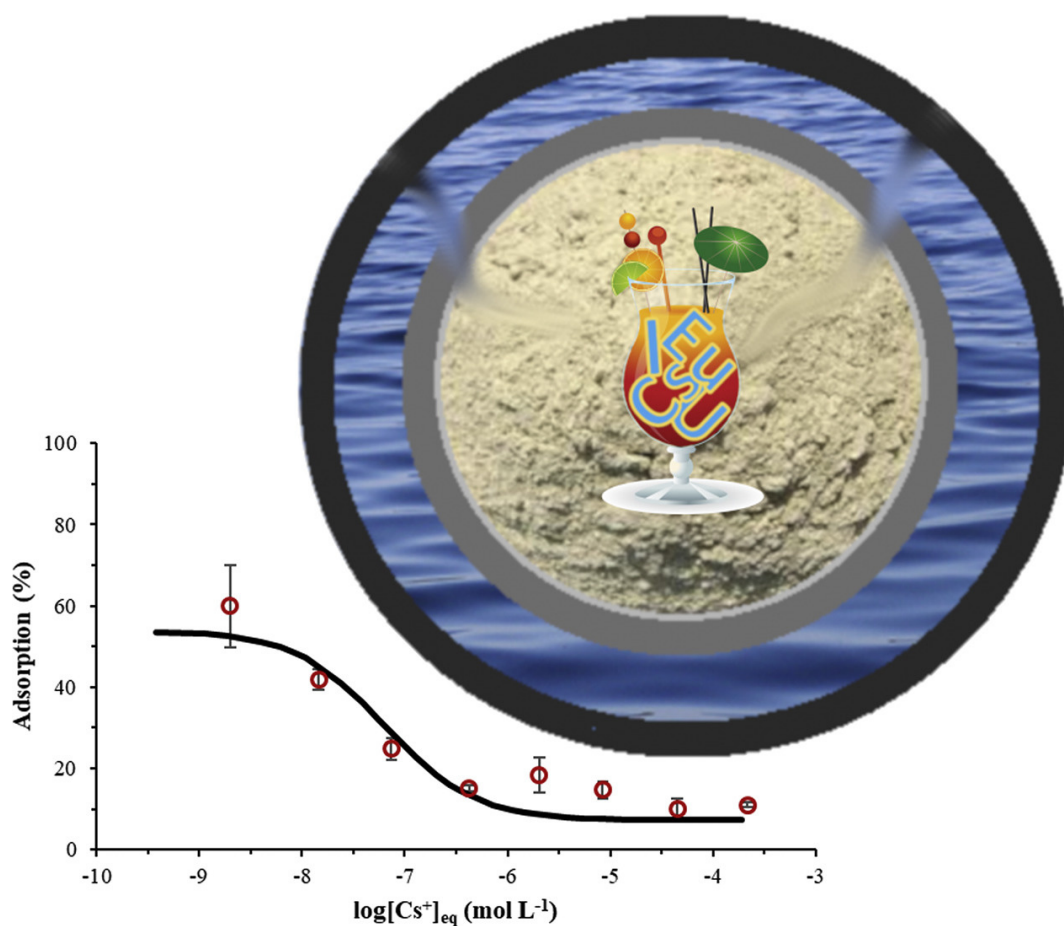


Figure 14. Adsorption and simulation of Cs^+ on Calcigel next to a schematic nearfield of a stored so-called waste cocktail surrounded by bentonite (Graphical abstract of Adsorption of caesium on raw Ca-bentonite in high saline solutions: influence of concentration, mineral composition, other radionuclides and modelling).



Research paper

Adsorption of caesium on raw Ca-bentonite in high saline solutions: Influence of concentration, mineral composition, other radionuclides and modelling

Kristina Brix^{a,*}, Christina Hein^b, Aaron Haben^a, Ralf Kautenburger^a

^a Institute of Inorganic Chemistry – WASTE-Elemental Analysis Group, Saarland University, Saarbrücken, Germany

^b Analytical and Ecological Chemistry, Trier University, Trier, Germany



ARTICLE INFO

Keywords:

Adsorption
Artificial cement pore water
Caesium
High level nuclear waste disposal
Raw bentonite
Specific ion interaction theory

ABSTRACT

Concentration depended retention of Cs⁺ was analysed in alkaline and very high saline solutions (0.1–5 M), mainly NaCl but also in an artificial cement pore water (ACW), representing conditions in a potential high level nuclear waste disposal in northern Germany. Adsorbent agent was Calcigel, a raw Ca-bentonite proposed as a clay based buffer material, which was used as supplied. Batch experiments were carried out in a wide concentration range (5–250,000 nmol L⁻¹) and subsequently, the aqueous phase was analysed via mass spectrometry with inductively coupled plasma (ICP-MS). The adsorption still depended on the Cs⁺ concentration in every medium and decreased with increasing electrolyte concentration, in general. In nanomolar concentration range, the retention was above 50% but dropped rapidly to only approximately 10% when ionic strength exceeded 1 M. The amount of Cs⁺ leached out of the clay appeared to be commensurate with electrolyte concentration. Ion exchange modelling was done using specific ion interaction theory to calculate activity coefficients. Two surface complexations were chosen to describe different adsorption sites on Calcigel. One with high selectivity for Cs⁺ (logK_{Cs} = 8.14) and very low capacity, such as frayed edges sites in micaceous minerals, the other one based on cationic exchange capacity of Calcigel and rather unselective for Cs⁺ (logK_{Cs} = 1.96). With refined selectivity constants, it was possible to describe experimental data quite perfect. However, determined values for constants differ from those found to be best for lower ionic strength. In addition, adsorption on raw Ca-bentonite was compared with that on Na-montmorillonite as a single mineral. Lower dependence on concentration was determined on single mineral in 0.1 M NaCl (79% to 53% adsorption on Na-montmorillonite, 89% to 36% on Ca-bentonite), but at higher ionic strengths the differences between the investigated clays diminished. The Cs⁺ adsorption on Calcigel was also analysed in presence of Eu³⁺, UO₂²⁺ and I⁻, representing potential competing ions attendant in high level nuclear waste. Here, almost no relevant influence could be detected, except at highest investigated concentration and ionic strength > 1 M. At an initial concentration [Cs⁺]_i = 250 μmol L⁻¹, the adsorption declined remarkably in presence of other ions from approximately 10% adsorption to at least 0–5%.

1. Introduction

Nowadays, one great task for humanity is to construct a high level nuclear waste (HLW) repository to protect the environment from radiant material for the next hundreds of thousands of years (Bredehoeft et al., 1978; Weber et al., 2009; Freiesleben, 2013). At this time, worldwide only one HLW repository in granite bedrock is under construction in the municipality Eurajoki, Finland (Miller and Marcos, 2007). The hazardous substances in HLW are mainly uranium, used as nuclear fuel (Bacher, 1949) and a lot of its fission products, e.g. iodine-

129, a highly volatile and because of its anionic character highly mobile beta emitter, which can lead to thyroid cancer after consumption of contaminated foods (Malone et al., 1991). Also, Am and other actinides can cause serious harm to living beings owing to their chemical and radio-toxicity (Breitenstein and Palmer, 1989; Taylor, 1989). But also Cs isotopes, which have a high solubility and mobility (Staunton and Roubaud, 1997; Poinssot et al., 1999; Bradbury and Baeyens, 2000), are part of the nuclear waste. They are considered as the main origin of radioactivity in the first 100 years of a repository (Cherif et al., 2017) and following this, the main source of soil's contamination, if there

* Corresponding author at: Institute of Inorganic Chemistry – WASTE-Elemental Analysis Group, Campus C4.1, 66123 Saarbrücken, Germany.

E-mail address: kristina.brix@uni-saarland.de (K. Brix).

<https://doi.org/10.1016/j.clay.2019.105275>

Received 13 June 2019; Received in revised form 14 August 2019; Accepted 21 August 2019
0169-1317/ © 2019 Elsevier B.V. All rights reserved.

would be a release of radioactivity into the environment (Avery, 1996; Strebl et al., 1999). Furthermore, Cs-135 will even outlast several thousands of years due to its long half-life ($t_{1/2} = 2.3 \cdot 10^6$ years) (Gaboreau et al., 2012).

The international consensus is to build a HLW disposal in deep geological formations (Poinssot et al., 1999; Freiesleben, 2013) such as salt rock, granite bedrock or clay. Northern Germany has a voluminous deposit of clay from lower Cretaceous (Mutterlose and Bornemann, 2000), which is considered as a possible host rock. Because of its contact to present salt rock formations, the supposed clay pore water can consist of up to 5 M NaCl in combination with other, higher charged cations, e.g. Ca^{2+} and Mg^{2+} (Klinge et al., 2002; Boulard and Kautenburger, 2018). Furthermore, cement will be used for construction and as abutment of a potential repository. Over time, the contact with the clay pore water leads to corrosion of the cementitious materials and thus to the formation of a high saline, hyperalkaline solution with pH 12–13 for thousands of years (Berner, 1992; Gaucher and Blanc, 2006; Dauzeres et al., 2010; Kitamura et al., 2013). Despite this, studies concerning Cs^+ adsorption on clay or clay minerals in background electrolytes with pH > 10 are uncommon (Abdel-Karim et al., 2016).

In addition to a potential clay host rock, another sort of clay will be used as a barrier between the radionuclides and the environment. Bentonite, containing mainly montmorillonite, is scheduled as buffer and backfill material (Savage et al., 1999; Becerro et al., 2009; Lommerzheim and Jobmann, 2015). Due to its huge swelling capacity and capability of adsorbing cations on its negatively charged surface, it is predestined to protect the surrounding environment from contamination with radionuclides (Tripathy et al., 2004; Ito, 2006; Lommerzheim and Jobmann, 2015).

To guarantee the long-term safety of a HLW disposal it is not sufficient to investigate the interactions between the technical barriers and radionuclides only at particular circumstances. It is necessary to know all possible and relevant interaction processes from the beginning of the deposition until after several thousand years. With respect to this, geochemical modelling is a helpful tool to predict changes in mineral composition and retention mechanisms. There are different models to describe Cs^+ adsorption onto clays and clay minerals. On illite, it is commonly accepted that there are up to three different adsorption sites based on mineral's cationic exchange capacity (CEC), namely frayed edge sites (FES), type II and planar sites (Poinssot et al., 1999; Bradbury and Baeyens, 2000; Fuller et al., 2014). There is only a small amount of FES (~0.25% of CEC) but they are very sensitive for ions with low hydration energy, e.g. Cs^+ and K^+ and can immobilise the ions irreversibly (Cornell, 1993; Bostick et al., 2002; Vejsada et al., 2005). On these sites, Na^+ has only an impact, when its concentration exceeds this of Cs^+ by some orders (Bradbury and Baeyens, 2000; Vejsada et al., 2005). The main component of bentonite is montmorillonite and there are some slightly different approaches to predict the adsorption behaviour. Missana et al. (2014) suggest two different adsorption sites, which were theoretically described as surface complexes. First site type, called T1, is similar to FES in illite, with a small capacity but high selectivity for Cs^+ . The second binding site, T2, has a higher capacity, which is based on the clay's CEC, but has also a lower selectivity for Cs^+ . Because of this, it can be assumed, that there is a competition effect between different cations on higher metal concentrations. Cherif et al. (2017) proposed a two-site model based on a cationic exchange and a surface complexation site to describe some available experimental data on clay minerals and clays. Such studies are predominantly based on single mineral considerations. In contrast to this, there are no single mineral clay formations in nature. The used materials will be a mixture of different compositions and phases. So it is also necessary to investigate natural materials without pre-treatment such as sieving or acid digestion theoretically and in the laboratory, but currently, there are only a few studies on absolutely raw clays (Hurel et al., 2002; Vejsada et al., 2005; Maes et al., 2008; Baborová et al., 2018).

Additionally, there are even less studies investigating Cs^+ adsorption in solutions with high ionic strengths (Liu et al., 2004) and none combining very high salinity, hyperalkalinity and non-pre-treated clay.

In this study, the retention of Cs^+ on non-pre-treated Calcigel (former Montigel), a raw Ca-bentonite and potential buffer and backfill material in a HLW repository was investigated with laboratory experiments as well theoretically via geochemical modelling. For the first time, both were done in very high saline NaCl based solutions (0.1 to 5 M) under hyperalkaline conditions (pH 12.5–13), reflecting realistic conditions in a HLW repository in northern Germany. For comparison with single clay minerals, the retention on Na-montmorillonite was also investigated. Furthermore, Cs^+ adsorption is widely studied on clay minerals as single element (SE), but rarely in presence of other elements relevant in a HLW disposal (Gutierrez and Fuentes, 1996; Tran et al., 2018). Therefore, the influence of other potential radionuclides in a so called waste cocktail (WC), such as UO_2^{2+} and Eu^{3+} (as homologue for three valent actinides), where precipitation processes can play a major role in retention under the used conditions (Krestou et al., 2004; Naveau et al., 2005; Tertre et al., 2006) and I⁻ as anionic component of HLW on Cs^+ retention was also studied. Altogether this study presents new results for Cs^+ adsorption on a raw Ca-bentonite as buffer and backfill material under conditions close to nature such as hyperalkalinity and very high salinity in a HLW repository in contact to salt rock formations.

2. Materials and methods

2.1. Chemicals and standards

All solutions were prepared with Milli-Q deionised water ($18.2 \text{ M}\Omega \text{ cm}^{-1}$). Single element ICP-Standards of Eu^{3+} (10 g L^{-1} , Merck Millipore, Darmstadt, Germany), I^- (Inorganic Ventures, Christiansburg, USA), UO_2^{2+} (AccuStandard, New Haven, USA), Cs^+ (AccuStandard, New Haven, USA) and Ho(III) (Merck Millipore, Darmstadt, Germany) (each 1 g L^{-1}) with Certipur® quality were used as stock solutions for batch experiments and calibration solutions. The pH values were adjusted with NaOH (30%, suprapure, Merck Millipore, Darmstadt, Germany). NaOCl (8%, p.a.) for the oxidation of I^- to IO_3^- was purchased from AppliChem GmbH (Darmstadt, Germany). For the preparation of background electrolytes, different salts (NaCl , Na_2SO_4 , CaCl_2 , SrCl_2 and KCl) with premium-grade quality (Emsure) from Merck Millipore (Darmstadt, Germany) and Fe^{3+} -, Al^{3+} - and Ba^{2+} -standards (1 g L^{-1}) from Bernd Kraft (Duisburg, Germany) were used. In this study, Calcigel, a raw Ca-bentonite from Bavaria (Clariant, Muttentz, Switzerland) was used as supplied (Table 1). Na-montmorillonite was purchased from abcr GmbH (Karlsruhe, Germany). To realize the acidic measurement conditions, HNO_3 (69%, suprapure) from Carl Roth GmbH + Co. KG (Karlsruhe, Germany) was used. The applied plasma gas was Argon 5.0 (ALPHAGAZ™ 2, Air Liquide, France). Measurements of K^+ concentration were carried out with an Unicam 969 atomic absorption spectrometer (Thermo Scientific, Waltham, USA).

Table 1
Composition of Calcigel (Clariant, 2015).

Mineral	Content [%]
Montmorillonite	60–70
Silica	6–9
Feldspar	1–4
Kaolinite	1–2
Mica	1–6
Others	5–10

2.2. Preparation of solutions

As equilibration media, NaCl based solutions with different concentrations were prepared (0.1, 1, 5 M) and their pH adjusted at 13. In previous experiments, the leaching behaviour of Portland cement under hypersaline conditions was analysed (Boulard and Kautenburger, 2018). Based on these results with diluted Gipshtut solution as reference pore water (PW; 2.5 M NaCl, 0.02 M CaCl₂, 0.02 M Na₂SO₄ and 0.005 M KCl); an artificial cement pore water (ACW) was defined and prepared. The ACW contains 2.46 M NaCl, 32.4 mM CaCl₂·2H₂O, 20 mM Na₂SO₄, 5.1 mM KCl, 0.06 mM SrCl₂·6H₂O, 0.008 mM Fe, 0.005 mM Ba and 0.004 mM Al which were added stepwise to argon flushed Milli-Q water. Due to the flushing, the content of carbon dioxide in the water gets minimised, which prevents the precipitation of carbonates during the following pH adjustment at 12.5 with NaOH.

2.3. Batch experiments and samples for mass spectrometry measurement

The bentonite was not pre-treated but pre-equilibrated before the adsorption batch experiments. For these experiments 10 mL salt solution was added to 40 mg Ca-bentonite ($s/l = 4 \text{ g L}^{-1}$) in a 15 mL centrifuge tube, followed by equilibration in a horizontal shaker (Promax 1020, Heidolph, Schwabach, Germany) at 25 °C for 72 h. After this, analyte was added in different concentrations (5, 25, 100, 500, 2500, 10,000, 50,000 and 250,000 nmol L⁻¹), in WC experiments same concentration was added for each of them. Again, samples were shaken for 72 h. The phase separation was performed in an Eppendorf centrifuge (Centrifuge 5804R, Eppendorf, Hamburg, Germany) with 10,000 rpm (12,857 g) for 10 min at 25 °C. All samples were prepared as triplicates. For ICP-MS measurements without I⁻ from 10 µL to 3.33 mL supernatant (depending on dilution level) were added to 6.36 mL Milli-Q water, 300 µL HNO₃ (69%) and 10 µL Ho (10 ppm stock solution) as internal standard. After this, samples were filled up to a total volume of 10 mL, if necessary. Samples containing I⁻ cannot get measured under acidic conditions directly. The I⁻ forms volatile HI or I₂ and adsorbs on the ICP-MS interface leading to an instable signal and a memory effect. Therefore, I⁻ gets oxidised to IO₃⁻ using 10 µL NaOCl (0.6% stock solution) (Takayanagi, 1986) at least 1 h before adding any acidic solution. Details for preparation can be found elsewhere (Brix et al., 2017). For calibration, solutions in different media with analyte concentrations from 0.5 to 500 nmol L⁻¹ were prepared the same way as samples for ICP-MS measurement.

2.4. Elemental quantification

A commercial ICP-MS system from Agilent (7500cx, Santa Clara, USA) with a Cetac auto sampler (ASX 500) and a high matrix introduction system for higher salt concentrations up to 3% (HMI, Agilent) was used for the quantification of the elements in this study. For samples with low salinity, a default method with operating parameters given in Table 2 has been used. Actually, 1 M NaCl solution has a salt content of nearly 6% and the ionic strength of ACW and 5 M NaCl is even higher. Due to this, a transient ICP-MS method was designed (Hein et al., 2017). This method enables the quantification of elements in up to 5 M saline solution without dilution or sample clean-up steps by

Table 2

Mass spectrometry with inductively coupled plasma (ICP-MS) measurement parameters.

ICP-MS	Agilent 7500cx
RF-power	1550 W
Cooling/auxiliary gas	15.0/1.05 L min ⁻¹
Dwell times	300 ms (3 × 100 ms) per mass
Repetition	3 times

Table 3

Selectivity coefficients logK normalised against Na⁺.

Selectivity coefficient logK	This study	Missana et al. ^a
Cs ⁺ (T1)	8.14	7.64
K ⁺ (T1)	2.20	2.50
Ca ²⁺ (T1)	0.76	0.76
Cs ⁺ (T2)	1.96	1.70
K ⁺ (T2)	0.00	0.57
Ca ²⁺ (T2)	0.00	0.29

^a Missana et al. (2014).

online dilution and decreasing the sample uptake time to only 10 s combined with time-resolved measurement.

2.5. Ion exchange modelling

The modelling of Cs⁺ adsorption was carried out with PHREEQC interactive v3.4 (Parkhurst and Appelo, 2013) using a modified SIT database (Duro et al., 2012). It is based on the work of Missana et al. (2014), where two different adsorption sites were supposed for smectite minerals. Both adsorption sites are described as surface complexes, one with a small capacity and high selectivity for Cs⁺ (T1) and the other one based on cationic exchange capacity of the mineral (T2). Due to equilibration of the Ca-bentonite with NaCl based solutions before the adsorption step, it was assumed for modelling that every exchangeable cation was substituted by Na⁺. Therefore, values for Na-smectite were used and iteratively refined to obtain the best accordance with the experimental data (Table 3). Other data used for modelling was the CEC of Calcigel = 58.7·10⁻⁵ eq g⁻¹ (Clariant, 2015) and the specific surface area = 493 m² g⁻¹ (Müller-Vonmoos and Kahr, 1983). T1 site density of Calcigel was refined in this study and determined to 1.05·10⁻⁵ sites nm⁻². Since Cs⁺ does normally not precipitate (Dzene et al., 2015), except in presence of e.g. activated antigorite (Mg₃Si₂O₅(OH)₄) (Lei et al., 2019), no mineral considerations were included in the model.

In SIT database activity coefficients of ionic species are calculated via specific ion interaction theory (SIT) developed by Brønsted and extended by Guggenheim and Scatchard, which provides reliable results for ionic strengths < 3.5 mol L⁻¹ (Brønsted, 1922; Guggenheim, 1935; Scatchard, 1936; Guggenheim, 1966; Séby et al., 2001). Calculations are based on the Debye-Hückel equation for diluted systems completed by a species interaction coefficient ϵ . These coefficients describe the interactions between oppositely charged ions and were included in the used database as $\epsilon(\text{Cs}^+, \text{Cl}^-) = 0.15$ and $\epsilon(\text{K}^+, \text{Cl}^-) = 0.15$ as proposed for $T = 25 \text{ °C}$ from P. Sipos (2008). Sipo also suggests $\epsilon(\text{Na}^+, \text{Cl}^-) = 0.14$ for NaCl concentrations up to 6 mol L⁻¹, but with respect to this, no compliance could be found between the model and the experimental data anymore. In contrast to this, Preis and Gamsjäger (2001) showed, that the species interaction coefficient $\epsilon(\text{Na}^+, \text{Cl}^-) = 0.03$ by default in SIT database can also be applied for higher NaCl electrolyte concentrations up to 7 mol L⁻¹, which is in good accordance with the experimental data by employing it in the model. PHREEQC input files for SIT modelling based on Table 3 are provided in the supporting information (SI Fig.A1 and Fig.A2).

3. Results and discussions

3.1. Modelling of Cs⁺ retention and influence of ionic strength

Cs⁺ adsorption was investigated at ionic strengths from 0.1 M to 5 M NaCl under alkaline conditions. Fig. 1 gives an overview of the K_d values for different Cs⁺ concentrations at different ionic strengths. Given standard deviations were differences between three independent samples. K_d values decreased almost invariably with increasing Cs⁺ concentration from > 400 L kg⁻¹ to < 200 L kg⁻¹ independent of background electrolyte. Furthermore, K_d tended to decrease with

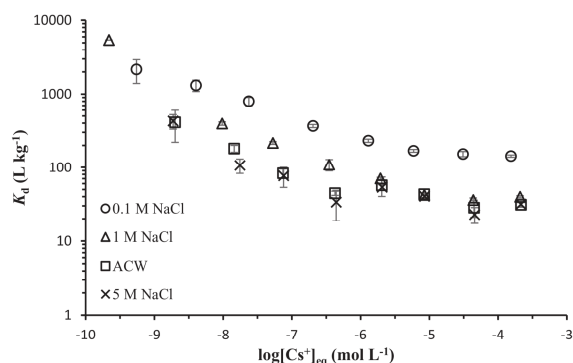


Fig. 1. K_d values of Cs^+ adsorption on Ca-bentonite at different initial concentrations in 0.1 M, 1 M and 5 M NaCl at pH 13 as well as in artificial cement pore water (ACW) at pH 12.5.

increasing ionic strength especially at higher Cs^+ concentrations. These effects were not as distinctive represented in Fig. 1 as they were in absolute, non-logarithmic considerations. Below, to take a closer look at the Cs^+ retention, adsorption is shown in absolute percent and a theoretical model that fits all of the experimental data in this study with one set of parameters is presented.

In 0.1 M NaCl at pH 13 the total Na^+ concentration was about 0.23 mol L^{-1} due to the pH adjustment with NaOH. K^+ content was determined as $30 \mu\text{mol L}^{-1}$ because it was considered as a major competing ion for the specific adsorption sites at low Cs^+ concentrations (Cornell, 1993; Staunton and Roubaud, 1997; Vejsada et al., 2005). Due to its natural composition, it cannot be excluded, that some Cs^+ was leached out of Calcigel during equilibration with the background solution. Leached Cs^+ from Calcigel ($[\text{Cs}^+]_0$) was determined as $[\text{Cs}^+]_0 = 0.5 \text{ nmol L}^{-1}$ after equilibration of Calcigel with this 0.1 M NaCl solution. In Fig. 2 the adsorption of Cs^+ on Calcigel in percent at different concentrations and the modelled adsorption curve is shown. Cs^+ adsorption strongly depended on concentration. This could be attributed to different adsorption sites, named T1 and T2 in the model.

For small initial Cs^+ concentrations ($[\text{Cs}^+]_i \leq 100 \text{ nmol L}^{-1}$) the experimental retention was above 70% with a maximum of $89 \pm 3\%$ at the lowest concentration. The adsorption then decreased slowly to a minimum of 36% at the highest analysed Cs^+ concentration ($250 \mu\text{mol L}^{-1}$). Two plateaus were visible, representing the T1 and T2 sites for Cs^+ adsorption. T1 sites had a capacity of $34.38 \text{ nmol L}^{-1}$, which was in good compliance with the distinctly decreasing of Cs^+ adsorption at concentrations above 25 nmol L^{-1} , the end of the first plateau. The second plateau represented the T2 sites, based on CEC with

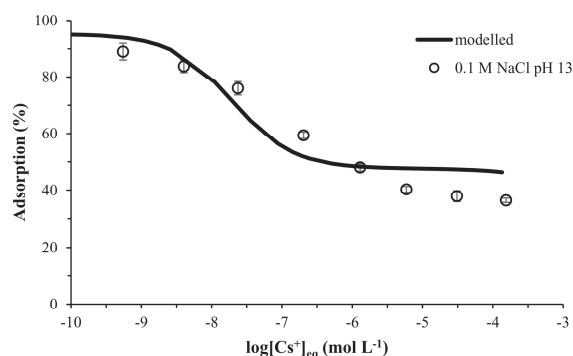


Fig. 2. Concentration depended percentual adsorption of Cs^+ on Calcigel in 0.1 M NaCl at pH 13 and modelled curve using specific ion interaction theory.

a capacity of $2.358 \text{ mmol L}^{-1}$. It began at an initial Cs^+ concentration of $10 \mu\text{mol L}^{-1}$, assigning the area where T1 did not affect the retention anymore. The area between ($[\text{Cs}^+]_i = 100$ to 2500 nmol L^{-1}) represents the concentration range, where both adsorption sites were involved in Cs^+ retention. In the calculated model, the Cs^+ adsorption was overestimated in both plateau areas and seemed to be left-shifted during the slope. For small Cs^+ concentrations, the adsorption was almost quantitative (90–95%), although Na^+ and K^+ were distinctly competing for adsorption places. Due to its high excess compared to K^+ and Cs^+ , Na^+ was occupying most of the T1 sites until $[\text{Cs}^+]_i = 20 \text{ nmol L}^{-1}$, despite an eightfold lower affinity of Na^+ to the T1 sites. K^+ only played a minor role in competing with Cs^+ , even at very low concentrations. The overestimation of adsorption in T1 dominated area by up to 5% indicated, that in the model, a too strong affinity of Cs^+ to this type of sites or too low competition with K^+ were considered. The affinity of Cs^+ was half of an order higher and this of K^+ slightly lower than suggested by Missana et al. (see Table 3), but they were chosen to obtain the best fit for all ionic strengths investigated in this study. An overall discussion of chosen model parameters and comparison between known values in the literature will follow at the end of this section. Examining modelled adsorption on T2 plateau, it was noticeable that the adsorption was overestimated by almost 10%, indicating a too strong affinity of Cs^+ against Na^+ to these sites, similar to T1. The left-shifting of the slope area, which means less retention (around 8–10%) of Cs^+ compared to experimental data, could be avoided by choosing a higher density of T1 sites. At $[\text{Cs}^+]_i = 100 \text{ nmol L}^{-1}$ almost the same amount of Cs^+ was immobilised at T1 and T2 sites indicating the turning point of the modelled curve. In experimental data, this point was approximately reached at $[\text{Cs}^+]_i = 500 \text{ nmol L}^{-1}$.

In summary, Cs^+ adsorption in 0.1 M NaCl at pH 13 on Calcigel was high at small concentrations, even if it does not contain pure montmorillonite, the influence of other minerals and potential inhomogeneity of the adsorption material were not significant in the experiments. The further trend of the adsorption curve was similar: the adsorption slowly decreased but stayed above 35% even for very high Cs^+ concentrations ($250 \mu\text{mol L}^{-1}$). According to the literature, the Cs^+ retention decreased with increasing analyte concentration (Staunton and Roubaud, 1997; Fuller et al., 2014; Missana et al., 2014; Baborová et al., 2018). Also, differences between the independent experiments were with 3% standard deviation at most very small. The modelling fitted almost perfectly the course of the experimental adsorption curve but was a little shifted to mainly higher retention. Differences were maximal about 12% in absolute percentage of adsorption and would seem many times lower considering a logarithmic description of the data.

Increasing the ionic strength from 0.1 M to 1 M NaCl led to a different adsorption curve (Fig. 3). Maximum retention of Cs^+ was achieved with 84% at the lowest investigated concentration $[\text{Cs}^+]_i = 5 \text{ nmol L}^{-1}$. With increasing concentration the adsorption decreased faster than in 0.1 M NaCl until it reached a plateau where approximately 14% of total Cs^+ were immobilised ($[\text{Cs}^+]_i \geq 10 \mu\text{mol L}^{-1}$). The K^+ concentration was determined as $[\text{K}^+] = 39 \mu\text{mol L}^{-1}$ and the leached Cs^+ from Calcigel as $[\text{Cs}^+]_0 = 5 \text{ nmol L}^{-1}$. It is remarkable, that 10-fold increasing of background electrolyte concentration led to a ten times higher value for $[\text{Cs}^+]_0$. This indicated a strong competition for Calcigel's adsorption sites between Na^+ and the Cs^+ natural occurring in this clay, under these conditions. Furthermore, the uncertainty of the lowest investigated Cs^+ concentration increased from 3% (0.1 M NaCl) to 5% and the measured value was not completely trustful anymore, because it was in the range of the background Cs^+ concentration. Nevertheless, the whole measurement row was according to the two sites model.

The Cs^+ adsorption dropped rapidly after the smallest investigated concentration from 84% to 61% inducing a longer, steeper slope as in 0.1 M NaCl, so no T1 plateau was noticeable in the experimental data.

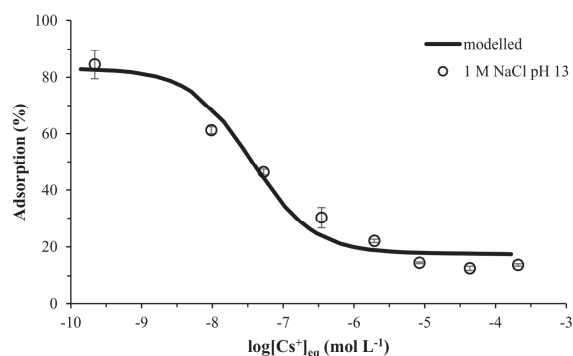


Fig. 3. Concentration depended percentual adsorption of Cs^+ on Calcligel in 1 M NaCl at pH 13 and modelled curve using specific ion interaction theory.

Finally, the adsorption on T2 plateau was over 20% lower in 1 M NaCl compared to 0.1 M NaCl. Modelled data, which fitted experimental data rather perfect at this ionic strength, could give information about whether increased Na^+ or K^+ concentration is responsible for these effects. In the model, contrary to the experiments, a T1 plateau was visible until the total Cs^+ concentration exceeded 20 nmol L^{-1} . In contrast to the lower ionic strength, the amount of K^+ bounded to T1 sites never transcended the amount of Cs^+ . Anymore, the Na^+ concentration at T1 sites exceeded this of Cs^+ until $[\text{Cs}^+]_i = 50 \text{ nmol L}^{-1}$, which was more than double compared to 0.1 M NaCl. Due to these findings, the main competitor for Cs^+ at T1 sites was Na^+ with its very high concentration. K^+ only played a minor role, if any. The perfect fit of the slope hinted to a well-adjusted T1 site density, other than in 0.1 M NaCl. The turning point of the modelled curve was around $[\text{Cs}^+]_i = 300 \text{ nmol L}^{-1}$, where the Cs^+ bounded to T2 sites was only a little bit higher than immobilised at T1 sites. At the T2 plateau, the modelled data overestimates the Cs^+ retention about 3–4%, which was also the area of greatest differences between model and experiments. This also indicated a too high adsorption affinity for T2 sites considered for Cs^+ , but not as distinctive as in 0.1 M NaCl.

Increasing the NaCl concentration around ten times led to a decreasing immobilisation of Cs^+ on Calcligel. This effect was even more drastic at high Cs^+ concentrations, where only 14% of the total Cs^+ could adsorb. With a 5% standard deviation at maximum in all cases, the results were well reproducible. These experimental findings were almost in perfect agreement with the proposed model for Cs^+ adsorption on raw Calcligel. Due to the excess of Na^+ , the leached K^+ only played a minor role in competing for adsorption places.

In ACW, the analysed solution which simulates realistic conditions for the technical barrier in a HLW, not only the NaCl concentration was increased up to 2.5 M, there were also a lot of other potential competing cations for Cs^+ in comparatively high concentrations. The main competitors next to Na^+ were considered K^+ with a content of 5.1 mmol L^{-1} and Ca^{2+} with 32.4 mmol L^{-1} in ACW. Ca^{2+} also occurs naturally in Calcligel since it is a Ca-bentonite, but its affinity to binding sites was low compared to this of Cs^+ and K^+ , so it was only considered in ACW because of its comparatively high concentration in the solution. The amount of Cs^+ leached out of the clay was determined as $[\text{Cs}^+]_0 = 16 \text{ nmol L}^{-1}$. Again, the leached Cs^+ seemed to be commensurate to the ionic strength of the background solution, increasing around three times by raising the ionic strength from 1 M to approximately 3 M. In Fig. 4 the concentration depended adsorption of Cs^+ on Calcligel in ACW is shown. Similar to the results in 1 M NaCl, the uncertainty of the lowest investigated Cs^+ concentration increased (10%), probably due to the high background of Cs^+ leached out of Calcligel. Since the background value exceeded the experimental concentration, results have to be considered carefully.

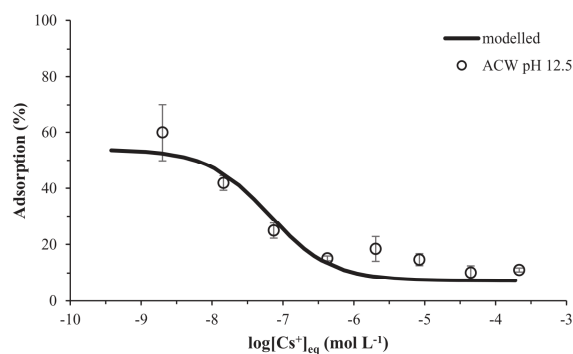


Fig. 4. Concentration depended percentual adsorption of Cs^+ on Calcligel in artificial cement pore water (ACW) at pH 12.5 and modelled curve using specific ion interaction theory.

As already seen in 1 M NaCl, high adsorption ($> 50\%$) could only be achieved at the lowest analysed Cs^+ concentration, so no T1 plateau could be seen in the experimental data. Afterwards, the retention decreased already at lower initial concentrations compared to the experiments discussed before to a plateau where only 10–18% of the total Cs^+ were immobilised. Maximum adsorption was about $60 \pm 10\%$, decreasing with increasing Cs^+ concentration to $42 \pm 3\%$ followed by $25 \pm 3\%$, reaching the T2 plateau with a retention of $15 \pm 1\%$ at a comparatively low initial concentration of 500 nmol L^{-1} . At $[\text{Cs}^+]_i = 2.5 \mu\text{mol L}^{-1}$ the adsorption seemed to rise again ($18 \pm 4\%$), but with respect to the measurement uncertainties, the curve's trend remained constant. The adsorption minimum was about $10 \pm 2\%$ at $[\text{Cs}^+]_i = 50 \mu\text{mol L}^{-1}$. Similar to 1 M NaCl, the modelled curve based on refined modelling parameters described the experimental data rather perfect. A T1 plateau was visible in this curve up to $[\text{Cs}^+]_i = 15 \text{ nmol L}^{-1}$. As a result of their high concentrations, besides Na^+ , K^+ and Ca^{2+} occupied more T1 sites than Cs^+ at the lowest modelled concentration (1 nmol L^{-1}). With increasing Cs^+ concentration this effect diminished through the extrusion of K^+ and Ca^{2+} . At a concentration of 50 nmol L^{-1} Cs^+ occupied the most of available T1 adsorption sites, similar as in 1 M NaCl. The slope could be fitted very well. This indicated again, the implemented T1 site density in the model was close to the real value for raw, non-treated Calcligel. The turning point of the modelled curve, where Cs^+ adsorption at the T2 sites exceeded the amount at the T1 sites, was between $[\text{Cs}^+]_i = 500 \text{ nmol L}^{-1}$ and 1000 nmol L^{-1} , which also marked the beginning of the T2 plateau. An explanation for this is the strong competition for adsorption places at both sites under these conditions, even if the affinity from K^+ and Ca^{2+} to T2 sites was not higher than that of Na^+ . The retention of Cs^+ in the area of the T2 plateau was with 7–11% underestimated in the model by 3–4% compared to the experimental data. This value equalled the overestimation in 1 M NaCl and could only be explained by a too low affinity of Cs^+ for T2 sites compared to K^+ , Ca^{2+} and Na^+ or a too small capacity of T2 sites. The latter was not very likely since the T2 sites were considered to be only depending on the CEC of the clay.

Compared to pure 1 M NaCl solution, the Cs^+ adsorption in ACW as a very complex medium was not dramatically reduced. Additional K^+ and Ca^{2+} from ACW mainly affected the Cs^+ specific T1 sites at small concentrations leading to a smaller precentral adsorption maximum. Increasing the Na^+ concentration once more to 2.5 M was responsible for a shift of the beginning of T2 plateau to smaller initial Cs^+ concentrations. Differences between independent experiments were especially noticeable at the smallest investigated concentration (10%), because of the high background value of Cs^+ leached out of Calcligel. Other differences were not $> 4\%$ at most. Similar to 1 M NaCl, the modelled curve was in very good compliance with the experimental

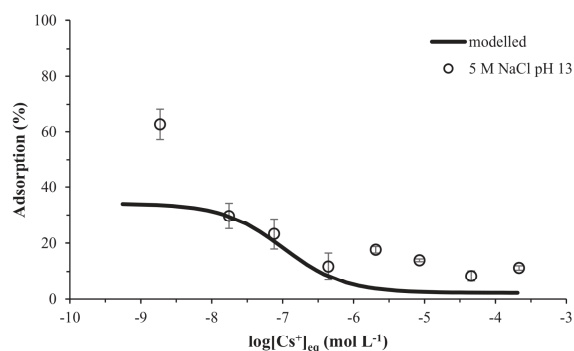


Fig. 5. Concentration depended percentual adsorption of Cs⁺ on Calcigel in 5 M NaCl at pH 13 and modelled curve using specific ion interaction theory.

data.

Finally, the Cs⁺ retention was analysed in 5 M NaCl solution. The K⁺ content was found to be 74 μmol L⁻¹, which doubled the value found in 1 M NaCl solution. This indicated no linear correlation between the ionic strength and the amount of K⁺ leached out of the bentonite. However, the leached Cs⁺ concentration was about 21 nmol L⁻¹. This was near the extrapolated value from the other background solutions [Cs⁺]₀ = 25 nmol L⁻¹, indicating one more time a linear correlation between the ionic strength and leached Cs⁺. Again, the lowest investigated Cs⁺ concentration by experiments was lower than the leached Cs⁺ background level. The outcome of this were significant uncertainties in independent experiments at this concentration (5%) and a not completely trustful absolute adsorption value for [Cs⁺]_i = 5 nmol L⁻¹.

In Fig. 5 the adsorption of Cs⁺ on Calcigel in 5 M NaCl solution is shown. The concentration dependence of Cs⁺ retention decreased significantly compared to the solutions with lower salinity, especially 0.1 M or 1 M NaCl solution. At [Cs⁺]_i = 5 nmol L⁻¹, the experimentally determined adsorption was about 63 ± 5%, rapidly decreasing to 30 ± 5% and 23 ± 5% at the following concentrations. Subsequently, the adsorption reached a plateau where only 8–18% of the total Cs⁺ were immobilised. In the experimental data, no T1 plateau was visible as it was the case for former media except for 0.1 M NaCl. Contrary to the solutions with lower salinity, the modelled curve could not describe the trend of the experiments entirely. The adsorption was underestimated in every area except the slope. In the T1 dominated area, a plateau was visible in the model up to [Cs⁺]_i = 25 nmol L⁻¹, but the maximum retention was about 30% lower than in the experiments. Possible reasons for this were a too low selectivity for Cs⁺ at T1 sites, which was in contrary to the other media or the uncertainty of first experimental measurement value. It is also mentionable, that a better agreement with the model and experiments could be reached by lowering T1 site density leading to a steeper slope instead of a plateau. As observed previously, K⁺ only played a minor role in inhibiting the Cs⁺ adsorption. In the area of the T2 plateau, the adsorption of Cs⁺ was almost completely suppressed by Na⁺. This also indicated a too low affinity of Cs⁺ to T2 sites compared to the experiments, where the adsorption of around 10% of total Cs⁺ still took place.

Summing up, the adsorption of Cs⁺ on raw Ca-bentonite depended on the Cs⁺ concentration in all investigated media. With increasing ionic strength this dependence decreased such as the adsorption by itself. For solutions with lower salinity, this relation was already known in the literature (Missana et al., 2014; Staunton and Roubaud, 1997; Vejsada et al., 2005), so the results of this study are in good compliance with these findings. K⁺ and Ca²⁺ played only a minor role in the inhibition of Cs⁺ retention when the Na⁺ concentration was in so many orders higher than the concentration of K⁺ and Ca²⁺. Despite this, the

influence of K⁺ and Ca²⁺ on the Cs⁺ retention on Calcigel was only relevant, when their concentration ratio in the background solution compared to Na⁺ was in the same range like it was in ACW. There was almost no difference in the retention rate of Cs⁺ at high concentrations (≥ 10 μmol L⁻¹) in solutions with salinity greater-than-or-equal-to 1 M NaCl. The retention was with at least about 8–18% not very effective but it still existed. The introduced model for the Cs⁺ adsorption on raw Calcigel, containing different minerals, in high saline solutions, was almost always in very good compliance with the experimental data. There were some small differences in absolute values: the adsorption tended to get overrated in 0.1 M and 1 M NaCl and underestimated in ACW and 5 M NaCl, particularly in the T2 area. One explanation can be the neglect of secondary minerals. In high saline solutions, especially at non-natural pH values such as 13, mineral phases can dissolve and others can be formed and precipitate (Gates and Bouazza, 2010; Gaucher and Blanc, 2006; Ye et al., 2016). This can lead to different selectivity constants for the clay mixture under varying conditions. Following this, the set of parameters for modelling had not to be the same for every medium, same applied for the CEC, which can change too. As an example, the T1 site density was underrated in 0.1 M NaCl. Leaching and dissolving of minerals at higher ionic strengths could lead to more competing cations in solution. If they occupied the T1 sites in reality and were not considered in the model, a lower amount of these sites had to be implemented in the model to match the experimental data. Another reason can be the use of raw Ca-bentonite and consequently the inhomogeneity of this material. Only 40 mg were used for each batch experiment, so there was no guarantee, that every 40 mg always consisted of the same amount of the same mineral phases. Furthermore, the selectivity constants for Cs⁺ adsorption on Calcigel were significantly higher than Missana et al. determined for smectite minerals. Equally, those for K⁺ and Ca²⁺ were lower (see Table 3). Modelling retention in 0.1 M (and more concentrated) NaCl via Davies equation (Davies, 1938) valid for ionic strengths < 0.5 M instead of SIT led to a different set of ideal parameters (SI Table A1 and Fig. A3–6). These Davies-gained selectivity constants were in better agreement with those proposed from Missana et al. These findings indicate, that ideal adsorption parameters determined via Davies equation have not to be completely transferable to very high ionic strengths and vice versa. Same hinted the SIT modelling using parameters suggested by Cherif et al. (2017) leading to a partial drastic overestimation of the Cs⁺ retention at T1 sites and a continuous underrating at T2 sites (SI Fig. A7–10). The here presented selectivity coefficients (Table 3) were refined to describe our experimental data in absolute, non-logarithmic values best and consistent. With a few exceptions, it was possible to simulate the Cs⁺ adsorption on raw bentonite theoretically in very high saline and complex solutions almost perfect.

3.2. Comparison with pure montmorillonite

The retention potential of raw Ca-bentonite was compared with this of a pure Na-montmorillonite mineral. In high saline solutions, it is assumed that the natural exchangeable cations in the clay get substituted by the cations of the background electrolyte (Staunton and Roubaud, 1997; Poinssot et al., 1999; Missana et al., 2014). Therefore, every Ca²⁺ located in the interlayer of Calcigel was expected to be exchanged with Na⁺ during pre-equilibration. In a potential HLW repository, this would be the case, when the pore water of the surrounding host rock gets in contact with the buffer material before the radionuclides get released out of the containers.

Fig. 6 gives an overview of the Cs⁺ adsorption on Calcigel and Na-montmorillonite in 0.1 M NaCl at pH 13, respectively. Additionally, the standard deviations of three independent experiments are shown. First, different trends of the adsorption curves were noticeable. For Calcigel a clear dependence on the Cs⁺ concentration was visible (as discussed in Section 3.1), for Na-montmorillonite this could not be seen directly. *K_d* values were ranging between 1000 and 300 over the whole

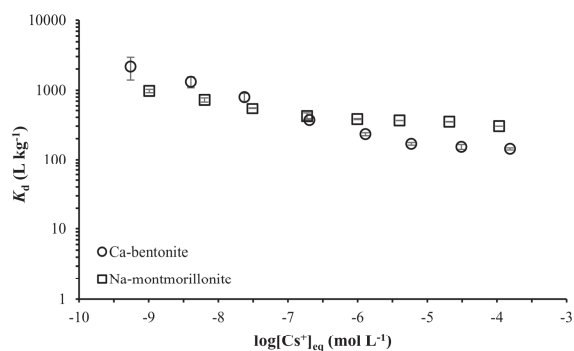


Fig. 6. Concentration depended K_d values of Cs^+ adsorption on Ca-bentonite and Na-montmorillonite in 0.1 M NaCl at pH 13.

concentration range, decreasing slightly with increasing concentration. In the literature, maximal analytical uncertainties are often given only as a constant value for all measurement results such as $\log K_d \pm 0.15$ (Bradbury and Baeyens, 2000; Missana et al., 2014) or $\log K_d \pm 0.2$ (Chikkamath et al., 2019), with respect to this, no significant differences would be found between the adsorption on Calcigel and Na-montmorillonite (SI Fig. A11).

To get a closer look at the adsorption behaviour of Cs^+ on raw bentonite and the clay mineral a percentual application of the Cs^+ retention is given in the next figures. In Fig. 7 the percentual adsorption of Cs^+ on Ca-bentonite and Na-montmorillonite is shown. With this approach, more differences between the raw bentonite and the montmorillonite mineral could be seen, especially at higher Cs^+ concentrations. The Cs^+ adsorption on Na-montmorillonite was with 80% at maximum 9–10% lower than the adsorption on Calcigel in the T1 dominated area. At $[\text{Cs}^+]_i = 500 \text{ nmol L}^{-1}$ both graphs were crossing and the amount of immobilised Cs^+ was almost equal for both adsorbing materials. Afterwards, the adsorption on Calcigel decreased remarkably to a minimum of 36% whereas the adsorption on Na-montmorillonite remained almost constant above 50%. Differences in both clays were at first the content of montmorillonite. Na-montmorillonite consists of pure montmorillonite whereas Calcigel is a mixture of varying minerals, containing 60–80% montmorillonite. Since in every batch experiment 40 mg of solid was used, montmorillonite-content, considered as main mineral responsible for the Cs^+ retention in Calcigel, differed by up to 40%. This could be the reason for a lower adsorption on Calcigel at high Cs^+ concentrations. Also, Calcigel is a raw clay where a lot of potential competing cations could get leached out occupying the adsorption sites in the clay interlayer, whereas in Na-montmorillonite only Na^+ should play a significant role. Contrary to

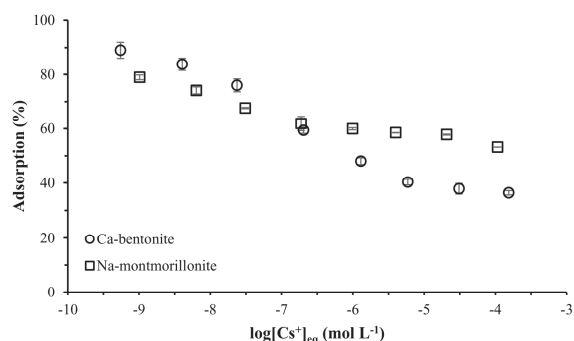


Fig. 7. Percentual retention of Cs^+ on Ca-bentonite and Na-montmorillonite in 0.1 M NaCl at pH 13 for different concentrations.

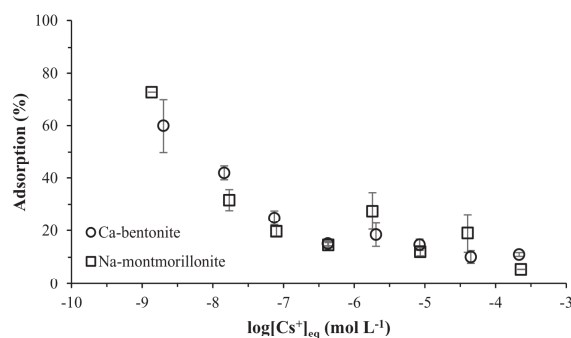


Fig. 8. Percentual retention of Cs^+ on Ca-bentonite and Na-montmorillonite in artificial cement pore water (pH 12.5) at different concentrations.

this, the leached K^+ content from Na-montmorillonite was determined to $68 \mu\text{mol L}^{-1}$ which approximately doubled the value leached out of Calcigel under these conditions ($30 \mu\text{mol L}^{-1}$). However, this can be an explanation for the lower retention of Cs^+ on the single mineral at low concentrations. The influence of K^+ as a competitor to Cs^+ is the highest in T1 dominated area. In conclusion, the Cs^+ adsorption on Na-montmorillonite did not depend on concentration as much as in Ca-bentonite and the deviations between independent experiments were smaller in the homogeneous material. This finding is in a good agreement with actual results for Cs^+ adsorption onto SWy-1 montmorillonite from the Clay Minerals Repository (Durrant et al., 2018).

The comparison between the raw clay and the homogeneous montmorillonite was also drawn in ACW as complex, but close to a real pore water solution, typical for a HLW disposal containing cement or concrete as one of the technical barriers. In Fig. 8 the retention of Cs^+ on Calcigel and the clay mineral in ACW is shown. At this very high ionic strength, there were almost no noticeable differences between the two materials. For the lowest Cs^+ concentration, the retention was about $73 \pm 0\%$ in Na-montmorillonite compared to $60 \pm 10\%$ in Calcigel, but with respect to standard deviations, this difference was not significant. However, an explanation for these potential differences can be again the divergence in amount of the mineral responsible for the Cs^+ adsorption. At higher concentrations, the increase of the standard deviation for the pure mineral and the amount of immobilised Cs^+ was about the same as in Ca-bentonite (16%). In contrast to 0.1 M NaCl, in ACW are many different cations, which can compete with Cs^+ for the adsorption sites resulting in a lower Cs^+ retention over the whole analysed concentration range. Due to this, the inhomogeneity of Calcigel and its potential leached out cations had no significant effect on the Cs^+ retention anymore, so the adsorption was almost equal between the natural material and the pure clay mineral.

The comparison of the Cs^+ retention on Calcigel with pure Na-montmorillonite led to different results in the used background solutions. In 0.1 M NaCl solution, the inhomogeneity of Calcigel had a visible effect on the Cs^+ adsorption in contrast to ACW with an ionic strength of about 3 M and remarkable differences could be seen between the two investigated adsorption agents. In most cases, the presence of competing cations in Ca-bentonite led to a lower percentual adsorption. The same trend has been found by Semenkova et al. (2018), where the highest adsorption of Cs^+ on raw bentonite (Kutch clay) was one order of magnitude ($\log K_d \approx 3$) lower compared to purified Kutch clay ($\log K_d \approx 4$), where potential competing cations are already leached out. Other results could be found in ACW. Here, almost no differences could be observed, because of the bulk of different, high concentrated cations (compared to initial Cs^+ concentration) already existing in the solution.

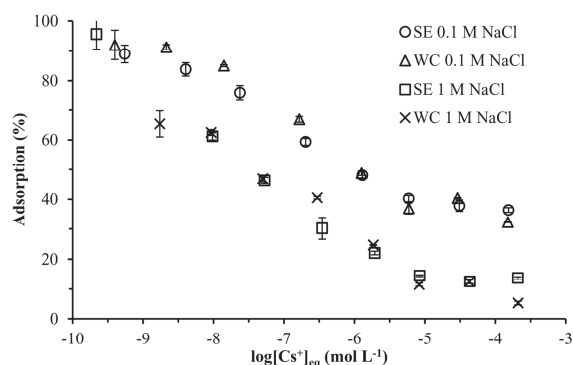


Fig. 9. Concentration depended percentual adsorption of Cs^+ on Calcigel in 0.1 M and 1 M NaCl (pH 13, respectively) investigated as single element (SE) and waste cocktail (WC, including UO_2^{2+} , Eu^{3+} , Cs^+ and I^-).

3.3. Influence of Eu^{3+} , UO_2^{2+} and I^-

Just as no single mineral or pre-treated clay will be installed in a HLW disposal, Cs will not be stored isolated from other radionuclides in the nuclear waste. If there is a release out of the containers someday, it will be a cocktail of different radionuclides encountering the buffer material, which was represented by Calcigel in this study. Therefore, the Cs^+ adsorption on Calcigel was also investigated in the presence of other radionuclides, namely UO_2^{2+} as unspent nuclear fuel, Eu^{3+} in representation of three-valent actinides such as Am^{3+} and I^- as a fission product of UO_2^{2+} and anionic component of HLW. In Fig. 9 the percentual adsorption of Cs^+ on Calcigel in 0.1 M and 1 M NaCl is shown as SE and in the WC. The results for UO_2^{2+} , Eu^{3+} and I^- are not shown here. However, since there is a change in the swelling capacity and permeability of montmorillonite depended on whether Na^+ or Cs^+ is the major interlayer cation (Takahashi and Tachi, 2019), differences in the retention behaviour of at least UO_2^{2+} and Eu^{3+} are expected.

Adsorption strongly depended on the initial Cs^+ concentration under all investigated conditions. In 0.1 M NaCl, only small differences between SE and WC experiments could be seen in the slope area, where small discrepancies have the highest impact, but the trend remained the same. At higher salinity (1 M), the retention data was equal for SE and WC except at three measurement points. The discrepancy of 10% in the slope ($[\text{Cs}^+]_i = 500 \text{ nmol L}^{-1}$) could be attributed to small uncertainties concerning the experiments. This point should be a little higher in SE and a little lower in WC experiments, following the curve's trend exactly. At the highest investigated Cs^+ concentration, the adsorption in WC almost vanished ($5 \pm 1\%$), which could indicate a competing or another negative effect of UO_2^{2+} , Eu^{3+} or even I^- at very high concentrations. It would be interesting if this effect is reproducible holding either the Cs^+ or the concentration of other ions constant at $250 \mu\text{mol L}^{-1}$. The most discrepancy could be seen at the lowest Cs^+ concentration where the adsorption was about $95 \pm 5\%$ in SE in contrast to only $65 \pm 4\%$ in WC experiments. This significant decrease of the Cs^+ adsorption indicated a strong competition between Cs^+ and either other elements relevant for HLW or ions leached out of the clay due to their presence. Since no relevant increase in the retention of other ions in the WC could be observed (non-published data), the latter is more likely. Altogether, in 0.1 M and 1 M NaCl, waste cocktail ions only had a minor impact on the immobilisation of Cs^+ in the analysed concentration range, if any, except at the lowest and highest analysed concentrations in 1 M solution.

In Fig. 10 the Cs^+ retention in ACW and 5 M NaCl is constituted at different concentrations determined via SE and WC experiments. As seen before in solutions with lower salinity, there were no great differences between the SE and WC measurements. Additionally, there

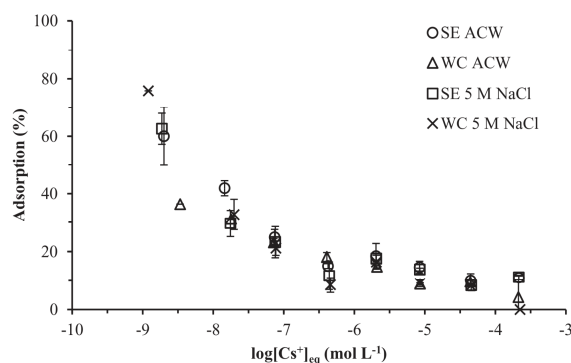


Fig. 10. Concentration depended percentual adsorption of Cs^+ on Calcigel in artificial cement pore water (ACW, pH 12.5) and 5 M NaCl (pH 13) investigated as single element (SE) and waste cocktail (WC, including UO_2^{2+} , Eu^{3+} , Cs^+ and I^-).

were almost no discrepancies between the two considered media. The adsorption rapidly decreased from 60% to around 10% at higher concentrations. Equal to 1 M NaCl, the greatest differences between SE and WC could be seen at the lowest and the highest initial Cs^+ concentration. At $[\text{Cs}^+]_i = 5 \text{ nmol L}^{-1}$ the retention was higher in WC than in SE in 5 M NaCl and lower in ACW. In ACW the effect could be regarded to be similar as in 1 M NaCl, that cations leached out of the clay due to the occurrence of other HLW relevant elements competed against Cs^+ for adsorption places. On the contrary to ACW, in 5 M NaCl, the Cs^+ retention was apparently increasing with additional ions in solution. If the reason for this was a precipitate caused by UO_2^{2+} , Eu^{3+} or I^- containing Cs^+ e.g. as co-precipitate, this effect should even be greater at higher concentrations. Most likely this phenomenon could be attributed to measurement uncertainties resulting from Cs^+ background (21 nmol L^{-1}) exceeding the analysed concentration. Moreover, it cannot be said, that this is not also the explanation for the effect in ACW ($[\text{Cs}^+]_0 = 16 \text{ nmol L}^{-1}$). At the highest analysed concentration, the adsorption was noticeably lower in presence of the WC than in SE experiments, as seen in 1 M NaCl before. The reproducibility of this effect is very high saline solutions indicated, that a real competing effect is very likely. Summarising the Cs^+ adsorption results for the SE and WC experiments, the main influence on the Cs^+ retention on Calcigel could be attributed to the salinity of the pore water solution. Further investigations as mentioned above have to be done here.

4. Conclusion

For the first time, Cs^+ adsorption on non-pre-treated, raw Ca-bentonite was investigated via batch experiments and simulated with ion exchange modelling combining hyperalkaline (pH 12.5–13) and high saline (up to 5 M) adsorption conditions. Overall, the Cs^+ adsorption especially depended on its initial concentration in all used background solutions (0.1, 1, 5 M NaCl) also in the artificial cement pore water ($I \approx 3 \text{ M}$) realistic e.g. for a HLW disposal in northern Germany. In the nanomolar Cs^+ concentration range, the retention was still above 50% under all investigated conditions, but dropped rapidly with the increasing Cs^+ concentration when the ionic strength exceeds 1 M. This influence of the highly selective Cs^+ binding sites even under the drastic conditions used in this study should be considered when scheduling a HLW repository. For modelling the Cs^+ adsorption on Calcigel, a SIT based two site model was proposed, which simulated the experimental data in absolute values very good. The gained selectivity constants for Cs^+ differ from those in literature calculated for lower ionic strengths via Davies equation, but are in the same order of magnitude. It is noticeable, that the influence of K^+ and Ca^{2+} as competitor

for Cs⁺ at T2 binding sites vanished in the investigated high saline solutions.

Especially in the comparatively low saline solution (0.1 M NaCl), some differences between the natural material and pure Na-montmorillonite were visible, showing the necessity to analyse not only single mineral phases. Those diminished with increasing ionic strength, due to the high excess of the electrolyte ions compared to the leached competing ions from the clay and the clay mineral. Furthermore, the influence of selected other elements relevant in HLW (Eu³⁺, UO₂²⁺, I⁻) on the Cs⁺ immobilisation was mainly visible at very low Cs⁺ concentrations (5 nmol L⁻¹) as well as at the highest investigated concentration (250 μmol L⁻¹). Here, further experiments have to be done to investigate this effect, also with other competing elements, to simulate geochemical conditions close to nature.

Acknowledgement

This work was supported by the German Federal Ministry of Economics and Energy (BMWV), represented by the Project Management Agency Karlsruhe (PTKA-WTE) (grant numbers O2E10991 and O2E11415D), and we would like to thank our project partners for the kind collaboration.

Appendix A. Supplementary data

Supplementary data to this article can be found online at <https://doi.org/10.1016/j.clay.2019.105275>.

References

Parkhurst, D.L., Appelo, C.A.J., 2013. Description of input and examples for PHREEQC Version 3-a computer program for speciation, batch-reaction, one-dimensional transport, and inverse geochemical calculations. In: U.S. Geological Survey, Chapter 43 of Section A, Groundwater Book 6, Modeling Techniques.

Tertre, E., Berger, G., Simoni, E., Castet, S., Giffaut, M., Loubet, E., Catalette, H., 2006. Europium retention onto clay minerals from 25 to 150 °C: experimental measurements, spectroscopic features and sorption modelling. *Geochim. Cosmochim. Acta* 70, 4563–4578. <https://doi.org/10.1016/j.gca.2006.06.1568>.

Abdel-Karim, A.M., Zaki, A.A., Elwan, W., El-Naggar, M.R., Gouda, M.M., 2016. Experimental and modelling investigations of cesium and strontium adsorption onto clay of radioactive waste disposal. *Appl. Clay Sci.* 132–133, 391–401. <https://doi.org/10.1016/j.clay.2016.07.005>.

Avery, S.V., 1996. Fate of caesium in the environment: distribution between the abiotic and biotic components of aquatic and terrestrial ecosystem. *J. Environ. Radioact.* 30 (2), 139–171. [https://doi.org/10.1016/0265-931X\(96\)89276-9](https://doi.org/10.1016/0265-931X(96)89276-9).

Baborová, L., Vopálka, D., Cervinka, R., 2018. Sorption of Sr and Cs onto Czech natural bentonite: experiments and modelling. *J. Radioanal. Nucl. Chem.* 318, 2257–2262. <https://doi.org/10.1007/s10967-018-6196-3>.

Bacher, R.F., 1949. The development of nuclear reactors. *Bull. Am. Acad. Arts Sci.* 2 (6), 2–4. <https://doi.org/10.2307/3823874>.

Becerro, A.I., Mantovani, M., Escudero, A., 2009. Mineralogical stability of phyllosilicates in hyperalkaline fluids: influence of layer nature, octahedral occupation and presence of tetrahedral Al. *Am. Mineral.* 94, 1187–1197. <https://doi.org/10.2138/am.2009.3164>.

Berner, U.R., 1992. Evolution of pore water chemistry during degradation of cement in a radioactive waste repository environment. *Waste Manag.* 12, 201–219. [https://doi.org/10.1016/0956-053X\(92\)90049-O](https://doi.org/10.1016/0956-053X(92)90049-O).

Bostick, B.C., Vairavamurthy, M.A., Karthikeyan, K.G., Chorover, J., 2002. Cesium adsorption on clay minerals: an EXAFS spectroscopic investigation. *Environ. Sci. Technol.* 36, 2670–2676. <https://doi.org/10.1021/es0156892>.

Boulard, L., Kautenburger, R., 2018. Short-term elemental release from Portland cement concrete by hypersaline leaching conditions. *Adv. Cem. Res.*, 1800085. <https://doi.org/10.1680/jadcr.18.00085>.

Bradbury, M.H., Baeyens, B., 2000. A generalised sorption model for the concentration dependent uptake of caesium by argillaceous rock. *J. Contam. Hydrol.* 42, 141–163. [https://doi.org/10.1016/S0169-7722\(99\)00094-7](https://doi.org/10.1016/S0169-7722(99)00094-7).

Bredelhoeft, J.D., England, A.W., Stewart, D.B., Trask, N.J., Winograd, I.J., 1978. Geologic disposal of high-level radioactive wastes—earth-Science perspectives. *U.S. Geological Survey* 779. <https://doi.org/10.3133/cir779>.

Breitenstein, B.D., Palmer, H.E., 1989. Lifetime follow-up of the 1976 americium accident victim. *Radiat. Prot. Dosim.* 26 (1), 317–322. <https://doi.org/10.1093/oxfordjournals.rpd.a080424>.

Brix, K., Hein, C., Sander, J.M., Kautenburger, R., 2017. Simultaneous quantification of iodine and high valent metals via ICP MS under acidic conditions in complex matrices. *Talanta* 167, 532–536. <https://doi.org/10.1016/j.talanta.2017.02.056>.

Brønsted, J.N., 1922. Studies on Solubility. IV. The principle of the specific interactions of

ions. *J. Am. Chem. Soc.* 44, 877–898. <https://doi.org/10.1021/ja01426a001>.

Cherif, M.A., Martin-Garin, A., Gérard, F., Bildstein, O., 2017. A robust and parsimonious model for caesium sorption on clay minerals and natural clay minerals. *Appl. Geochem.* 87, 22–37. <https://doi.org/10.1016/j.apgeochem.2017.10.017>.

Chikkamath, S., Patel, M.A., Kar, A.S., Raut, V.V., Tomar, B.S., Manjanna, J., 2019. Sorption of Cs(I) on Fe-montmorillonite relevant to geological disposal of HLW. *Radiochim. Acta* 107 (5), 387–396. <https://doi.org/10.1515/ract-2018-3016>.

Clariant, 2015. Product Information: Calcigel, Switzerland.

Cornell, R.M., 1993. Sorption of cesium on minerals: a review. *J. Radioanal. Nucl. Chem.* 171, 483–500. <https://doi.org/10.1007/BF02219872>.

Dauzeres, A., Le Bescop, P., Sardini, P., Cau Dit Coumes, C., 2010. Physico-chemical investigation of clay/cement-based materials interaction in the context of geological waste disposal: experimental approach and results. *Cem. Concr. Res.* 40, 1327–1340. <https://doi.org/10.1016/j.cemconres.2010.03.015>.

Davies, C.W., 1938. The extent of dissociation of salts in water. Part VIII. An equation for the mean ionic activity coefficient of an electrolyte in water, and a revision of the dissociation constants of some sulphates. *J. Chem. Soc.* 2093–2098. <https://doi.org/10.1039/JR9380002093>.

Duro, L., Grivé, M., Giffaut, E., 2012. ThermoChimie, the ANDRA Thermodynamic Database. *Mater. Res. Soc. Symp.* 1475, 589–592. <https://doi.org/10.1557/opl.2012.637>.

Durrant, C.B., Begg, J.D., Kersting, A.B., Zavarin, M., 2018. Cesium sorption reversibility and kinetics on illite, montmorillonite and kaolinite. *Sci. Total Environ.* 610–611, 511–520. <https://doi.org/10.1016/j.scitotenv.2017.08.122>.

Dzene, L., Tertre, E., Hubert, F., Ferrage, E., 2015. Nature of the sites involved in the process of cesium desorption from vermiculite. *J. Colloid Interface Sci.* 455, 254–260. <https://doi.org/10.1016/j.jcis.2015.05.053>.

Freiesleben, H., 2013. Final disposal of radioactive waste. *EPJ Web Conf* 54, 01006. <https://doi.org/10.1051/epjconf/20135401006>.

Fuller, A.J., Shaw, S., Peacock, C.L., Trivedi, D., Small, J.S., Abrahamson, L.G., Burke, I.T., 2014. Ionic strength and pH dependent multi-site sorption of Cs onto a micaceous aquifer sediment. *Appl. Geochem.* 40, 32–42. <https://doi.org/10.1016/j.apgeochem.2013.10.017>.

Gaboreau, S., Claret, F., Crouzet, C., Giffaut, E., Tournassat, C., 2012. Caesium uptake by Callovian-Oxfordian clayrock under alkaline perturbation. *Appl. Geochem.* 27, 1194–1201. <https://doi.org/10.1016/j.apgeochem.2012.02.002>.

Gates, W.P., Bouazza, A., 2010. Bentonite transformations in strongly alkaline solutions. *Geotext. Geomembr.* 28, 219–225. <https://doi.org/10.1016/j.geotextmem.2009.10.010>.

Gaucher, E.C., Blanc, P., 2006. Cement/clay interactions – a review: experiments natural analogues, and modelling. *Waste Manag.* 26, 776–788. <https://doi.org/10.1016/j.wasman.2006.01.027>.

Guggenheim, E.A., 1935. The specific thermodynamic properties of aqueous solutions of strong electrolytes. *Philos. Mag.* 19, 588–643. <https://doi.org/10.1080/14786443508561403>.

Guggenheim, E.A., 1966. *Applications of Statistical Mechanics*. Oxford University Press.

Gutierrez, M., Fuentes, H.R., 1996. A mechanistic modelling of montmorillonite contamination by cesium sorption. *Appl. Clay Sci.* 11, 11–24. [https://doi.org/10.1016/0169-1317\(96\)00006-3](https://doi.org/10.1016/0169-1317(96)00006-3).

Hein, C., Sander, J.M., Kautenburger, R., 2017. New approach of a transient ICP-MS measurement method for samples with high salinity. *Talanta* 164, 477–782. <https://doi.org/10.1016/j.talanta.2016.06.059>.

Hurel, C., Marmier, N., Séby, F., Giffaut, E., Bourg, A.C.M., Fromage, F., 2002. Sorption behaviour of caesium on a bentonite sample. *Radiochim. Acta* 90, 695–698. <https://doi.org/10.1524/ract.2002.90.9-11.2002.695>.

Ito, H., 2006. Compaction properties of granular bentonites. *Appl. Clay Sci.* 31, 47–55. <https://doi.org/10.1016/j.clay.2005.08.005>.

Kitamura, A., Fujiwara, K., Mihara, M., Cowper, M., Kamei, G., 2013. Thorium and americium solubilities in cement pore water containing superplasticiser compared with thermodynamic calculations. *J. Radioanal. Nucl. Chem.* 298, 485–493. <https://doi.org/10.1007/s10967-013-2618-4>.

Klinge, H., Köthe, A., Ludwig, R., Zwirner, R., 2002. *Geologie und Hydrogeologie des Deckgebirges über dem Salzstock Gorleben*. *Z. Angew. Geol.* 2, 7–15.

Krestou, A., Xenidis, A., Panias, D., 2004. Mechanism of aqueous uranium(VI) uptake by hydroxyapatite. *Miner. Eng.* 17, 373–381. <https://doi.org/10.1016/j.mineng.2003.11.019>.

Lei, Z., Li, X., Huang, P., Hu, H., Li, Z., Zhang, Q., 2019. Mechanochemical activation of antigorite to provide active magnesium for precipitating cesium from the existences of potassium and sodium. *Appl. Clay Sci.* 168, 223–229. <https://doi.org/10.1016/j.clay.2018.11.015>.

Liu, C., Zachara, J.M., Smith, S.C., 2004. A cation exchange model to describe Cs⁺ sorption at high ionic strength in subsurface sediments at Hanford site, USA. *J. Contam. Hydrol.* 68, 217–238. [https://doi.org/10.1016/S0169-7722\(03\)00143-8](https://doi.org/10.1016/S0169-7722(03)00143-8).

Lommerzhelm, A., Jobmann, M., 2015. *Endlagerkonzept sowie Verfüll- und Verschlusskonzept für das Standortmodell Nord. AnSichT Technical Report*.

Maes, N., Salah, S., Jacques, D., Aertsens, M., Gompel, M.V., De Cannière, P., Velitchkova, N., 2008. Retention of Cs in Boom Clay: comparison of data from batch sorption tests and diffusion experiments on intact clay cores. *Phys. Chem. Earth* 33, 149–155. <https://doi.org/10.1016/j.pce.2008.10.002>.

Malone, J., Unger, J., Delange, F., Lagasse, R., Dumont, J.E., 1991. Thyroid consequences of Chernobyl accident in the countries of the European Community. *J. Endocrinol. Invest.* 14, 701–717. <https://doi.org/10.1007/BF03347899>.

Miller, B., Marcos, N., 2007. *Process Report – FEPs and Scenarios for a Spent Fuel Repository at Olkiluoto*. (POSIVA 12).

Missana, T., Benedicto, A., García-Gutiérrez, M., Alonso, U., 2014. Modelling cesium retention onto Na-, K-, and Ca-smectite: effects of ionic strength, exchange and

- competing cations on the determination of selectivity coefficients. *Geochim. Cosmochim. Acta* 128, 266–277. <https://doi.org/10.1016/j.gca.2013.10.007>.
- Müller-Vonmoos, M., Kahr, G., 1983. Mineralogische Untersuchungen von Wyoming Bentonit MX-80 und Montigel. NAGRA Technical Report 12.
- Mutterlose, J., Bornemann, A., 2000. Distribution and facies patterns of Lower Cretaceous sediments in northern Germany: a review. *Cretac. Res.* 21, 733–759. <https://doi.org/10.1006/cres.2000.0232>.
- Naveau, A., Monteil-Rivera, F., Dumonceau, J., Boudesocque, S., 2005. Sorption of europium on a goethite surface: influence of background electrolyte. *J. Contam. Hydrol.* 77, 1–16. <https://doi.org/10.1016/j.jconhyd.2004.10.002>.
- Poinssot, C., Baeyens, B., Bradbury, M.H., 1999. Experimental and modelling studies of caesium sorption on illite. *Geochim. Cosmochim. Acta* 63 (19/20), 3217–3227. [https://doi.org/10.1016/S0016-7037\(99\)00246-X](https://doi.org/10.1016/S0016-7037(99)00246-X).
- Preis, W., Gamsjäger, H., 2001. Thermodynamic investigation of phase equilibria in metal carbonate-water-carbon dioxide systems. *Monatsh. Chem.* 132, 1327–1346. <https://doi.org/10.1007/s007060170020>.
- Savage, D., Lind, A., Arthur, R.C., 1999. Review of the Properties and Uses of Bentonite as a Buffer and Backfill Material. (SKI Report 9).
- Scatchard, G., 1936. Concentrated solutions of strong electrolytes. *Chem. Rev.* 19, 309–327. <https://doi.org/10.1021/cr60064a008>.
- Séby, F., Potin-Gautier, M., Giffaut, E., Borge, G., Donard, O.F.X., 2001. A critical review of thermodynamic data for selenium species at 25°C. *Chem. Geol.* 171, 173–194. [https://doi.org/10.1016/S0009-2541\(00\)00246-1](https://doi.org/10.1016/S0009-2541(00)00246-1).
- Semenkova, A.S., Fvsiunina, M.V., Verma, P.K., Mohapatra, P.K., Petrov, V.G., Seregina, I.F., Bolshov, M.A., Krupskaya, V.V., Romanchuk, A.Y., Kalmykov, S.N., 2018. Cs⁺ sorption onto Kutch clays: influence of competing ions. *Appl. Clay Sci.* 166, 88–93. <https://doi.org/10.1016/j.clay.2018.09.010>.
- Sipos, P., 2008. Application of the specific Ion Interaction Theory (SIT) for ionic products of aqueous electrolyte solutions of very high concentrations. *J. Mol. Liq.* 143, 13–16. <https://doi.org/10.1016/j.molliq.2008.04.003>.
- Staunton, S., Roubaud, M., 1997. Adsorption of ¹³⁷Cs on montmorillonite and illite: effect of charge compensating cation, ionic strength, concentration of Cs, K and fulvic acid. *Clay Clay Miner.* 45 (2), 251–260. <https://doi.org/10.1346/CCMN.1997.0450213>.
- Strebl, F., Gerzabek, M.H., Bossew, P., Kienzl, K., 1999. Distribution of radiocaesium in an Austrian forest stand. *Sci. Total Environ.* 226, 75–83. [https://doi.org/10.1016/S0048-9697\(98\)90051-1](https://doi.org/10.1016/S0048-9697(98)90051-1).
- Takahashi, H., Tachi, Y., 2019. 3D-microstructure analysis of compacted Na- and Cs-montmorillonite with nanofocus X-ray computed tomography and correlation with macroscopic transport properties. *Appl. Clay Sci.* 168, 211–222. <https://doi.org/10.1016/j.clay.2018.11.008>.
- Takayanagi, K., 1986. The oxidation of iodide to iodate for the polarographic determination of total iodine in natural waters. *Talanta* 33 (5), 451–454. [https://doi.org/10.1016/0039-9140\(86\)80115-1](https://doi.org/10.1016/0039-9140(86)80115-1).
- Taylor, D.M., 1989. The biodistribution and toxicity of plutonium, americium and neptunium. *Sci. Total Environ.* 83, 217–225. [https://doi.org/10.1016/0048-9697\(89\)90094-6](https://doi.org/10.1016/0048-9697(89)90094-6).
- Tran, E.L., Teutsch, N., Klein-BenDavid, O., Weisbrod, N., 2018. Uranium and cesium sorption to bentonite colloids under carbonate-rich environments: implications for radionuclide transport. *Sci. Total Environ.* 643, 260–269. <https://doi.org/10.1016/j.scitotenv.2018.06.162>.
- Tripathy, S., Sridharan, A., Schanz, T., 2004. Swelling pressures of compacted bentonites from diffuse double layer theory. *Can. Geotech. J.* 41, 437–450. <https://doi.org/10.1139/t03-096>.
- Vejsada, J., Hradil, D., Řanda, Z., Jelínek, E., Štulík, K., 2005. Adsorption of cesium on Czech smectite-rich clays – a comparative study. *Appl. Clay Sci.* 30, 53–66. <https://doi.org/10.1016/j.clay.2005.03.003>.
- Weber, W.J., Navrotsky, A., Stefanovsky, S., Vance, E.R., Vernaz, E., 2009. Materials science of high-level nuclear waste immobilization. *MRS Bull.* 34, 46–53. <https://doi.org/10.1557/mrs2009.12>.
- Ye, W.M., He, Y., Chen, Y.G., Chen, B., Cui, Y.J., 2016. Thermochemical effects on the smectite alteration of GMZ bentonite for deep geological repository. *Environ. Earth Sci.* 75, 906–916. <https://doi.org/10.1007/s12665-016-5716-0>.

Supporting Information For

Adsorption of caesium on raw Ca-bentonite in high saline solutions: influence of concentration, mineral composition, other radionuclides and modelling

Kristina Brix^{a*}, Christina Hein^b, Aaron Haben^a, Ralf Kautenburger^a

^aInstitute of Inorganic Chemistry – WASTE-Elemental analysis group, Saarland University, Saarbrücken, Germany

^bAnalytical and Ecological Chemistry, Trier University, Trier, Germany

*Corresponding author at: Institute of Inorganic Chemistry – WASTE-Elemental analysis group, Campus C4.1, 66123 Saarbrücken, Germany

E-mail address: kristina.brix@uni-saarland.de (K. Brix)

```

SIT
-epsilon
K+    Cl-    0.15
Cs+   Cl-    0.15
SURFACE_MASTER_SPECIES
      Hfo_s  Hfo_sOH
      Hfo_w  Hfo_wOH
SURFACE_SPECIES
# Cs Sorption T1 und T2
      Hfo_sOH = Hfo_sOH
      log_k   0.00

      Hfo_wOH = Hfo_wOH
      log_k   0.00
# Na
      Hfo_sOH + Na+ = Hfo_sONa + H+
      log_k   0.00

      Hfo_wOH + Na+ = Hfo_wONa + H+
      log_k   0.00
# Cs
      Hfo_sOH + Cs+ = Hfo_sOCs + H+
      log_k   8.14
      Hfo_wOH + Cs+ = Hfo_wOCs + H+
      log_k   1.96
# K
      Hfo_sOH + K+ = Hfo_sOK + H+
      log_k   2.20
      Hfo_wOH + K+ = Hfo_wOK + H+
      log_k   0.00
# Ca
      Hfo_sOH + Ca+2 = Hfo_sOCa+ + H+
      log_k   0.76
      Hfo_wOH + Ca+2 = Hfo_wOCa+ + H+
      log_k   0.00

TITLE
SOLUTION 1
  temp      25
  pH        13
  pe         4
  redox     pe
  units     g/l
  density   1
  Cl        3.545
  Cs        0.001 uMol/l
  K         2.85 mg/l
  N(5)     0.001 uMol/l
  Na        5.29
  -water    1 # kg
SURFACE 1
  -sites DENSITY
  Hfo_sOH   0.0000105   493   4
  Hfo_wOH   0.72
END

```

Fig. A1. PHREEQC input for the modelling of 1 nmol L⁻¹ Cs⁺ in 0.1 M NaCl by using specific ion interaction theory. For other concentrations Cs and N(5) were varied from 1-250,000 nmol L⁻¹.

SOLUTION 2		SOLUTION 3		SOLUTION 4	
temp	25	temp	25	temp	25
pH	13	pH	12.5	pH	13
pe	4	pe	4	pe	4
redox	pe	redox	pe	redox	pe
units	g/l	units	mmol/l	units	g/l
density	1.306	density	1.375	density	1.488
Cl	35.45	Cl	2.53 mol/L	Cl	177.25
Cs	0.001 uMol/l	Cs	0.001 uMol/l	Cs	0.001 uMol/l
N(5)	0.001 uMol/l	K	5.1	N(5)	0.001 uMol/l
Na	25.99	N(5)	0.001 uMol/l	Na	117.99
K	1.53 mg/L	Na	2.52 mol/L	K	3.30 mg/L
-water	1 # kg	Ca	32.4	-water	1 # kg
		Sr	0.06		
		Fe(3)	0.008		
		Ba	0.005		
		Al	0.004		
		S(6)	20		
		-water	1 # kg		

Fig. A2. PHREEQC solution input for the modelling in 1 M NaCl (Solution 2), artificial cement pore water (Solution 3) and 5 M NaCl (Solution 4) at $[Cs^+]_i = 1 \text{ nmol L}^{-1}$ by using specific ion interaction theory.

Table A1

Selectivity coefficients $\log K$ normalised against Na^+ refined for Davies-modelling.

Selectivity coefficient $\log K$	This study	Missana et al. ^a
Cs^+ (T1)	7.79	7.64
K^+ (T1)	2.50	2.50
Ca^{2+} (T1)	0.76	0.76
Cs^+ (T2)	1.80	1.70
K^+ (T2)	0.57	0.57
Ca^{2+} (T2)	0.29	0.29

^a (Missana et al., 2014)

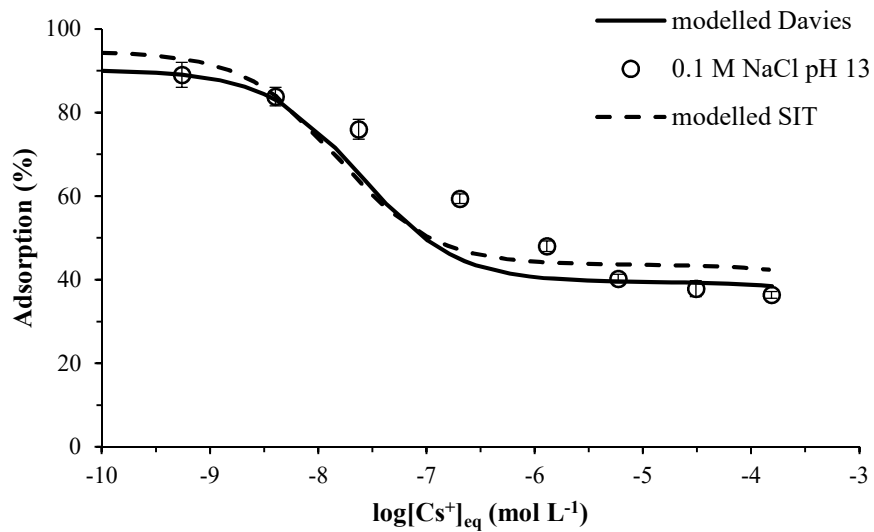


Fig. A3. Concentration depended percental adsorption of Cs^+ on Calcigel in 0.1 M NaCl at pH 13 and with Davies equation and specific ion interaction theory modelled curves calculated with ideal parameters for Davies modelling.

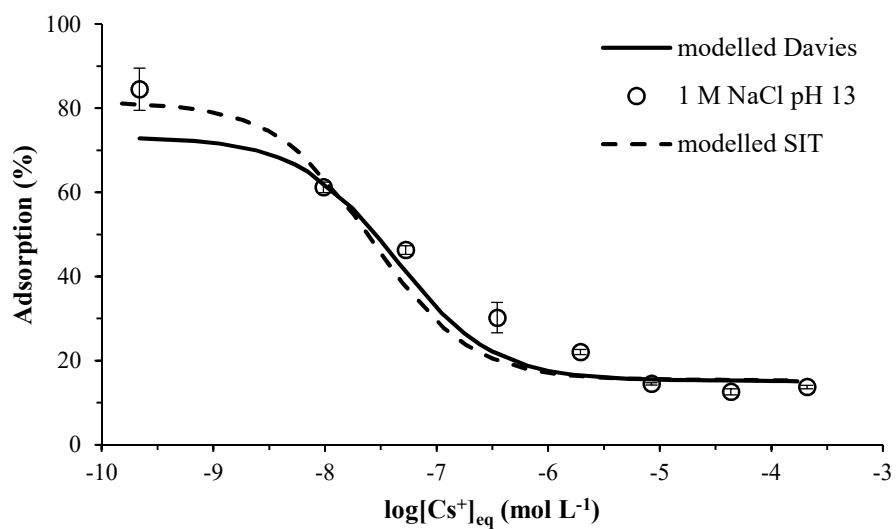


Fig. A4. Concentration depended percental adsorption of Cs^+ on Calcigel in 1 M NaCl at pH 13 and with Davies equation and specific ion interaction theory modelled curves calculated with ideal parameters for Davies modelling.

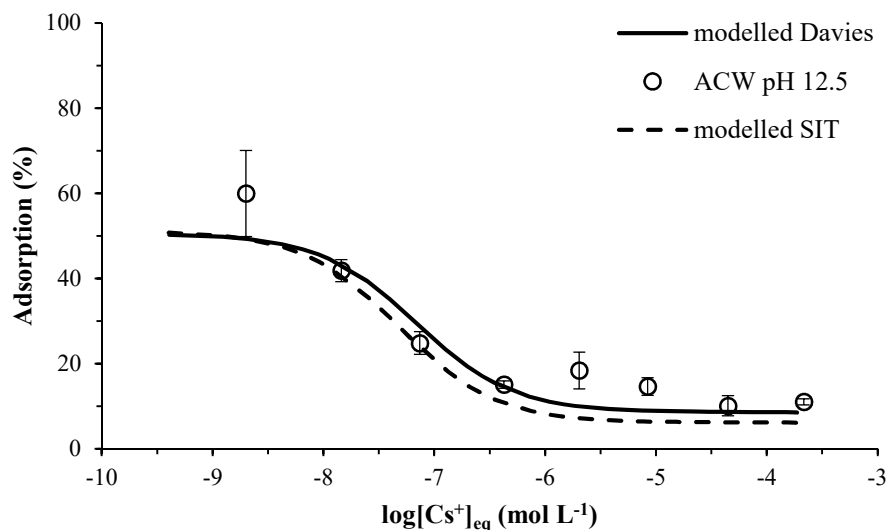


Fig. A5. Concentration depended percental adsorption of Cs^+ on Calcigel in artificial cement pore water (ACW) at pH 12.5 and with Davies equation and specific ion interaction theory modelled curves calculated with ideal parameters for Davies modelling.

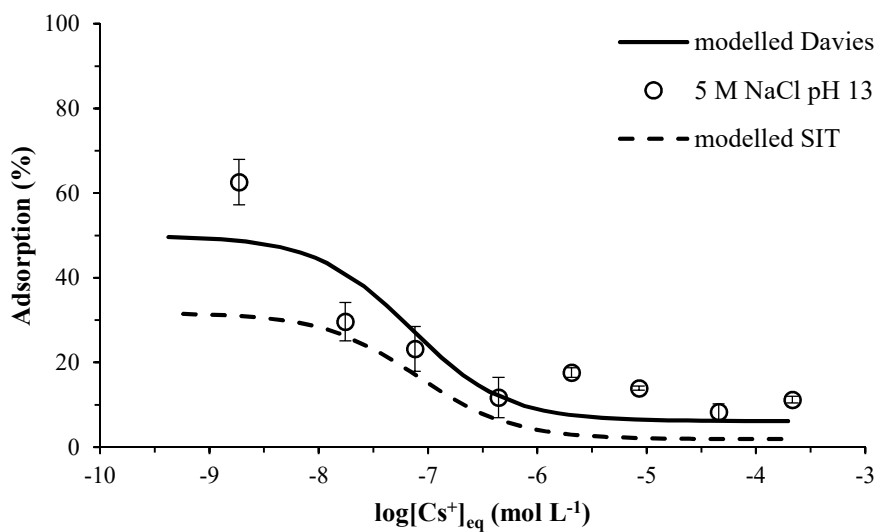


Fig. A6. Concentration depended percental adsorption of Cs^+ on Calcigel in 5 M NaCl at pH 13 and with Davies equation and specific ion interaction theory modelled curves calculated with ideal parameters for Davies modelling.

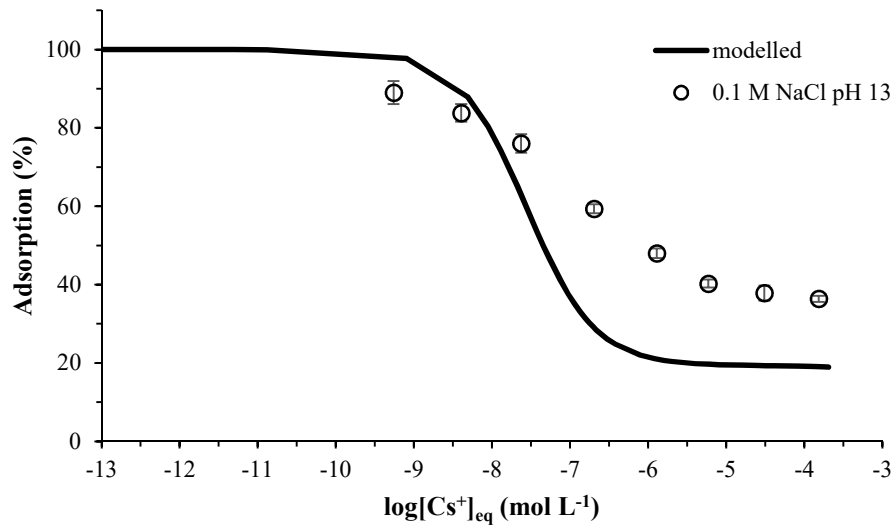


Fig. A7. Concentration depended percental adsorption of Cs^+ on Calcigel in 0.1 M NaCl at pH 13 and modelled curve via specific ion interaction theory calculated with parameter from Cherif et al. (Surface complexation site density = $1.05 \cdot 10^{-5}$ sites nm^{-2}) (Cherif et al., 2017).

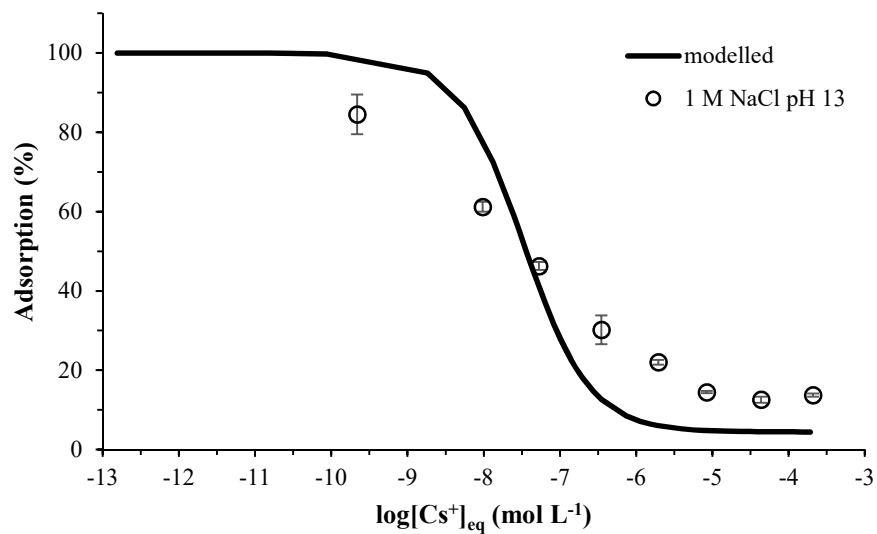


Fig. A8. Concentration depended percental adsorption of Cs^+ on Calcigel in 1 M NaCl at pH 13 and SIT modelled curve via specific ion interaction theory calculated with parameter from Cherif et al. (Surface complexation site density = $1.05 \cdot 10^{-5}$ sites nm^{-2}) (Cherif et al., 2017).

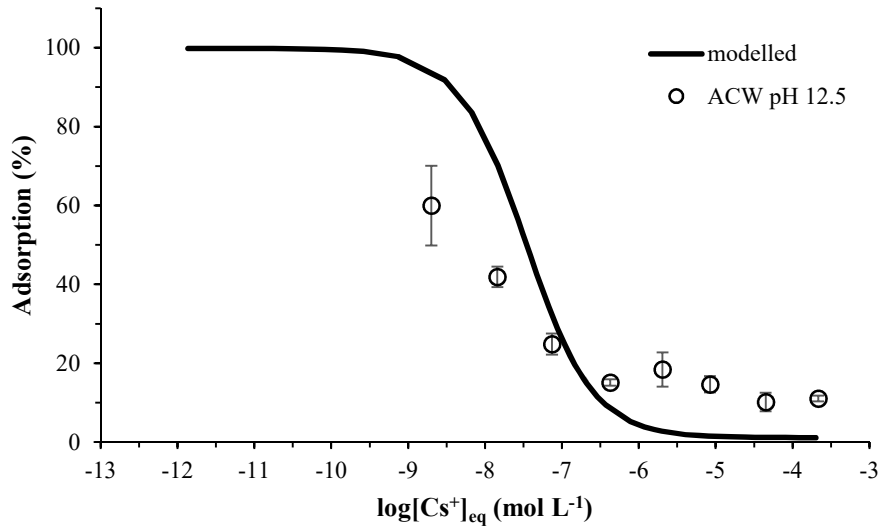


Fig. A9. Concentration depended percental adsorption of Cs^+ on Calcigel in artificial cement pore water (ACW) at pH 12.5 and SIT modelled curve via specific ion interaction theory calculated with parameter from Cherif et al. (Surface complexation site density = $1.05 \cdot 10^{-5}$ sites nm^{-2}) (Cherif et al., 2017).

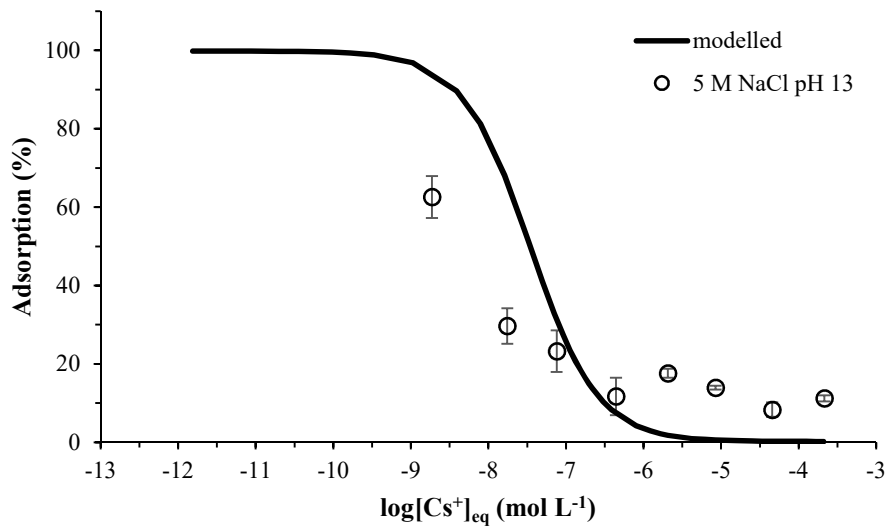


Fig. A10. Concentration depended percental adsorption of Cs^+ on Calcigel in 5 M NaCl at pH 13 and SIT modelled curve via specific ion interaction theory calculated with parameter from Cherif et al. (Surface complexation site density = $1.05 \cdot 10^{-5}$ sites nm^{-2}) (Cherif et al., 2017).

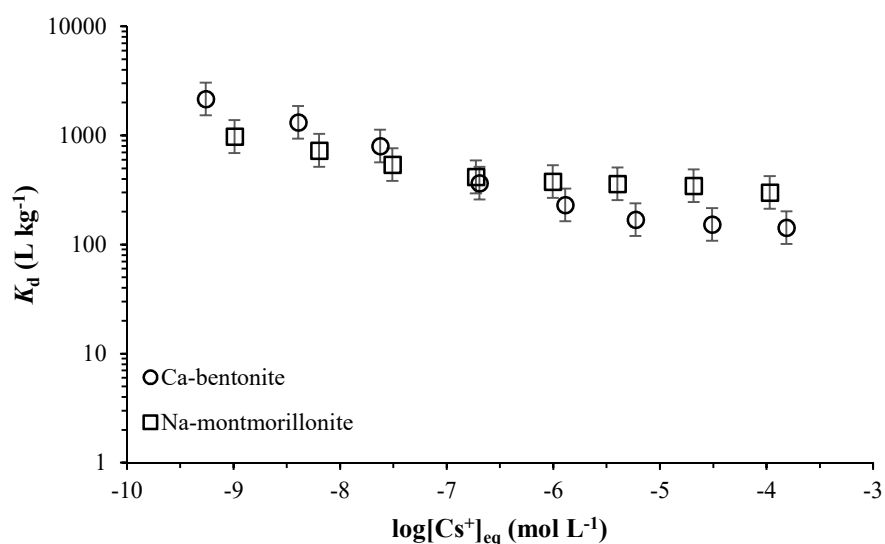


Fig. A11. Concentration depended K_d values of Cs^+ adsorption on Ca-bentonite and Na-montmorillonite in 0.1 M NaCl with standardised uncertainty of $\log K_d \pm 0.15$.

References

- Cherif, M.A., Martin-Garin, A., Gérard, F., Bildstein, O., 2017, A robust and parsimonious model for caesium adsorption on clay minerals and natural clay minerals, *Appl. Geochem.* 87, 22-37. <https://doi.org/10.1016/j.apgeochem.2017.10.017>.
- Missana, T., Benedicto, A., García-Gutiérrez, M., Alonso, U., 2014, Modelling cesium retention onto Na-, K-, and Ca-smectite: effects of ionic strength, exchange and competing cations on the determination of selectivity coefficients, *Geochim. Cosmochim. Acta* 128, 266-277. <https://doi.org/10.1016/j.gca.2013.10.007>.

4. Summary and outlook

This work deals with the retention of elements relevant for a HLW disposal on different clays and contributes to a long-term safety case for a potential HLW disposal in clay formations, especially in the model region northern Germany. Various experiments and theoretical studies concerning the retention of Eu^{3+} , UO_2^{2+} and Cs^+ on OPA as reference host rock and Calcigel as potential buffer and backfill material were performed. The gained results describe the behaviour of elements relevant for a HLW disposal under realistic conditions (with the exception of the solid to liquid ratio, used in the batch experiments).

On OPA, the retention of Eu^{3+} increases with increasing pH value. It exceeds 50% in 0.01 M SP and PW (0.4 M) at both temperatures (25 and 60 °C) for $\text{pH} > 6$. In the case of UO_2^{2+} , the retention is low in the neutral pH range, due to the formation of the neutral $\text{Ca}_2\text{UO}_2(\text{CO}_3)_3$ aquo complex. It increases again at $\text{pH} \geq 9$. In the presence of humic acid, the retention of both metals increases under the investigated conditions. These results show that OPA could be a sufficient host rock for a HLW disposal in relation to the retention of UO_2^{2+} and three valent actinides. This is even the case under realistic conditions such as high salinity, $\text{pH} > 7$, room and elevated temperature and the presence of clay organic matter (Figure 15 and 16).

Cs^+ can be immobilised by Calcigel under alkaline conditions (pH 12.5-13) in high and very high saline background electrolytes (0.1-5 M NaCl, ACW) (Figure 17). That also applies in the presence of other HLW relevant elements (Eu^{3+} , UO_2^{2+} and I). In complex solutions (such as ACW), the inhomogeneity of the natural material Calcigel has no influence on the Cs^+ retention. With regard to the Cs^+ retention, Calcigel is a suitable buffer material for a HLW disposal even under conditions occurring in northern Germany.

The developed ion exchange models for OPA and Calcigel are in very good agreement with the experimental data. The gained modelling parameters can be evaluated by applying them to other experiments under different conditions.

A new method to quantify iodine via ICP-MS under acidic conditions was developed. The robustness was shown by different pH values (7 and 12.5) and ionic strengths (Milli-Q water to 5 M NaCl) of the background electrolyte. Only a small amount of one additional chemical ($18 \text{ mg L}^{-1} \text{ NaOCl}$ for iodine concentrations $\leq 127 \text{ } \mu\text{g L}^{-1}$) is needed and the reaction time is with 1-72 h very flexible. This method is not only useful in repository research. It simplifies the iodine quantification in presence of high valent metals in many, also very complex solutions such as urine or seawater.

Since the storage of dangerous materials such as HLW for around one million years is a very extensive topic, there is still a lot of research to do. The presented experiments concerning OPA and Calcigel should be conducted with interchanged adsorbents to obtain data at realistic conditions. Additionally, the retention behaviour of iodide and other elements relevant for HLW should also get investigated at the same conditions as it was done in this work. Due to probable precipitation effects, the geochemical modelling will be challenging in the hyperalkaline pH range. Nevertheless, hyperalkaline and high saline pore water is expected in the model for an HLW in northern Germany and was rarely considered in the literature, yet.

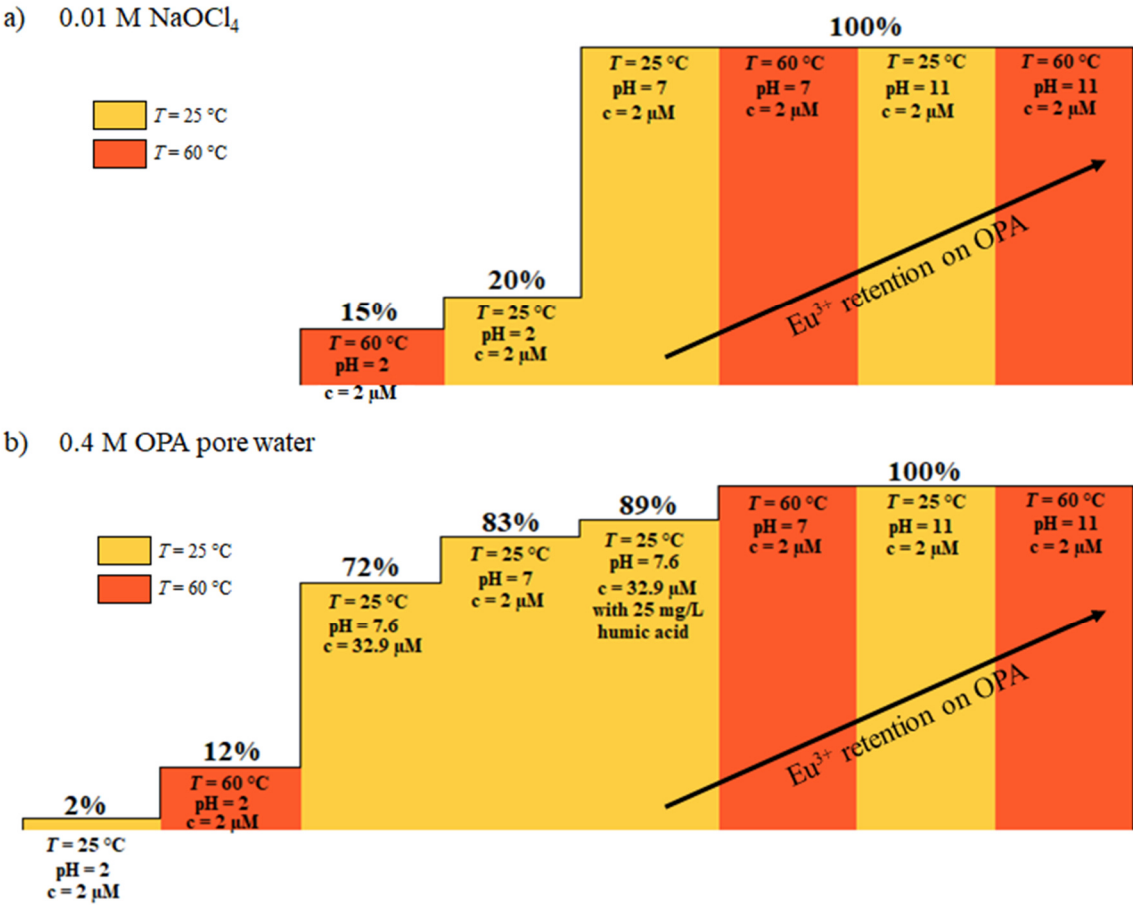


Figure 15. Retention of Eu³⁺ on Opalinus Clay (OPA) under different conditions in 0.01 M NaOCl₄ (a) and in OPA reference pore water (b).

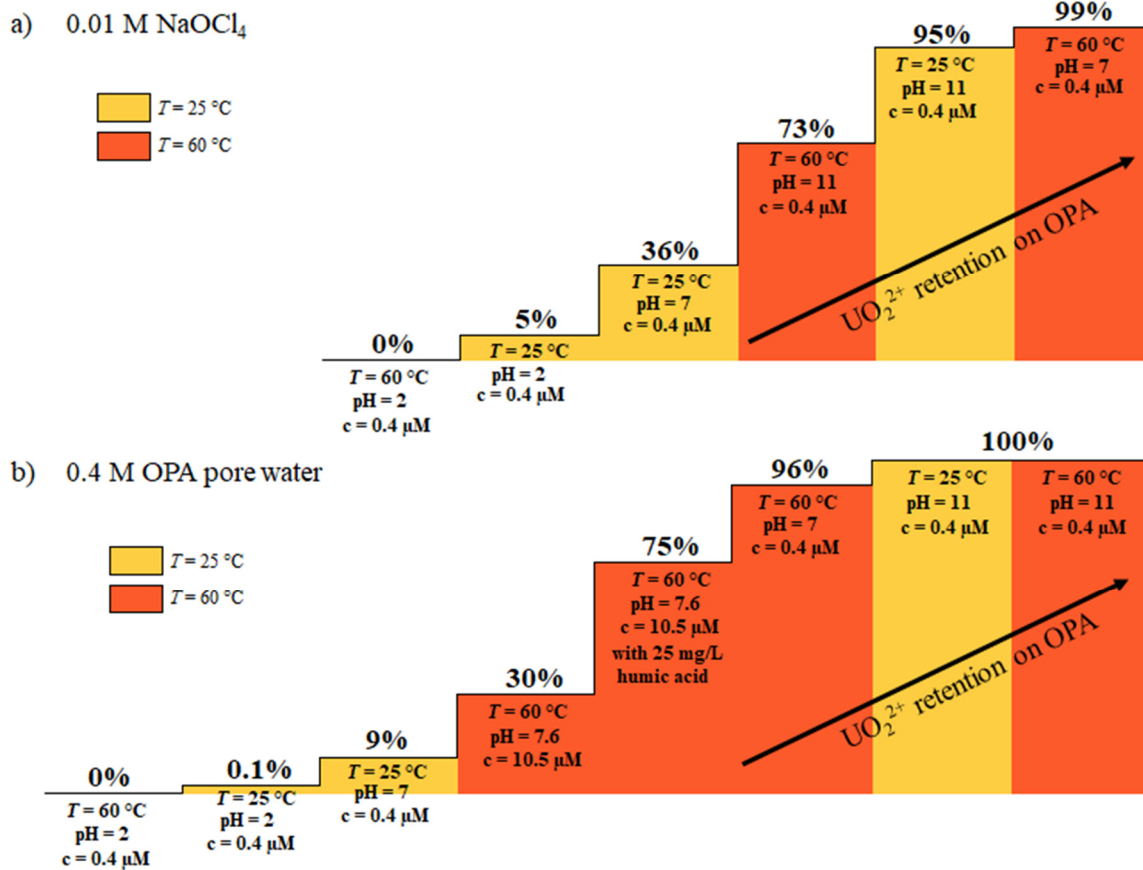


Figure 16. Retention of UO₂²⁺ on Opalinus Clay (OPA) under different conditions in 0.01 M NaOCl₄ (a) and in OPA reference pore water (b).

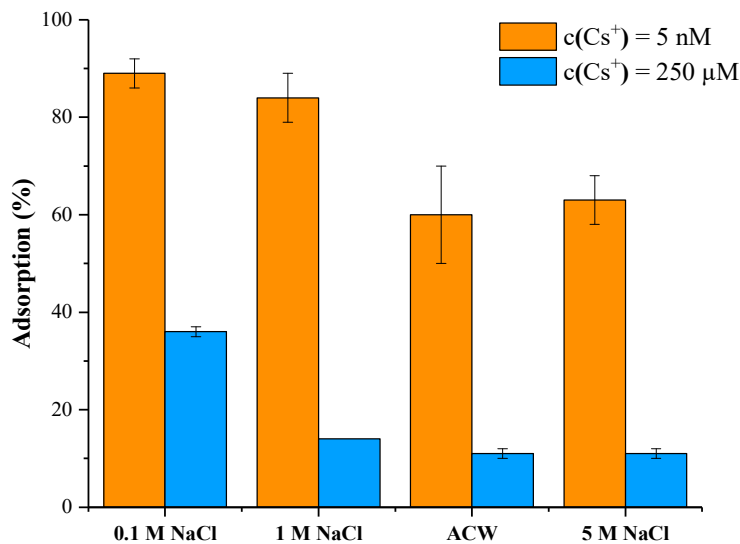


Figure 17. Adsorption of the lowest (5 nM) and highest (250 μM) investigated initial Cs⁺ concentration on Calcigel in 0.1-5 M NaCl pH 13 and artificial cement pore water (ACW, pH 12.5, I ≈ 3 M).

5. References

- Aaltonen, I., Engström, J., Front, K., Gehör, S., Kosunen, P., Kärki, A., Mattila, J., Paananen, M., Paulamäki, S., 2016. Geology of Olkiluoto.
- Agilent Technologies, 2005. ICP-MS - Inductively Coupled Mass Spectrometry - A Primer.
- Al-Ammar, A., Reitznerová, E., Barnes, R.M., 2001. Thorium and iodine memory effects in inductively-coupled plasma mass spectrometry. *Fresenius. J. Anal. Chem.* 370, 479–482. <https://doi.org/10.1007/s002160100837>
- Allison, J.D., Brown, D.S., Novo-Gradac, K.J., 1991. MINTEQA2/PRODEFA2, a geochemical assessment model for environmental systems: Version 3.0 User's Manual. Environmental Research Laboratory, Athens.
- Appelo, C.A.J., Van Loon, L.R., Wersin, P., 2010. Multicomponent diffusion of a suite of tracers (HTO, Cl, Br, I, Na, Sr, Cs) in a single sample of Opalinus Clay. *Geochim. Cosmochim. Acta* 74, 1201–1219. <https://doi.org/10.1016/j.gca.2009.11.013>
- Arayro, J., Dufresne, A., Zhou, T., Ioannidou, K., Ulm, J.-F., Pellenq, R., Béland, L.K., 2018. Thermodynamics, kinetics, and mechanics of cesium sorption in cement paste: a multiscale assessment. *Phys. Rev. Mater.* 2, 053608. <https://doi.org/10.1103/PhysRevMaterials.2.053608>
- Baborová, L., Vopálka, D., Červinka, R., 2018. Sorption of Sr and Cs onto Czech natural bentonite: experiments and modelling. *J. Radioanal. Nucl. Chem.* 318, 2257–2262. <https://doi.org/10.1007/s10967-018-6196-3>
- Baeyens, B., Bradbury, M.H., 1997. A mechanistic description of Ni and Zn sorption on Namontmorillonite Part I: titration and sorption measurements. *J. Contam. Hydrol.* 27, 199–222. [https://doi.org/10.1016/S0169-7722\(97\)00008-9](https://doi.org/10.1016/S0169-7722(97)00008-9)
- Baisden, P.A., Choppin, G.R., 2007. Nuclear Waste Management and the Nuclear Fuel Cycle. EOLSS Publishers, Oxford, UK.
- Barkleit, A., Kretzschmar, J., Tsushima, S., Acker, M., 2014. Americium(III) and europium(III) complex formation with lactate at elevated temperatures studied by spectroscopy and quantum chemical calculations. *Dalt. Trans.* 43, 11221–11232. <https://doi.org/10.1039/C4DT00440J>
- Bartlett, G.S., Houts, P.S., Byrnes, L.K., Miller, R.W., 1983. The near disaster at Three Mile Island. *Int. J. Mass Emerg. Disasters* 1, 19–42.
- Bateman, K., Coombs, P., Noy, D.J., Pearce, J.M., Wetton, P., Haworth, A., Linklater, C., 1999.

- Experimental simulation of the alkaline disturbed zone around a cementitious radioactive waste repository: numerical modelling and column experiments. *Geol. Soc. London, Spec. Publ.* 157, 183–194. <https://doi.org/10.1144/GSL.SP.1999.157.01.14>
- Bengtsson, A., Pedersen, K., 2017. Microbial sulphide-producing activity in water saturated Wyoming MX-80, Asha and Calcigel bentonites at wet densities from 1500 to 2000 kgm⁻³. *Appl. Clay Sci.* 137, 203–212. <https://doi.org/10.1016/j.clay.2016.12.024>
- Bennett, D.G., Gens, R., 2008. Overview of European concepts for high-level waste and spent fuel disposal with special reference waste container corrosion. *J. Nucl. Mater.* 379, 1–8. <https://doi.org/10.1016/j.jnucmat.2008.06.001>
- Berner, U.R., 1992. Evolution of pore water chemistry during degradation of cement in a radioactive waste repository environment. *Waste Manag.* 12, 201–219. [https://doi.org/10.1016/0956-053X\(92\)90049-O](https://doi.org/10.1016/0956-053X(92)90049-O)
- Bethke, C.M., Farrell, B., Yeakel, S., 2019. *GWB Essentials Guide*. Aqueous Solutions LLC, Champaign.
- Bhattacharyya, K.G., Gupta, S. Sen, 2008. Adsorption of a few heavy metals on natural and modified kaolinite and montmorillonite: a review. *Adv. Colloid Interface Sci.* 140, 114–131. <https://doi.org/10.1016/j.cis.2007.12.008>
- Blum, W.E.H., 2007. *Bodenkunde in Stichworten*, 6th ed. Gebr. Borntraeger, Berlin, Stuttgart.
- Bradbury, M.H., Baeyens, B., 2011. Predictive sorption modelling of Ni(II), Co(II), Eu(III), Th(IV) and U(VI) on MX-80 bentonite and Opalinus Clay: a “bottom-up” approach. *Appl. Clay Sci.* 52, 27–33. <https://doi.org/10.1016/j.clay.2011.01.022>
- Bradbury, M.H., Baeyens, B., 2009. Sorption modelling on illite Part I: titration measurements and the sorption of Ni, Co, Eu and Sn. *Geochim. Cosmochim. Acta* 73, 990–1003. <https://doi.org/10.1016/j.gca.2008.11.017>
- Bradbury, M.H., Baeyens, B., 2000. A generalised sorption model for the concentration dependent uptake of caesium by argillaceous rocks. *J. Contam. Hydrol.* 42, 141–163. [https://doi.org/10.1016/S0169-7722\(99\)00094-7](https://doi.org/10.1016/S0169-7722(99)00094-7)
- Bradbury, M.H., Baeyens, B., 1997. A mechanistic description of Ni and Zn sorption on Na-montmorillonite Part II: modelling. *J. Contam. Hydrol.* 27, 223–248. [https://doi.org/10.1016/S0169-7722\(97\)00007-7](https://doi.org/10.1016/S0169-7722(97)00007-7)
- Bradl, H.B., 2004. Adsorption of heavy metal ions on soils and soils constituents. *J. Colloid Interface Sci.* 277, 1–18. <https://doi.org/10.1016/j.jcis.2004.04.005>
- Bräuer, V., Reh, M., Schulz, P., Schuster, P., Sprado, K.H., 1994. Endlagerung stark wärmeentwickelnder radioaktiver Abfälle in tiefen geologischen Formationen

- Deutschlands - Untersuchung und Bewertung von Regionen in nichtsalinaren Formationen.
- Breitenstein Jr., B.D., Palmer, H.E., 1989. Lifetime Follow-up of the 1976 Americium Accident Victim. *Radiat. Prot. Dosimetry* 26, 317–322. <https://doi.org/10.1093/oxfordjournals.rpd.a080424>
- Brønsted, J.N., 1922. Studies on solubility. IV. The principle of the specific interaction of ions. *J. Am. Chem. Soc.* 44, 877–898. <https://doi.org/10.1021/ja01426a001>
- Brouwer, E., Baeyens, B., Maes, A., Cremers, A., 1983. Cesium and rubidium ion equilibria in illite clay. *J. Phys. Chem.* 87, 1213–1219. <https://doi.org/10.1021/j100230a024>
- Browner, R.F., Boorn, A.W., 1984. The Achilles' Heel of Atomic Spectroscopy? *Anal. Chem.* 56, 786A–798A. <https://doi.org/10.1021/ac00271a001>
- Bruchertseifer, H., Cripps, R., Guentay, S., Jaekel, B., 2003. Analysis of iodine species in aqueous solutions. *Anal. Bioanal. Chem.* 375, 1107–1110. <https://doi.org/10.1007/s00216-003-1779-3>
- Brunauer, S., Emmett, P.H., Teller, E., 1938. Adsorption of gases in multimolecular layers. *J. Am. Chem. Soc.* 60, 309–319. <https://doi.org/10.1021/ja01269a023>
- Buchheim, B., Persson, L., 1992. Chemotoxicity of nuclear waste repositories. *Nucl. Technol.* 97, 303–315. <https://doi.org/10.13182/NT92-A34638>
- Bundesamt für Strahlenschutz, 2017a. Geschichte des Endlagers Morsleben https://archiv.bge.de/archiv/www.endlager-morsleben.de/Morsleben/DE/themen/endlager/geschichte/geschichte_dossierd7e7.html?cms_notFirst=true&cms_docId=7586480 (accessed 19.07.19).
- Bundesamt für Strahlenschutz, 2017b. Die Geschichte der Asse https://archiv.bge.de/archiv/www.asse.bund.de/Asse/DE/themen/was-ist/geschichte/geschichte_node.html (accessed 19.07.19).
- Bundesamt für Strahlenschutz, 2017c. Das Endlager Konrad im Überblick https://archiv.bge.de/archiv/www.endlager-konrad.de/Konrad/DE/themen/endlager/ueberblick/ueberblick_node.html (accessed 19.07.19).
- Bundesgesellschaft für Endlagerung, 2019. Kurzinformationen zum Endlager Morsleben <https://www.bge.de/de/morsleben/kurzinformationen/> (accessed 19.07.19).
- Bundesgesellschaft für Geowissenschaften und Rohstoffe, 2007. Endlagerung radioaktiver Abfälle in Deutschland - Untersuchung und Bewertung von Regionen mit potenziell geeigneten Wirtsgesteinsformationen.

- Cao, X., Zheng, L., Hou, D., Hu, L., 2019. On the long-term migration of uranyl in bentonite barrier for high-level radioactive waste repositories: the effect of different host rocks. *Chem. Geol.* 525, 46–57. <https://doi.org/10.1016/j.chemgeo.2019.07.006>
- Chang, P.-H., Li, Z., Jean, J.-S., Jiang, W.-T., Wang, C.-J., Lin, K.-H., 2012. Adsorption of tetracycline on 2:1 layered non-swelling clay mineral illite. *Appl. Clay Sci.* 67–68, 158–163. <https://doi.org/10.1016/j.clay.2011.11.004>
- Cherif, M.A., Martin-Garin, A., Gérard, F., Bildstein, O., 2017. A robust and parsimonious model for caesium sorption on clay minerals and natural clay materials. *Appl. Geochemistry* 87, 22–37. <https://doi.org/10.1016/j.apgeochem.2017.10.017>
- Clariant, 2015. Product Information: Calcigel. Switzerland.
- Collier, J.G., Davies, L.M., 1980. The accident at Three Mile Island. *Heat Transf. Eng.* 1, 56–67. <https://doi.org/10.1080/01457638008939563>
- Cornell, R.M., 1993. Adsorption of cesium on minerals: a review. *J. Radioanal. Nucl. Chem.* 171, 483–500. <https://doi.org/10.1007/BF02219872>
- Courdouan, A., Christl, I., Meylan, S., Wersin, P., Kretzschmar, R., 2007. Characterization of dissolved organic matter in anoxic rock extracts and in situ pore water of the Opalinus Clay. *Appl. Geochemistry* 22, 2926–2939. <https://doi.org/10.1016/j.apgeochem.2007.09.001>
- Courdouan, A., Christl, I., Rabung, T., Wersin, P., Kretzschmar, R., 2008. Proton and trivalent metal cation binding by dissolved organic matter in the Opalinus Clay and the Callovo-Oxfordian formation. *Environ. Sci. Technol.* 42, 5985–5991. <https://doi.org/10.1021/es8007358>
- Date, A.R., 1983. An introduction to inductively coupled plasma source mass spectrometry. *Trends Anal. Chem.* 2, 225–230. [https://doi.org/10.1016/0165-9936\(83\)87006-X](https://doi.org/10.1016/0165-9936(83)87006-X)
- Davies, C.W., 1938. 397. The extent of dissociation of salts in water. Part VIII. An equation for the mean ionic activity coefficient of an electrolyte in water, and a revision of the dissociation constants of some sulphates. *J. Chem. Soc.* 2093–2098. <https://doi.org/10.1039/JR9380002093>
- Debye, P., Hückel, E., 1923. Zur Theorie der Elektrolyte. I. Gefrierpunktserniedrigung und verwandte Erscheinungen. *Phys. Zeitschrift* 24, 185–206.
- Dickson, C.L., Glasser, F.P., 2000. Cerium(III, IV) in cement: implications for actinide (III, IV) immobilisation. *Cem. Concr. Res.* 30, 1619–1623. [https://doi.org/10.1016/S0008-8846\(00\)00362-8](https://doi.org/10.1016/S0008-8846(00)00362-8)
- Drozdovitch, V., Khrouch, V., Minenko, V., Konstantinov, Y., Khrutchinsky, A., Kutsen, S.,

- Kukhta, T., Shinkarev, S., Gavrilin, Y., Luckyanov, N., Voillequé, P., Bouville, A., 2019. Influence of the external and internal radioactive contamination of the body and the clothes on the results of the thyroidal ¹³¹I measurements conducted in Belarus after the Chernobyl accident. Part 1: Estimation of the external and internal radioactive c. *Radiat. Environ. Biophys.* 58, 195–214. <https://doi.org/10.1007/s00411-019-00784-3>
- Duffield, J.R., Williams, D.R., 1986. The environmental chemistry of radioactive waste disposal. *Chem. Soc. Rev.* 15, 291–307.
- Dzene, L., Tertre, E., Hubert, F., Ferrage, E., 2015. Nature of the sites involved in the process of cesium desorption from vermiculite. *J. Colloid Interface Sci.* 455, 254–260. <https://doi.org/10.1016/j.jcis.2015.05.053>
- Eisenbud, M., Krauskopf, K., Franca, E.P., Lei, W., Ballad, R., Linsalata, P., Fujimori, K., 1984. Natural analogues for the transuranic actinide elements: an investigation in Minas Gerais, Brazil. *Environ. Geol. Water Sci.* 6, 1–9. <https://doi.org/10.1007/BF02525564>
- Elbana, T.A., Selim, H.M., Akrami, N., Newman, A., Shaheen, S.M., Rinklebe, J., 2018. Freundlich sorption parameters for cadmium, copper, nickel, lead, and zinc for different soils: influence of kinetics. *Geoderma* 324, 80–88. <https://doi.org/10.1016/j.geoderma.2018.03.019>
- Emmett, P.H., Kummer, J.T., 1943. Kinetics of ammonia synthesis. *Ind. Eng. Chem.* 35, 677–683. <https://doi.org/10.1021/ie50402a012>
- Evans, N.D.M., 2008. Binding mechanisms of radionuclides to cement. *Cem. Concr. Res.* 38, 543–553. <https://doi.org/10.1016/j.cemconres.2007.11.004>
- Fermi, E., Amaldi, E., D'Agostino, O., Rasetti, F., Segrè, E., Rutherford, E., 1934. Artificial radioactivity produced by neutron bombardment. *Proc. R. Soc. London. Ser. A, Contain. Pap. a Math. Phys. Character* 146, 483–500. <https://doi.org/10.1098/rspa.1934.0168>
- Féron, D., Crusset, D., Gras, J.-M., 2009. Corrosion issues in the French high-level nuclear waste program. *CORROSION* 65, 213–223. <https://doi.org/10.5006/1.3319129>
- Flügge, S., 1939. Kann der Energieinhalt der Atomkerne technisch nutzbar gemacht werden? *Naturwissenschaften* 27, 402–410. <https://doi.org/10.1007/BF01489507>
- Freundlich, H., 1907. Über die Adsorption in Lösungen. *Zeitschrift für Phys. Chemie.* <https://doi.org/10.1515/zpch-1907-5723>
- Gao, N., Huang, Z., Liu, H., Hou, J., Liu, X., 2019. Advances on the toxicity of uranium to different organisms. *Chemosphere* 237, 124548. <https://doi.org/10.1016/j.chemosphere.2019.124548>

- Garrels, R.M., Thompson, M.E., 1962. A chemical model for sea water at 25°C and one atmosphere total pressure. *Am. J. Sci.* 260, 57–66. <https://doi.org/10.2475/ajs.260.1.57>
- Gaucher, E., Blanc, P., 2006. Cement/clay interactions - A review: experiments, natural analogues, and modeling. *Waste Manag.* 26, 776–788. <https://doi.org/10.1016/j.wasman.2006.01.027>
- Gens, A., Guimaraes, L. d. N., Garcia-Molina, A., Alonso, E.E., 2002. Factors controlling rock–clay buffer interaction in a radioactive waste repository. *Eng. Geol.* 64, 297–308. [https://doi.org/10.1016/S0013-7952\(02\)00026-1](https://doi.org/10.1016/S0013-7952(02)00026-1)
- Gens, A., Sánchez, M., Guimarães, L.D.N., Alonso, E.E., Lloret, A., Olivella, S., Villar, M. V, Huertas, F., 2009. A full-scale in situ heating test for high-level nuclear waste disposal: observations, analysis and interpretation. *Géotechnique* 59, 377–399. <https://doi.org/10.1680/geot.2009.59.4.377>
- Georgescu, A.-M., Nardou, F., Zichil, V., Nistor, I.D., 2018. Adsorption of lead(II) ions from aqueous solutions onto Cr-pillared clays. *Appl. Clay Sci.* 152, 44–50. <https://doi.org/10.1016/j.clay.2017.10.031>
- Ghadiri, M., Chrzanowski, W., Rohanizadeh, R., 2015. Biomedical applications of cationic clay minerals. *RSC Adv.* 5, 29467–29481. <https://doi.org/10.1039/C4RA16945J>
- Gibbs, J.W., 1878. On the equilibrium of heterogeneous substances. *Transactions Connecticut Acad. Arts Sci.* 3, 108–248, 343–534. <https://doi.org/10.2475/ajs.s3-16.96.441>
- Gimmi, T., 2008. Modelling field diffusion experiments in clay rock: influence of numerical representation of borehole and rock interface. *J. Environ. Sci. Sustain. Soc.* 2, 63–70. <https://doi.org/10.3107/jesss.2.63>
- Gray, A.L., 1975a. Mass-spectrometric analysis of solutions using an atmospheric pressure ion source. *Analyst* 100, 289–299. <https://doi.org/10.1039/AN9750000289>
- Gray, A.L., 1975b. Plasma sampling mass spectrometry for trace analysis of solutions. *Anal. Chem.* 47, 600–601. <https://doi.org/10.1021/ac60353a049>
- Gray, A.L., 1974. It all depends on the source. *Proc. Soc. Anal. Chem.* 11, 182–183. <https://doi.org/10.4324/9781315521091>
- Grivé, M., Duro, L., Colàs, E., Giffaut, E., 2015. Thermodynamic data selection applied to radionuclides and chemotoxic elements: an overview of the ThermoChimie-TDB. *Appl. Geochemistry* 55, 85–94. <https://doi.org/10.1016/j.apgeochem.2014.12.017>
- Guggenheim, E.A., 1935. L. The specific thermodynamic properties of aqueous solutions of strong electrolytes. *London, Edinburgh, Dublin Philos. Mag. J. Sci.* 19, 588–643. <https://doi.org/10.1080/14786443508561403>

- Gupta, S. Sen, Bhattacharyya, K.G., 2006. Adsorption of Ni(II) on clays. *J. Colloid Interface Sci.* 295, 21–32. <https://doi.org/10.1016/j.jcis.2005.07.073>
- Gutierrez, M., Fuentes, H.R., 1996. A mechanistic modeling of montmorillonite contamination by cesium sorption. *Appl. Clay Sci.* 11, 11–24. [https://doi.org/10.1016/0169-1317\(96\)00006-3](https://doi.org/10.1016/0169-1317(96)00006-3)
- Güven, N., 1990. Longevity of bentonite as buffer material in a nuclear-waste repository. *Eng. Geol.* 28, 233–247. [https://doi.org/10.1016/0013-7952\(90\)90010-X](https://doi.org/10.1016/0013-7952(90)90010-X)
- Hahn, O., Strassmann, F., 1939. Nachweis der Entstehung aktiver Bariumisotope aus Uran und Thorium durch Neutronenbestrahlung; Nachweis weiterer aktiver Bruchstücke bei der Uranspaltung. *Naturwissenschaften* 27, 89–95. <https://doi.org/10.1007/BF01488988>
- Hahn, R., Hein, C., Sander, J.M., Kautenburger, R., 2017. Complexation of europium and uranium with natural organic matter (NOM) in highly saline water matrices analysed by ultrafiltration and inductively coupled plasma mass spectrometry (ICP-MS). *Appl. Geochemistry* 78, 241–249. <https://doi.org/10.1016/j.apgeochem.2017.01.008>
- Hamed, M.M., Ahmend, I.M., Holiel, M., 2019. Retention behavior of anionic radionuclides using metal hydroxide sludge. *Radiochim. Acta.* <https://doi.org/10.1515/ract-2019-0010>
- Harvey, C.C., Lagaly, G., 2013. Chapter 4.2 - Industrial Applications, in: Bergaya, F., Lagaly, G. (Eds.), *Handbook of Clay Science, Developments in Clay Science*. Elsevier, pp. 451-490. <https://doi.org/10.1016/B978-0-08-098259-5.00018-4>
- Hayashi, M., Hughes, L., 2013. The Fukushima nuclear accident and its effect on global energy security. *Energy Policy* 59, 102–111. <https://doi.org/10.1016/j.enpol.2012.11.046>
- He, Y., Ye, W.-M., Chen, Y.-G., Cui, Y.-J., 2019. Effects of K⁺ solutions on swelling behavior of compacted GMZ bentonite. *Eng. Geol.* 249, 241–248. <https://doi.org/10.1016/j.enggeo.2018.12.020>
- Hein, C., Sander, J.M., Kautenburger, R., 2017. New approach of a transient ICP-MS measurement method for samples with high salinity. *Talanta* 164, 477–482. <https://doi.org/10.1016/j.talanta.2016.06.059>
- Hendriks, L., Ramkorun-Schmidt, B., Gundlach-Graham, A., Koch, J., Grass, R.N., Jakubowski, N., Günther, D., 2019. Single-particle ICP-MS with online microdroplet calibration: toward matrix independent nanoparticle sizing. *J. Anal. At. Spectrom.* 34, 716–728. <https://doi.org/10.1039/C8JA00397A>
- Henry, W., 1803. III. Experiments on the quantity of gases absorbed by water at different temperatures, and under different pressures. *Philos. Trans. R. Soc.* 93, 29–42. <https://doi.org/10.1098/rstl.1803.0004>

- Herbert, H.-J., Kasbohm, J., Sprenger, H., Fernández, A.M., Reichelt, C., 2008. Swelling pressures of MX-80 bentonite in solutions of different ionic strength. *Phys. Chem. Earth* 33, S327–S342. <https://doi.org/10.1016/j.pce.2008.10.005>
- Herbert, H.-J., Moog, H.C., 2002. Untersuchungen zur Quellung von Bentoniten in hochsalinaren Lösungen.
- Höglund, S., Eliasson, L., Allard, B., Andersson, K., Torstenfelt, B., 1985. Sorption of some fission products and actinides in concrete systems. *MRS Proc.* 50, 683–690. <https://doi.org/10.1557/PROC-50-683>
- Holleman, A.F., Wiberg, E., Wiberg, N., 2007. *Lehrbuch der Anorganischen Chemie*, 102nd ed. Walter de Gruyter & Co., Berlin.
- Hoth, P., Wirth, H., Bräuer, V., Krull, P., Feldrappe, H., 2007. Endlagerung radioaktiver Abfälle in tiefen geologischen Formationen Deutschlands - Untersuchung und Bewertung von Tongesteinsformationen.
- Houk, R.S., 1986. Mass spectrometry of inductively coupled plasmas. *Anal. Chem.* 58, 97A-105A. <https://doi.org/10.1021/ac00292a003>
- Houk, R.S., Fassel, V.A., Fiesch, G.D., Svec, H.J., Gray, A.L., Taylor, C.E., 1980. Inductively coupled argon plasma as an ion source for mass spectrometric determination of trace elements. *Anal. Chem.* 52, 2283–2289. <https://doi.org/10.1021/ac50064a012>
- Houk, R.S., Svec, H.J., Fassel, V.A., 1981. Mass spectrometric evidence for suprathreshold ionization in an inductively coupled argon plasma. *Appl. Spectrosc.* 35, 380–384. <https://doi.org/10.1366/0003702814732391>
- Hunt, J., 2008. Celebrating 25 Years of Inductively Coupled Plasma-Mass Spectrometry <https://www.americanlaboratory.com/913-Technical-Articles/764-Celebrating-25-Years-of-Inductively-Coupled-Plasma-Mass-Spectrometry/> (accessed 05.07.19).
- International Atomic Energy Agency, 2019. Nuclear Power Reactors in the World. Ref. Data Ser. 2.
- International Atomic Energy Agency, 2015. The Fukushima Daiichi Accident.
- International Atomic Energy Agency, 2009. Classification of Radioactive Waste.
- International Atomic Energy Agency, 1999. Inventory of radioactive waste disposals at sea.
- International Atomic Energy Agency, 1994. Classification of Radioactive Waste - A Safety Guide.
- International Atomic Energy Agency, 1981. Underground Disposal of Radioactive Wastes - Basic Guidance.
- International Maritime Organization, 2006. 1996 Protocol to the Convention on the Prevention

- of Marine Pollution by dumping of Wastes and other Matter 1972.
- Ishikawa, H., Amemiya, K., Yusa, Y., Sasaki, N., 1990. Comparison of fundamental properties of Japanese bentonites as buffer material for waste disposal. *Sci. Geol. Mem.* 107–115.
- Itoh, A., Ono, M., Suzuki, K., Yasuda, T., Nakano, K., Kaneshima, K., Inaba, K., 2018. Simultaneous determination of Cr, As, Se, and other trace metal elements in seawater by ICP-MS with hybrid simultaneous preconcentration combining iron hydroxide coprecipitation and solid phase extraction using chelating resin. *Int. J. Analytical Chem.* 9457095. <https://doi.org/10.1155/2018/9457095>
- Jahn, D., Korolczuk, S., 2012. German exceptionalism: the end of nuclear energy in Germany! *Env. Polit.* 21, 159–164. <https://doi.org/10.1080/09644016.2011.643374>
- Jahn, S., Sönke, J., 2013. Endlagerstandortmodell Nord (AnSichT) - Teil II - Zusammenstellung von Gesteinseigenschaften für den Langzeitsicherheitsnachweis.
- Jobmann, M., Bebiolka, A., Burlaka, V., Herold, P., Jahn, S., Lommerzheim, A., Maßmann, J., Meleshyn, A., Mrugalla, S., Reinhold, K., Rübel, A., Stark, L., Ziefle, G., 2017. Safety assessment methodology for a German high-level waste repository in clay formations. *J. Rock Mech. Geotech. Eng.* 9, 856-876. <https://doi.org/10.1016/j.jrmge.2017.05.007>
- Johnson, L.H., Niemeyer, M., Klubertanz, G., Siegel, P., Gribi, P., 2002. Calculations of the temperature evolution of a repository for spent fuel, vitrified high-level waste and intermediate level waste in Opalinus Clay.
- Joseph, C., 2013. The ternary system U(VI) / humic acid / Opalinus Clay. TU Dresden.
- Joseph, C., Schmeide, K., Sachs, S., Brendler, V., Geipel, G., Bernhard, G., 2011. Sorption of uranium(VI) onto Opalinus Clay in the absence and presence of humic acid in Opalinus Clay pore water. *Chem. Geol.* 284, 240–250. <https://doi.org/10.1016/j.chemgeo.2011.03.001>
- Joshi, S.R., 1987. Early Canadian results on the long-range transport of chernobyl radioactivity. *Sci. Total Environ.* 63, 125–137. [https://doi.org/10.1016/0048-9697\(87\)90041-6](https://doi.org/10.1016/0048-9697(87)90041-6)
- Kautenburger, R., 2014. A new timescale dimension for migration experiments in clay: proof of principle for the application of miniaturized clay column experiments (MCCE). *J. Radioanal. Nucl. Chem.* 300, 255-262. <https://doi.org/10.1007/s10967-014-3017-1>
- Kautenburger, R., Beck, H.P., 2010. Influence of geochemical parameters on the sorption and desorption behaviour of europium and gadolinium onto kaolinite. *J. Environ. Monit.* 12, 1295–1301. <https://doi.org/10.1039/B914861B>
- Kautenburger, R., Beck, H.P., 2008. Waste disposal in clay formations: influence of humic acid on the migration of heavy-metal pollutants. *ChemSusChem* 2008, 1, 295-297.

<https://doi.org/10.1002/cssc.200800014>

- Kazakov, V.S., Demidchik, E.P., Astakhova, L.N., 1992. Thyroid cancer after Chernobyl. *Nature* 359, 21. <https://doi.org/10.1002/ijc.25448>.
- King, F., Kolář, M., 2019. Lifetime predictions for nuclear waste disposal containers. *CORROSION* 75, 309–323. <https://doi.org/10.5006/2994>
- Klinge, H., Köthe, A., Ludwig, R.-R., Zwirner, R., 2002. Geologie und Hydrogeologie des Deckgebirges über dem Salzstock Gorleben. *Zeitschrift für Angew. Geol.* 2, 7–15.
- Kockel, F., Krull, P., 1995. Endlagerung stark wärmeentwickelnder radioaktiver Abfälle in tiefen geologischen Formationen Deutschlands - Untersuchung und Bewertung von Salzformationen.
- Kommission Lagerung hoch radioaktiver Abfallstoffe, 2016. Verantwortung für die Zukunft - Ein faires und transparentes Verfahren für die Auswahl eines nationalen Endlagerstandortes.
- Krauskopf, K.B., 1986. Thorium and rare-earth metals as analogs for actinide elements. *Chem. Geol.* 55, 323–335. [https://doi.org/10.1016/0009-2541\(86\)90033-1](https://doi.org/10.1016/0009-2541(86)90033-1)
- Kubo, A., Tanabe, K., Suzuki, G., Ito, Y., Ishimaru, T., Kasamatsu-Takasawa, N., Tsumune, D., Mizuno, T., Watanabe, Y.W., Arakawa, H., Kanda, J., 2018. Radioactive cesium concentrations in coastal suspended matter after the Fukushima nuclear accident. *Mar. Pollut. Bull.* 131, 341–346. <https://doi.org/10.1016/j.marpolbul.2018.04.042>
- Kursten, B., Smailos, E., Azkarate, I., Werme, L., Smart, N.R., Santarini, G., 2004. COBECOMA - State-of-the-art document on the CORrosion BEhaviour of COntainer MAterials.
- Kutsen, S., Khrutchinsky, A., Minenko, V., Voillequé, P., Bouville, A., Drozdovitch, V., 2019. Influence of the external and internal radioactive contamination of the body and the clothes on the results of the thyroidal ¹³¹I measurements conducted in Belarus after the Chernobyl accident---Part 2: Monte Carlo simulation of response of detectors near. *Radiat. Environ. Biophys.* 58, 215–226. <https://doi.org/10.1007/s00411-019-00785-2>
- Langmuir, I., 1918. The adsorption of gases on plane surfaces of glass, mica and platinum. *J. Am. Chem. Soc.* 40, 1361–1403. <https://doi.org/10.1021/ja02242a004>
- Lee, S., Bi, X., Reed, R.B., Ranville, J.F., Herckes, P., Westerhoff, P., 2014. Nanoparticle size detection limits by single particle ICP-MS for 40 elements. *Environ. Sci. Technol.* 48, 10291–10300. <https://doi.org/10.1021/es502422v>
- Lee, W.E., Ojovan, M.I., Stennett, M.C., Hyatt, N.C., 2006. Immobilisation of radioactive waste in glasses, glass composite materials and ceramics. *Adv. Appl. Ceram.* 105, 3–12.

<https://doi.org/10.1179/174367606X81669>

- Leggett, R.W., Williams, L.R., Melo, D.R., Lipsztein, J.L., 2003. A physiologically based biokinetic model for cesium in the human body. *Sci. Total Environ.* 317, 235–255. [https://doi.org/10.1016/S0048-9697\(03\)00333-4](https://doi.org/10.1016/S0048-9697(03)00333-4)
- Lesniewski, J.E., Zheng, K., Lecchi, P., Dain, D., Jorabchi, K., 2019. High-sensitivity elemental mass spectrometry of fluorine by ionization in plasma afterglow. *Anal. Chem.* 91, 3773–3777. <https://doi.org/10.1021/acs.analchem.8b05851>
- Li, P., Kim, N.H., Siddaramaiah, Lee, J.H., 2009. Swelling behavior of polyacrylamide/laponite clay nanocomposite hydrogels: pH-sensitive property. *Compos. Part B Eng.* 40, 275–283. <https://doi.org/10.1016/j.compositesb.2009.01.001>
- Link, C., 2018. Suche nach Atomendlager - Auch Baden-Württemberg ist im Fokus <https://www.stuttgarter-nachrichten.de/inhalt.suche-nach-atomendlager-auch-baden-wuerttemberg-ist-im-fokus.92bd473e-de69-4fbc-a36e-403c0a728657.html> (accessed 18.07.19).
- Lippold, H., Müller, N., Kupsch, H., 2005. Effect of humic acid on the pH-dependent adsorption of terbium (III) onto geological materials. *Appl. Geochemistry* 20, 1209-1217. <https://doi.org/10.1016/j.apgeochem.2005.01.004>
- Lips, M., 2005. Water chemistry in pressurized water reactors – A Gösgen-specific overview. *Chim. Int. J. Chem.* 59, 929–937. <https://doi.org/10.2533/000942905777675372>
- Liu, L.-N., Chen, Y.-G., Ye, W.-M., Cui, Y.-J., Wu, D.-B., 2018. Effects of hyperalkaline solutions on the swelling pressure of compacted Gaomiaozi (GMZ) bentonite from the viewpoint of Na⁺ cations and OH⁻ anions. *Appl. Clay Sci.* 161, 334–342. <https://doi.org/10.1016/j.clay.2018.04.023>
- Lobo, L., Pereiro, R., Fernández, B., 2018. Opportunities and challenges of isotopic analysis by laser ablation ICP-MS in biological studies. *TrAC Trends Anal. Chem.* 105, 380–390. <https://doi.org/10.1016/j.trac.2018.05.020>
- Löhr, K., Borovinskaya, O., Tourniaire, G., Panne, U., Jakubowski, N., 2019. Arraying of single cells for quantitative high throughput laser ablation ICP-TOF-MS. *Anal. Chem.* in press. <https://doi.org/10.1021/acs.analchem.9b00198>
- Lommerzheim, A., Jobmann, M., 2015. Endlagerkonzept sowie Verfüll- und Verschlusskonzept für das Endlagerstandortmodell NORD.
- Ma, Z., Gamage, R.P., Rathnaweera, T., Kong, L., 2019. Review of application of molecular dynamic simulations in geological high-level radioactive waste disposal. *Appl. Clay Sci.* 168, 436–449. <https://doi.org/10.1016/j.clay.2018.11.018>

- Madsen, F.T., 1998. Clay mineralogical investigations related to nuclear waste disposal. *Clay Miner.* 33, 109–129. <https://doi.org/10.1180/000985598545318>
- Marksberry, D., Gonzalez, F., Hamburger, K., 2016. Three Mile Island Accident of 1979 - Knowledge - Management Digest - Overview.
- Martens-Menzel, R., 2011. *Physikalische Chemie in der Analytik*, 2nd ed. Vieweg+Teubner, Wiesbaden.
- Marty, N.C.M., Fritz, B., Clément, A., Michau, N., 2010. Modelling the long term alteration of the engineered bentonite barrier in an underground radioactive waste repository. *Appl. Clay Sci.* 47, 82–90. <https://doi.org/10.1016/j.clay.2008.10.002>
- Massat, L., Cuisinier, O., Bihannic, I., Claret, F., Pelletier, M., Masrouri, F., Gaboreau, S., 2016. Swelling pressure development and inter-aggregate porosity evolution upon hydration of a compacted swelling clay. *Appl. Clay Sci.* 124–125, 197–210. <https://doi.org/10.1016/j.clay.2016.01.002>
- Medved', I., Černý, R., 2019. Modeling of radionuclide transport in porous media: a review of recent studies. *J. Nucl. Mater.* 526, 151765. <https://doi.org/10.1016/j.jnucmat.2019.151765>
- Meitner, L., Frisch, O.R., 1939a. Products of the fission of the uranium nucleus. *Nature* 143, 471–472. <https://doi.org/10.1038/143471a0>
- Meitner, L., Frisch, O.R., 1939b. Disintegration of uranium by neutrons: a new type of nuclear reaction. *Nature* 143, 239–240. <https://doi.org/10.1038/143239a0>
- Melnikov, P., Zaroni, L.Z., 2010. Clinical effects of cesium intake. *Biol. Trace Elem. Res.* 135, 1–9. <https://doi.org/10.1007/s12011-009-8486-7>
- Meyer, S., López-Serrano, A., Mitze, H., Jakubowski, N., Schwerdtle, T., 2018. Single-cell analysis by ICP-MS/MS as a fast tool for cellular bioavailability studies of arsenite. *Metallomics* 10, 73–76. <https://doi.org/10.1039/C7MT00285H>
- Miller, B., Marcos, N., 2007. *Process Report - FEPs and Scenarios for a Spent Fuel Repository at Olkiluoto.*
- Missana, T., Benedicto, A., García-Gutiérrez, M., Alonso, U., 2014a. Modeling cesium retention onto Na-, K- and Ca-smectite: effects of ionic strength, exchange and competing cations on the determination of selectivity coefficients. *Geochim. Cosmochim. Acta* 128, 266–277. <https://doi.org/10.1016/j.gca.2013.10.007>
- Missana, T., García-Gutiérrez, M., Benedicto, A., Ayora, C., De-Pourcq, K., 2014b. Modelling of Cs sorption in natural mixed-clays and the effects of ion competition. *Appl. Geochemistry* 49, 95–102. <https://doi.org/10.1016/j.apgeochem.2014.06.011>

- Missana, T., García-Gutiérrez, M., Mingarro, M., Alonso, U., 2019. Selenite retention and cation coadsorption effects under alkaline conditions generated by cementitious materials: the case of C–S–H phases. *ACS Omega* 4, 13418–13425. <https://doi.org/10.1021/acsomega.9b01637>
- Missana, T., García-Gutiérrez, M., Alonso, Ú., 2004. Kinetics and irreversibility of cesium and uranium sorption onto bentonite colloids in a deep granitic environment. *Appl. Clay Sci.* 26, 137–150. <https://doi.org/10.1016/j.clay.2003.09.008>
- Mitrano, D.M., Barber, A., Bednar, A., Westerhoff, P., Higgins, C.P., Ranville, J.F., 2012. Silver nanoparticle characterization using single particle ICP-MS (SP-ICP-MS) and asymmetrical flow field flow fractionation ICP-MS (AF4-ICP-MS). *J. Anal. At. Spectrom.* 27, 1131–1142. <https://doi.org/10.1039/C2JA30021D>
- Molero, J., Sanchez-Cabeza, J.A., Merino, J., Mitchell, P.I., Vidal-Quadras, A., 1999. Impact of ¹³⁴Cs and ¹³⁷Cs from the Chernobyl reactor accident on the Spanish Mediterranean marine environment. *J. Environ. Radioact.* 43, 357–370. [https://doi.org/10.1016/S0265-931X\(98\)00067-8](https://doi.org/10.1016/S0265-931X(98)00067-8)
- Monfared, M., Sulem, J., Delage, P., Mohajerani, M., 2011. A laboratory investigation on thermal properties of the Opalinus Claystone. *Rock Mech. Rock Eng.* 44, 735–747. <https://doi.org/10.1007/s00603-011-0171-4>
- Montes-H, G., Marty, N., Fritz, B., Clement, A., Michau, N., 2005. Modelling of long-term diffusion–reaction in a bentonite barrier for radioactive waste confinement. *Appl. Clay Sci.* 30, 181–198. <https://doi.org/10.1016/j.clay.2005.07.006>
- Mueller, L., Traub, H., Jakubowski, N., Drescher, D., Baranov, V.I., Kneipp, J., 2014. Trends in single-cell analysis by use of ICP-MS. *Anal. Bioanal. Chem.* 406, 6963–6977. <https://doi.org/10.1007/s00216-014-8143-7>
- Müller-Vonmoss, M., Kahr, G., 1983. Mineralogische Untersuchungen von Wyoming Bentonit MX-80 und Montigel.
- Mutterlose, J., Bornemann, A., 2000. Distribution and facies patterns of Lower Cretaceous sediments in northern Germany: a review. *Cretac. Res.* 21, 733–759. <https://doi.org/10.1006/cres.2000.0232>
- Nagatani, K., Kiribayashi, S., Okada, Y., Otake, K., Yoshida, K., Tadokoro, S., Nishimura, T., Yoshida, T., Koyanagi, E., Fukushima, M., Kawatsuma, S., 2013. Emergency response to the nuclear accident at the Fukushima Daiichi nuclear power plants using mobile rescue robots. *J. F. Robot.* 30, 44–63. <https://doi.org/10.1002/rob.21439>
- Nagra, 2002. Projekt Opalinuston - Synthese der geowissenschaftlichen

- Untersuchungsergebnisse, Entsorgungsnachweis für abgebrannte Brennelemente, verglaste hochaktive sowie langlebige mittelaktive Abfälle.
- Neles, J., Mohr, S., Schmidt, G., 2008. Endlagerung von wärmeentwickelnden radioaktiven Abfällen in Deutschland - Anhang Abfälle.
- Nichoison, K.W., Hedgecock, J.B., 1991. Behaviour of radioactivity from Chernobyl—weathering from buildings. *J. Environ. Radioact.* 14, 225–231. [https://doi.org/10.1016/0265-931X\(91\)90030-J](https://doi.org/10.1016/0265-931X(91)90030-J)
- Nohrstedt, D., 2008. The politics of crisis policymaking: Chernobyl and Swedish nuclear energy policy. *Policy Stud. J.* 36, 257–278. <https://doi.org/10.1111/j.1541-0072.2008.00265.x>
- Nordyke, R.A., Gilbert, Fred I., J., Harada, A.S.M., 1988. Graves' Disease: influence of age on clinical findings. *JAMA Intern. Med.* 148, 626–631. <https://doi.org/10.1001/archinte.1988.00380030132023>
- Novo, D.L.R., Mello, J.E., Rondan, F.S., Henn, A.S., Mello, P.A., Mesko, M.F., 2019. Bromine and iodine determination in human saliva: challenges in the development of an accurate method. *Talanta* 191, 415–421. <https://doi.org/10.1016/j.talanta.2018.08.081>
- Nuclear Energy Agency, 2016. Radioactive Waste Management Programmes in OECD/NEA Member Countries - Germany.
- Nuclear Energy Agency, 2005. Radioactive Waste Management Programmes in OECD/NEA Member Countries - Germany.
- Nuclear Energy Agency, 2002. Chernobyl: Assessment of radiological and health impacts - 2002 Update of Chernobyl: Ten Years On. <https://doi.org/10.1787/9789264184879-en>
- Parkhurst, D.L., Appelo, C.A.J., 2013. Description of input examples for PHREEQC Version 3 -A computer program for speciation, batch-reaction, one-dimensional transport and inverse geochemical calculations. U.S. Geological Survey Techniques and Methods, Denver.
- Pavlakakis, N., Pollock, C.A., McLean, G., Bartrop, R., 1996. Deliberate overdose of uranium: toxicity and treatment. *Nephron* 72, 313–317. <https://doi.org/10.1159/000188862>
- Peña, J., Torres, E., Turrero, M.J., Escribano, A., Martín, P.L., 2008. Kinetic modelling of the attenuation of carbon steel canister corrosion due to diffusive transport through corrosion product layers. *Corros. Sci.* 50, 2197–2204. <https://doi.org/10.1016/j.corsci.2008.06.004>
- Petros'yants, A.M., 1964. A decade of nuclear power engineering. *At. Energy* 16, 596–600. <https://doi.org/10.1007/BF01115662>
- Plancque, G., Moulin, V., Toulhoat, P., Moulin, C., 2003. Europium speciation by time-

- resolved laser-induced fluorescence. *Anal. Chim. Acta* 478, 11–22.
[https://doi.org/10.1016/S0003-2670\(02\)01486-1](https://doi.org/10.1016/S0003-2670(02)01486-1)
- Poinsot, C., Baeyens, B., Bradbury, M.H., 1999. Experimental and modelling studies of caesium sorption on illite. *Geochim. Cosmochim. Acta* 63, 3217–3227.
[https://doi.org/10.1016/S0016-7037\(99\)00246-X](https://doi.org/10.1016/S0016-7037(99)00246-X)
- Qiao, J., Xu, Y., 2018. Direct measurement of uranium in seawater by inductively coupled plasma mass spectrometry. *Talanta* 183, 18–23.
<https://doi.org/10.1016/j.talanta.2018.02.045>
- Radhakrishna, H.S., Chan, H.T., Crawford, A.M., Lau, K.C., 1989. Thermal and physical properties of candidate buffer-backfill materials for a nuclear fuel waste disposal vault. *Can. Geotech. J.* 26, 629–639. <https://doi.org/10.1139/t89-076>
- Rasheed, Z.S., Mohammed, R.S., Salim, S.R., Hassan, A.S., 2019. Compared effect exposure of radiation to the compounds blood. *Res. J. Pharm. Technol.* 12, 545–548.
<https://doi.org/10.5958/0974-360x.2019.00096.9>
- Reed, B.C., 2014. *The History and Science of the Manhattan Project*, 1st ed. Springer, Heidelberg, New York, Dordrecht, London.
- Reid, H.J., Bashammakh, A.A., Goodall, P.S., Landon, M.R., O'Connor, C., Sharp, B.L., 2008. Determination of iodine and molybdenum in milk by quadrupole ICP-MS. *Talanta* 75, 189–197. <https://doi.org/10.1016/j.talanta.2007.10.051>
- Reinhold, K., Jahn, S., Kühnlenz, T., Ptock, L., Sönke, J., 2013. *Endlagerstandortmodell Nord (AnSichT) - Teil I: Beschreibung des geologischen Endlagerstandortmodells.*
- Reponen, A., Jantunen, M., Paatero, J., Jaakkola, T., 1993. Plutonium fallout in Southern Finland after the chernobyl accident. *J. Environ. Radioact.* 21, 119–130.
[https://doi.org/10.1016/0265-931X\(93\)90049-D](https://doi.org/10.1016/0265-931X(93)90049-D)
- Rogovin, M., Frampton Jr., G.T., 1980. *Three Mile Island: a report to the commissioners and to the public. Volume I.* <https://doi.org/10.2172/5395798>
- Röhlig, K.-J., Geckeis, H., Mengel, K., 2012. Endlagerung radioaktiver Abfälle. *Chemie unserer Zeit* 46, 140–149. <https://doi.org/10.1002/ciuz.201200578>
- Rønnov-Jessen, V., Kirkegaard, C., 1973. Hyperthyroidism - a disease of old age? *Br. Med. J.* 1, 41–43. <https://doi.org/10.1136/bmj.1.5844.41>
- Salvatores, M., 2005. Nuclear fuel cycle strategies including partitioning and transmutation. *Nucl. Eng. Des.* 235, 805–816. <https://doi.org/10.1016/j.nucengdes.2004.10.009>
- Sander, J.M., 2017. *Entwicklung von Methoden zur Untersuchung der Metallmobilität in Ton und salinaren Systemen.* Saarland University.

- Santoiemma, G., 2018. Recent methodologies for studying the soil organic matter. *Appl. Soil Ecol.* 123, 546–550. <https://doi.org/10.1016/j.apsoil.2017.09.011>
- Scatchard, G., 1936. Concentrated solutions of strong electrolytes. *Chem. Rev.* 19, 309–327. <https://doi.org/10.1021/cr60064a008>
- Schmeide, K., Bernhard, G., 2010. Sorption of Np(V) and Np(IV) onto kaolinite: effects of pH, ionic strength, carbonate and humic acid. *Appl. Geochemistry* 25, 1238–1247. <https://doi.org/10.1016/j.apgeochem.2010.05.008>
- Seveque, J.L., de Cayeux, M.D., Elert, M., Nougier, H., 1992. Mathematical modelling of radioactive waste leaching. *Cem. Concr. Res.* 22, 477–488. [https://doi.org/10.1016/0008-8846\(92\)90091-9](https://doi.org/10.1016/0008-8846(92)90091-9)
- Shoesmith, D.W., 2006. Assessing the corrosion performance of high-level nuclear waste containers. *CORROSION* 62, 703–722. <https://doi.org/10.5006/1.3278296>
- Sinev, N.M., Baturov, B.B., Shmelev, V.M., 1964. Pathways of nuclear power development in the USSR. *Sov. At. Energy* 17, 973–981. <https://doi.org/10.1007/BF01116283>
- Soler, J.M., Steefel, C.I., Gimmi, T., Leupin, O.X., Cloet, V., 2019. Modeling the ionic strength effect on diffusion in clay. The DR-A experiment at Mont Terri. *ACS Earth Sp. Chem.* 3, 442–451. <https://doi.org/10.1021/acsearthspacechem.8b00192>
- Standortauswahlgesetz, 2013. Gesetz zur Suche und Auswahl eines Standortes für ein Endlager für Wärme entwickelnde radioaktive Abfälle und zur Änderung anderer Gesetze (Standortauswahlgesetz - StandAG), Bundesgesetz, Federal Republic of Germany.
- Staunton, S., Roubaud, M., 1997. Adsorption of ¹³⁷Cs on montmorillonite and illite: effect of charge compensating cation, ionic strength, concentration of Cs, K and fulvic acid. *Clays Clay Miner.* 45, 251–260. <https://doi.org/10.1346/CCMN.1997.0450213>
- Stewart, B.D., Mayes, M.A., Fendorf, S., 2010. Impact of uranyl-calcium-carbonato complexes on uranium(VI) adsorption to synthetic and natural sediments. *Environ. Sci. Technol.* 44, 928–934. <https://doi.org/10.1021/es902194x>
- Swan, E., Urquhart, A.R., 1926. Adsorption equations. *J. Phys. Chem.* 31, 251–276. <https://doi.org/10.1021/j150272a008>
- Taylor, D.M., 1989. The biodistribution and toxicity of plutonium, americium and neptunium. *Sci. Total Environ.* 83, 217–225. [https://doi.org/10.1016/0048-9697\(89\)90094-6](https://doi.org/10.1016/0048-9697(89)90094-6)
- Thomas, R., 2002a. A beginner's guide to ICP-MS Part IX: Mass analyzers: collision/reaction cell technology. *Spectroscopy* 17, 42–49.
- Thomas, R., 2002b. A beginner's guide to ICP-MS Part X: Detectors. *Spectroscopy* 17, 34–39.
- Thomas, R., 2001a. A beginner's guide to ICP-MS Part I. *Spectroscopy* 16, 38–42.

- Thomas, R., 2001b. A beginner's guide to ICP-MS Part II: The Sample-Introduction System. *Spectroscopy* 16, 56–61.
- Thomas, R., 2001c. A beginner's guide to ICP-MS Part III: The Plasma Source. *Spectroscopy* 16, 26–30.
- Thomas, R., 2001d. A beginner's guide to ICP-MS Part IV: The interface region. *Spectroscopy* 16, 26–34.
- Thomas, R., 2001e. A beginner's guide to ICP-MS Part V: The Ion Focusing System. *Spectroscopy* 16, 38–44.
- Thomas, R., 2001f. A beginner's guide to ICP-MS Part VI: The Mass Analyzer. *Spectroscopy* 16, 44–48.
- Thury, M., 2002. The characteristics of the Opalinus Clay investigated in the Mont Terri underground rock laboratory in Switzerland. *Comptes Rendus Phys.* 3, 923–933. [https://doi.org/10.1016/S1631-0705\(02\)01372-5](https://doi.org/10.1016/S1631-0705(02)01372-5)
- Thury, M., Bossart, P., 1999. The Mont Terri rock laboratory, a new international research project in a Mesozoic shale formation, in Switzerland. *Eng. Geol.* 52, 347–359. [https://doi.org/10.1016/S0013-7952\(99\)00015-0](https://doi.org/10.1016/S0013-7952(99)00015-0)
- Tiruneh, A.T., Debessai, T.Y., Bwembya, G.C., Nkambule, S.J., 2018. Combined clay adsorption-coagulation process for the removal of some heavy metals from water and wastewater. *Am. J. Environ. Eng.* 8, 25–35. <https://doi.org/10.5923/j.ajee.20180802.02>
- Tournassat, C., Bourg, I.C., Steefel, C.I., Bergaya, Faïza, 2015. Chapter 1 - Surface Properties of Clay Minerals, in: Tournassat, C., Steefel, C.I., Bourg, I.C., Bergaya, Faïza (Eds.), *Natural and Engineered Clay Barriers, Developments in Clay Science*. Elsevier, pp. 5–31. <https://doi.org/10.1016/B978-0-08-100027-4.00001-2>
- Tournassat, C., Tinnacher, R.M., Grangeon, S., Davis, J.A., 2018. Modeling uranium(VI) adsorption onto montmorillonite under varying carbonate concentrations: a surface complexation model accounting for the spillover effect on surface potential. *Geochim. Cosmochim. Acta* 220, 291–308. <https://doi.org/10.1016/j.gca.2017.09.049>
- Turner, H.C., Lee, Y., Weber, W., Melo, D., Kowell, A., Ghandhi, S.A., Amundson, S.A., Brenner, D.J., Shuryak, I., 2019. Effect of dose and dose rate on temporal gamma-H2AX kinetics in mouse blood and spleen mononuclear cells in vivo following cesium-137 administration. *BMC Mol. Cell Biol.* 20, 1–13. <https://doi.org/10.1186/s12860-019-0195-2>
- Unuabonah, E.I., Adebowale, K.O., Olu-Owolabi, B.I., 2007. Kinetic and thermodynamic studies of the adsorption of lead (II) ions onto phosphate-modified kaolinite clay. *J.*

- Hazard. Mater. 144, 386–395. <https://doi.org/10.1016/j.jhazmat.2006.10.046>
- Van Loon, L.R., Baeyens, B., Bradbury, M.H., 2005. Diffusion and retention of sodium and strontium in Opalinus clay: comparison of sorption data from diffusion and batch sorption measurements, and geochemical calculations. *Appl. Geochemistry* 20, 2351–2363. <https://doi.org/10.1016/j.apgeochem.2005.08.008>
- Van Loon, L.R., Soler, J.M., Bradbury, M.H., 2003. Diffusion of HTO, $^{36}\text{Cl}^-$ and $^{125}\text{I}^-$ in Opalinus Clay samples from Mont Terri: effect of confining pressure. *J. Contam. Hydrol.* 61, 73–83. [https://doi.org/10.1016/S0169-7722\(02\)00114-6](https://doi.org/10.1016/S0169-7722(02)00114-6)
- Van Loon, L.R., Wersin, P., Soler, J.M., Eikenberg, J., Gimmi, T., Hernán, P., Dewonck, S., Savoye, S., 2004. In-situ diffusion of HTO, $^{22}\text{Na}^+$, Cs^+ and I^- in Opalinus Clay at the Mont Terri underground rock laboratory. *Radiochim. Acta* 92, 757–763. <https://doi.org/10.1524/ract.92.9.757.54988>
- Vanhoe, H., Van Allemeersch, F., Versieck, J., Dams, R., 1993. Effect of solvent type on the determination of total iodine in milk powder and human serum by inductively coupled plasma mass spectrometry. *Analyst* 118, 1015–1019. <https://doi.org/10.1039/AN9931801015>
- Wada, T., Nemoto, Y., Shimamura, S., Fujita, T., Mizuno, T., Sohtome, T., Kamiyama, K., Morita, T., Igarashi, S., 2013. Effects of the nuclear disaster on marine products in Fukushima. *J. Environ. Radioact.* 124, 246–254. <https://doi.org/10.1016/j.jenvrad.2013.05.008>
- Wallenius, J., 2019. Maximum efficiency nuclear waste transmutation. *Ann. Nucl. Energy* 125, 74–79. <https://doi.org/10.1016/j.anucene.2018.10.034>
- Weißburger, U., 1996. The nuclear threat to the environment in Russia. *Econ. Bull.* 33, 17–28. <https://doi.org/10.1007/BF02233765>
- Wersin, P., Van Loon, L.R., Soler, J.M., Yllera, A., Eikenberg, J., Gimmi, T., Hernán, P., Boisson, J.-Y., 2004. Long-term diffusion experiment at Mont Terri: first results from field and laboratory data. *Appl. Clay Sci.* 26, 123–135. <https://doi.org/10.1016/j.clay.2003.09.007>
- Williams, D., 2002. Cancer after nuclear fallout: lessons from the Chernobyl accident. *Nat. Rev. Cancer* 2, 543–549. <https://doi.org/10.1038/nrc845>
- Wolery, T.J., 1992. EQ3/6, a software package for geochemical modeling of aqueous systems: Package overview and installation guide (Version 7.0). Lawrence Livermore National Laboratory, Livermore.
- Wolery, T.J., Jackson, K.J., Bourcier, W.L., Bruton, C.J., Viani, B. E., Knauss, K.G., Delany,

- J.M., 1988. The EQ3/6 software package for geochemical modeling: Current status, in: American Chemical Society (ACS) National Meeting. Los Angeles.
- Yamagata, N., 1962. The concentration of common cesium and rubidium in human body. *J. Radiat. Res.* 3, 9–30. <https://doi.org/10.1269/jrr.3.9>
- Ye, W.-M., Chen, Y.-G., Chen, B., Wang, Q., Wang, J., 2010. Advances on the knowledge of the buffer/backfill properties of heavily-compacted GMZ bentonite. *Eng. Geol.* 116, 12–20. <https://doi.org/10.1016/j.enggeo.2010.06.002>
- Zhang, C.L., Wieczorek, K., Xie, M.L., 2010. Swelling experiments on mudstones. *J. Rock Mech. Geotech. Eng.* 2, 44–51. <https://doi.org/10.3724/SP.J.1235.2010.00044>
- Zhang, Q., Zheng, M., Huang, Y., Kunte, H.J., Wang, X., Liu, Y., Zheng, C., 2019. Long term corrosion estimation of carbon steel, titanium and its alloy in backfill material of compacted bentonite for nuclear waste repository. *Sci. Rep.* 9, 3195. <https://doi.org/10.1038/s41598-019-39751-9>
- Zheng, L., Rutqvist, J., Xu, H., Birkholzer, J.T., 2017. Coupled THMC models for bentonite in an argillite repository for nuclear waste: illitization and its effect on swelling stress under high temperature. *Eng. Geol.* 230, 118–129. <https://doi.org/10.1016/j.enggeo.2017.10.002>